Price: 10 EUR

HUNGARIAN GROUP OF *fib*

CONCRETE STRUCTURES

ANNUAL TECHNICAL JOURNAL

2009

Vol. 10

CONCRETE STRUCTURES
Journal of the Hungarian Group of *fib*

Editor-in-chief:
Prof. György L. Balázs

Editors:
Prof. Géza Tassi
Dr. Herbert Träger

Founded by: Hungarian Group of *fib*
Publisher: Hungarian Group of *fib*
(*fib* = International Federation for Structural Concrete)

Editorial office:
Budapest University of Technology and Economics (BME)
Department of Construction Materials and Engineering Geology
Műegyetem rkp. 3., H-1111 Budapest
Phone: +36-1-463 4068
Fax: +36-1-463 3450
WEB http://www.fib.bme.hu
Editing of online version:
László Bene

Price: 10 EUR
Printed in 1000 copies

ISSN 1419-6441
online ISSN: 1586-0361

Cover:
Cable stayed Northern Danube bridge on M0 ring around Budapest, Hungary
Photo: Pál Csécsei

CONTENT

Sponsors:
Railway Bridges Foundation, ÉMI Kht., HÍDÉPÍTŐ Co.,
MÁV Co., MSC Hungarian SCETAUROUTE Consulting Co.,
Pfleiderer Lábatlani Vasbetonipari Co., Pont-*TERV* Co., UVATERV Co.,
MÉLYÉPTERV KOMPLEX Engineering Co., SW Umwelttechnik Hungary Ltd.,
Betonmix Consulting Ltd., BVM Épelem Ltd., CAEC Ltd., Pannon Freyssinet Ltd.,
STABIL PLAN Ltd., UNION PLAN Ltd., DCB Consulting Ltd.,
BME Dept. of Structural Engineering,
BME Dept. of Construction Materials and Engineering Geology

LINKS BETWEEN LONDON AND HUNGARY – HISTORY, CULTURE, CONSTRUCTION


Géza Tassi – György L. Balázs

*As a tradition of Journal CONCRETE STRUCTURES a review is presented every year on the technical and cultural links between Hungary and the city or country were the **fib** Symposium or Congress takes place. We are happy to remember now to the links between London and Budapest.*

1. INTRODUCTION

The population of the city of London is approximately equal to that of the entire population of Hungary. Of course, there are a great many other differences on both sides in subjects covered by this paper. The United Kingdom is abundant in politicians, scientists, men of letters, artists and engineers. All Hungarian schoolboys and schoolgirls know, for example, about Queen Victoria (1819-1901), Sir Isaac Newton (1643-1727), William Shakespeare (1564-1616), J. M. W. Turner (1775-1851) and G. Stephenson (1781-1848). One cannot, of course, compare the number of people speaking our respective languages of English and Hungarian. However, despite the difference, Hungarians are proud of their own number of outstanding statesmen, writers, poets, sculptors, painters, musicians and scientists. It is certain, that in the streets of London, one may come across almost every day at least five things having a Hungarian inventor, for example, the safety match (J. Irinyi, 1817-1895), the ball pen (L. J. Bíró, 1899-1986), vitamin C (A. Szent-Györgyi, 1893-1986), the computer (J. Neumann, 1903-1957) and the hologram (D. Gábor, 1900-1979). We Hungarians are also proud of our excellent sportsmen who are internationally famous as well as in London, such as F. Puskás (1927-2006) or S. Kocsis (1929-1979).

We seek not to make comparisons between London and Hungary, but to highlight the conjunctions of our history.

There are many benefits to congresses and symposia. Apart from the enormous exchange of professional knowledge, personal contact between delegates is of great value. These meetings help in getting to know better the host country and city, as well as the technical achievements of the organizers and foreign participants. We may say that it has become a tradition for this English language journal of the Hungarian Group of ***fib*** to present a paper on the traditional connections between the host of the meeting and Hungary. Of course, it is not possible to relate all facts and events which contributed to the better understanding between international links, however we hope that this article will bring London closer to Hungary and vice versa (Tassi, Balázs, Borosnyói, 2005).

2. HISTORICAL SNAPSHOTS

2.1 Preliminaries

Some years ago, at an international congress dealing with concrete structures, a British professor expressed his pleasant surprise to his Hungarian colleague about how well they can understood one another. ”This may be quite natural”, was the reply. “After all you must not forget – continued the Hungarian delegate - that the lands of both our countries once belonged to one and the same realm.” ‘What do you mean by that?’ the question was returned with some slight surprise. “Well, I mean in antiquity, the Imperium Romanum” came the reply. And indeed! During the rule of the emperor Hadrian and thereafter until 450 A. D. both a significant part of the British Isles (Britannia) and the half of the present Hungary (Pannonia) belonged to the Roman Empire as the map shows (Cornell, Matthews, 1982) *(Fig.1)*. Speaking not about the territory but rather of population, we note that in those times the Angles and Saxons were still on the continent and only heading in the future to the present Great Britain in order to come to an amalgamation with the Celtic and other population of the Isles. At this time, however, the Hungarian tribes might have lived on the eastern slopes of the Ural Mountain in Asia and it took almost half a millennium, until they occupied their present home in the Carpathian Basin.

Fig. 1: Map of the Roman Empire (4th 5th century A. D.)

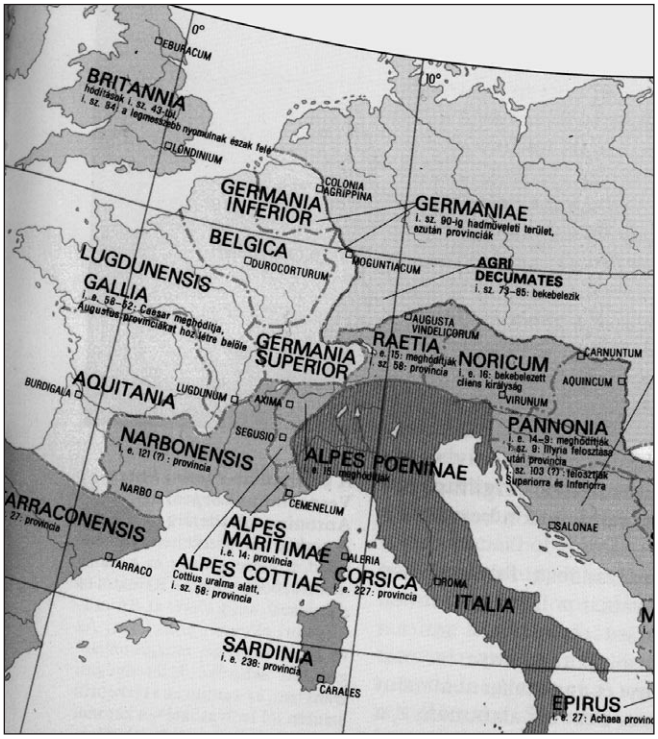

Certainly it took a long time until Hungary entered the European Community, where now both nations feel at home.

2.2 The Middle Ages

After the first millennium initial contacts were established between the first Hungarian King St. Stephen and Ethelred's brave son, Edmund Ironside (~981 – 1016). Edmund was at that time the king of the English, and had fought desperately against the Danish invaders lead by Canute the Great. In the year 1016 Edmund Ironside lost in battle and died. His widow had to flee with her two sons (Feiling, 1959). Of them Edward the Exile found refuge and a home in the Hungarian court of St. Stephen (Szent István) and according to a number of early English chronicles the young Edward married Agathe, a daughter of the Hungarian king. From their marriage a daughter, Margarete was borne in Hungary near Mecseknádasd (Baranya County) in the Fortress Réka. Margarete later became the wife of Malcolm III of Scotland (Lexikon des Mittelalters, 2003).

The address of Pope Urban II held at Clermont on the 27th of November, 1095 was the inception of a great European movement, the crusades, which influenced and encouraged English-Hungarian relations. Many knights and noblemen set forth from all of Europe, from England and from Hungary in order to recapture the Holy Land. Of the two main routes taken, one led through the Hungarian Kingdom and English crusaders were received with hospitality. During the long time of the crusades both the English and the Hungarian knights fought together in the fortress Margat (Marqab) among others. This fortress is located in Syria where presently large-scale excavations and reconstructions are in progress under the supervision of Hungarian experts (Runciman, 1995).

Meanwhile, the Hungarian Kingdom suffered much from the Mongol invasion as did other countries in Europe in the middle of the 13th century. The immense devastation caused by the Mongolian hordes awoke a great anxiety also in Britain in response to a detailed letter written by the Hungarian king Béla IV to the king Henry III. (Hóman, Szekfű, 1936). After the end of the first Hungarian royal dynasty in 1301 a new king was elected from the Angevins who were also involved in the history of England. No wonder, that the new Hungarian king, Anjou Louis the Great (Nagy Lajos), kept up friendly dialogue with the English court and succeeded in obtaining the sympathy and support of Edward III in his warfare against Naples in 1347 (Hóman, Szekfű, 1936).

After some years of transition, Sigismund (Zsigmond) of Luxemburg succeeded the Anjou kings on the Hungarian throne. In 1410 Sigismund also became the sovereign of the Holy Roman Empire. In this capacity he presided at the Council of Constance and he succeeded in terminating the schism of the western Church while condemning, among others, the doctrines of the English John Wyclif. After the battle at Agincourt, Emperor Sigismund did much to end the Hundred Years War between France and England. This was based on the Alliance of Canterbury which was concluded on 15th August, 1416 between the emperor Sigismund and the king Henry V. For this end Sigismund travelled personally to England and presented the insignia of the Order of the Dragon to the king Henry V *(Fig. 2)*. (Lexikon des Mittelalters, 2003).

Fig. 2: Order of Dragon donated by King Sigismund (Zsigmond) of Hungary to King Henry V of England

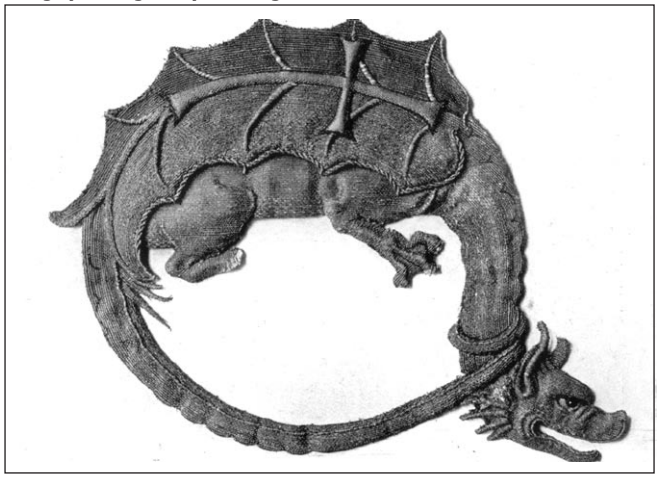

Defeat at the battle of Nikopolis 28th September, 1396, under the leadership of the emperor Sigismund, was the last act of the crusades in which one thousand English knights fought against the Turks. Among them was John Holland, the Duke of Exeter, who was one of the half brothers of the English king Richard II. (Lexikon des Mittelalters, 2003).

Remarkably there was no significant connection between England and Hungary under the reign of the greatest renaissance king of Hungary, Matthias (Mátyás) Corvinus. Some fifty years after, the collapse of Hungary under immense Turkish pressure, the unity of the Hungarian kingdom ceased to exist. Two kings were elected in controversy. One of them was Habsburg, Ferdinand and the other one János Zápolya. The latter contacted the English king Henry VIII for help against Ferdinand. Henry VIII expressed his sympathy for Zápolya, however, due to the great distance between their two countries, he declined to help. (Hóman, Szekfű, 1936).

2.3 Modern Times

A period of obscurity lasting about 150 years commenced for Hungary under the Turkish rule. The Turks were a great threat also to lands west of Hungary creating concern and interest in England. An example of this interest is the great number of maps of Hungary having been engraved in England, especially in London, during that period. Illustrated below in *Fig. 3* is a front page from one of these maps.

Fig. 3: Front page for map of Hungary engraved in London, XVIIth century

During the last decades of the Turkish occupation of Hungary there were, however, sporadic connections between our two countries principally in the area of learning and pedagogy. In the early 17th century a Hungarian student, Márton Szepsi Csombor, journeyed in Europe and the British Isles, visiting both London and Canterbury where he became especially interested in the schools. He then published his experiences in 1622 under the title "Europica Varietatis". Even to-day, active in London, there exists a Hungarian cultural circle using his name.

In the 18th century Queen Anne had a Hungarian painter named Jakab Bogdány (1660 Eperjes-1724 London). His

flower-piece to this day remains exhibited in Hampton Court under the number 222. (Bajzik, 1975).

After the expulsion of the Turks from Hungary English travellers took a greater interest in visiting our country. Some years earlier Edward Brown, the member of the Royal Society made a journey to Hungary as well as to other neighbouring countries. His experiences were published in London in 1673 (Brown, 1673). It is possible that Edward Brown succeeded in getting pictorial information about Hungary as the British Library in London has a beautiful collection of coloured drawings drawn by an unknown painter of costumes born in the 17th century in Transylvania, a region which was for a long time a part of Hungary.

It is the 19th century with the influences of the enlightenment which after a long sleep slowly brought significant changes for Hungary and here mention must be made above all of the great Hungarian patriot Count István Széchenyi (1791-1860) *(Fig. 4. b)* and of his experiences collected in England 1815-16, later 1822. He negotiated in London in 1832 about the steam shipping, the navigation of the Lower Danube and the possibility of a permanent bridge across the Danube. Due to the good results gained from the steam navigation on the River Danube Count Széchenyi urged the building of another steam ship but for the Lake Balaton (Széchenyi, 1846). This lake with its 80 km length and 5 km width in average practically cut in half the bordering country-sides. The steamer *(Fig. 5)* had finally been built, it was named "Kisfaludy" after a late Hungarian poet and furnished with a steam engine from the Greenwich factory of John Penn and Son. The ship had been set afloat 21st September, 1846 and she was able to transport 300 passengers. She served more than fifty years. Count Széchenyi was the pioneer of the construction of railways in Hungary, too. Due to his efforts the test runs of the railway were started 10th November, 1845 and the first public track was officially commissioned 15th July, 1846 with the locomotive "Buda" *(Fig. 6)*. The locomotives were, however, not from England but from the Belgian factory of Cockerill J. and Co. An English heritage is, however, the track-gauge stated originally by George Stephenson as 4 feet and 8.5 inches i. e. 1435 mm (Miklós, 1937). In 1848 Count Széchenyi was appointed to be the minister of transport and communal works in the first ministry of Hungary responsible to the parliament.

Fig. 4: Lajos Kossuth István Széchenyi

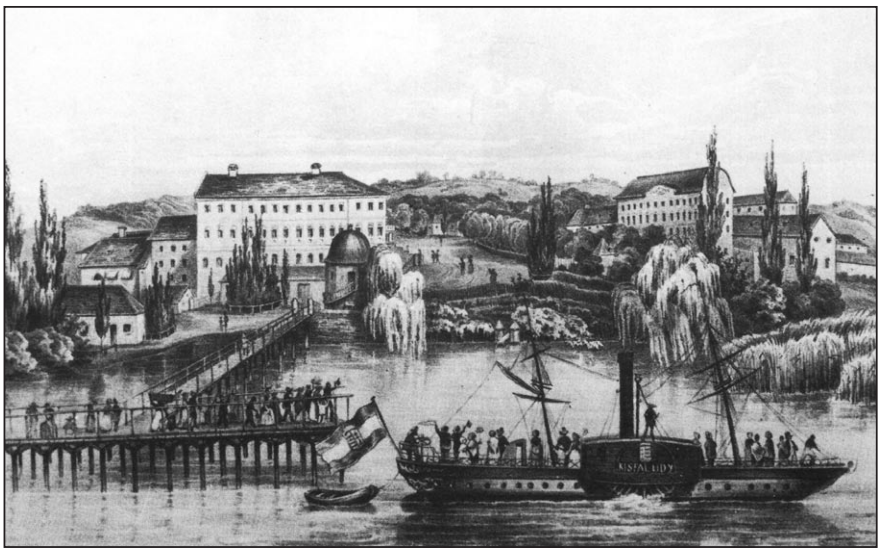

Fig. 5: The ship "Kisfaludy" manufactured in London

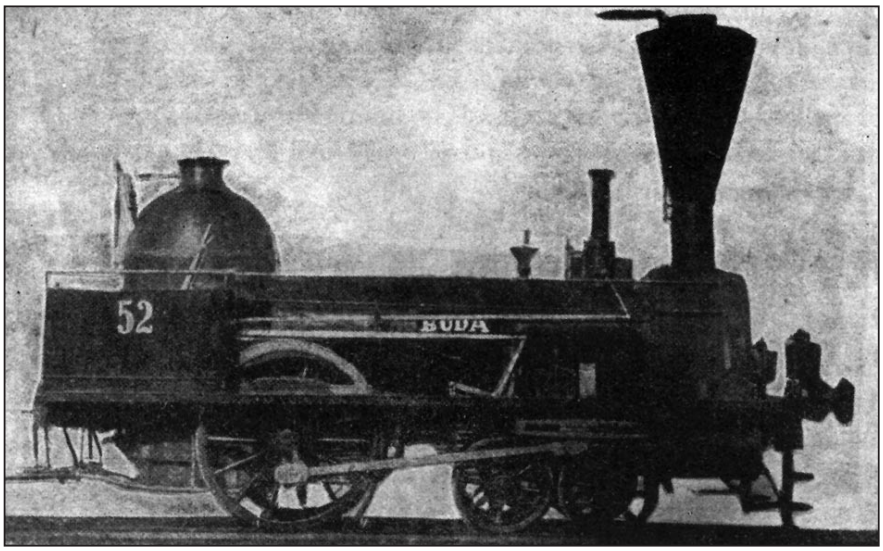

Fig 6: The first locomotive in Hungary designed by George Stephenson

It was also 1848 that irreconcilable controversies arouse between Hungary and the Austrian Empire that was to enforce its intentions with military means. Hungary came to the necessity of self defence and thus the war of the Hungarian independence commenced. Due to the initial successes the Hungarian parliament declared also the dethronement of the Habsburg dynasty (Barta, 1953), but finally the war of independence had been suppressed with ***the aid*** of tremendous Russian military forces.

A lot of Hungarian patriots had been executed or imprisoned by the Austrians and another lot had to flee the country. Many freedom-fighters could find refuge in England, among them also Lajos Kossuth (1802-1894) *(Fig. 4 a)*, the leader of the 1848 revolution and later governor of the country. He had a lecture tour in England in 1851, and then he lived in London from 1852 to 1861. His blue memorial tablet can be seen in London at 39 Chepstow Villas W11 even today.

The efforts and claims of the independence did not cease to exist in Hungary even after the lost war. One of the first line combatants of these endeavours was again Count Széchenyi who sarcastically attacked the Austrian Empire in an anonymous book having been published in London 1859. Its title was "Ein Blick auf den anonymen Rückblick" (A look at the Anonymous "Look Back"). As for the front-page of it, see *Fig. 7*), however, the identity of the author had soon been disclosed by the Austrian secret police. 1867 a reconciliation came about between Hungary and Austria and it was the beginning of a fruitful prosperity lasting until the World War I. Meanwhile, Hungary was successful at the fourth Summer Olympic Games held in London 1908 and won three gold, four silver and one bronze medals.

After the first frosty years between Great Britain and Hungary following World War I came a score of years' détente of that summit for Hungary might be the visit of the king Edward VIII started 8th September 1936.

The World War II brought Hungary and Great Britain on the opposite sides. Thanks to the salutary effects of the 14th Summer Olympic Games in London (1948) where the hostilities were beneficially put aside, resulting in 10 gold, 5 silver and 13 bronze medals for Hungary.

A great but at the end sorrowful event was in the late history of Hungary the revolution in 1956 that finally was beaten by the Soviet Army such as their predecessors the Tsarist Russia had beaten the Hungarian revolution 1848-1849. More than two hundred thousand Hungarian fellow-citizens left the country after the defeat of 1956. Great Britain was generous enough to give shelter to a lot of them and they became useful citizens

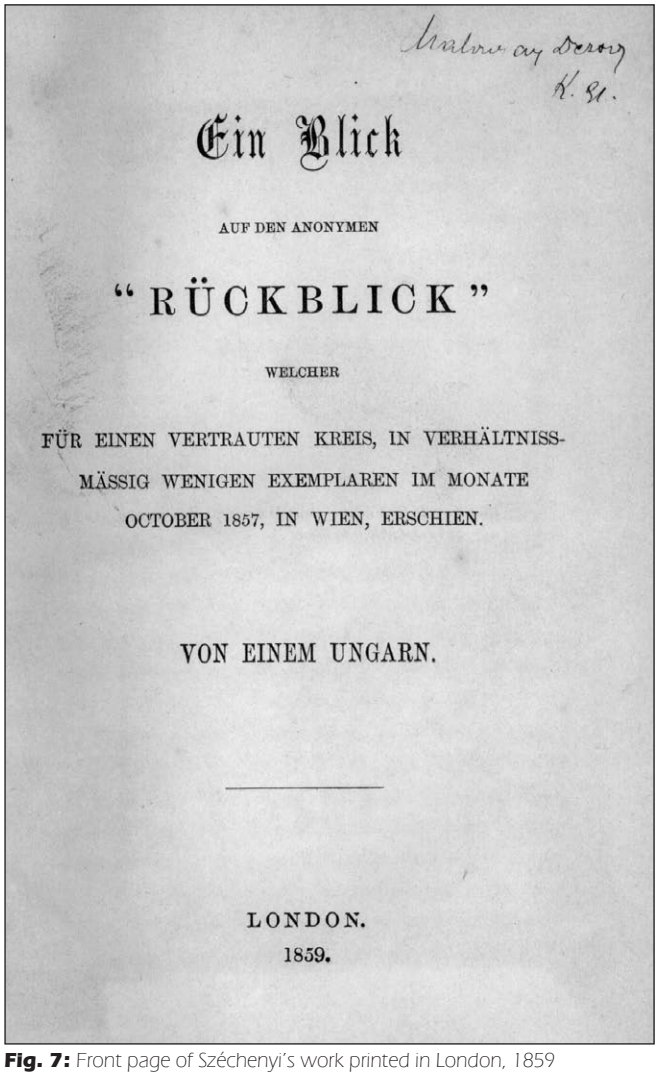
Ein Blick

AUF DEN ANONYMEN

"RÜCKBLICK"

WELCHER

FÜR EINEN VERTRAUTEN KREIS, IN VERHÄLTNISS-MÄSSIG WENIGEN EXEMPLAREN IM MONATE OCTOBER 1857, IN WIEN, ERSCHIEN.

VON EINEM UNGARN.

LONDON.
1859.

Fig. 7: Front page of Széchenyi's work printed in London, 1859

of their adopting country. Last but not least in love there are still two other outstanding events worth to mention of the late history of Hungary. One of them was the state visit of the British Prime Minister Mrs. Margaret Thatcher to Hungary 1993. The people of Hungary hope that Mrs. Thatcher was satisfied also with the red pepper which she bought in the great market-hall of Budapest. The other state visit was paid by Her Majesty the Queen 1993. At this time Her Majesty made an address to the Hungarian Parliament, too.

3. SCIENCE, LITERATURE, MUSIC AND FINE ARTS

Despite political differences between the two countries throughout the ages, free and effective communication in the areas of science and arts never ceased. Even just a rough outline of fruitful interactions in these areas would burst the scope of this paper.

Some identities, however, cannot be omitted, and firstly we refer to that of two economists:

Thomas (Tamás) Balogh (1905 Budapest – 1995 London) whose father Emil Balogh was chief engineer of the Budapest Transport Company. (During the time that he lived in London, Author[1] of this paper was in close correspondence with him.) Thomas Balogh was for a long time a tutor at Oxford's Balliol College. In recognition of his services to the Labour Party under the Wilson government, Thomas Balogh was awarded a peerage with the barony of Hampstead and thus his name in Great Britain is better known as Lord Thomas Balogh.

The other Hungarian born economist was Miklós Káldor (1908 Budapest – 1986 Cambridge) who became a significant representative of the Cambridge economic school of the Keynesian view. He was also awarded a peerage and became known as Lord Nicholas Kaldor. He was also an external member of the Hungarian Academy of Sciences.

Other significant names in Hungarian/English cross cultural activity are: Albert Szent-Györgyi (Budapest 1893-Woods Hole, USA 1986), medical doctor and biochemist, he studied in Hungary and also in Cambridge at the institute of biochemistry of F.G. Hopkins from where he gained his doctorate in Chemistry. He was already a professor in Szeged (Hungary) when he discovered Vitamin C and for this he was awarded the Nobel Prize in 1937. In 1943, as a member of an antifascist group, he contacted the British-American allied powers in Turkish territory.

Dennis (Dénes) Gábor (Budapest 1900 - London1979) *(Fig. 8)* studied at the Technical University of Budapest, later at Berlin Charlottenburg where he gained doctor degree. He worked in Germany and in Hungary, later as physicist he was employed at the British Thomson Corporation between 1934 and 1948. From 1948 onwards, he was a professor at the Imperial College of Science and Technology in London. (Author[1] of this paper was fortunate to meet him there in 1971.) Professor Gábor *(Fig. 8)* beside his more than 100 patents, elaborated the holographic methods gaining him the Nobel Prize in physics in 1971.

The examples above are significant but not complete. We could enumerate a long series of English writers and poets who are well known in Hungary. We are very fortunate that the greatest Hungarian poets and writers translated the pearls of English literature. It is therefore not a joke to say that "the most popular Hungarian playwright is William Shakespeare". On the other hand, there are excellent Hungarian poets and writers whose works are known in English translation. We met

Fig. 8: *Dennis (Dénes) Gábor*

citizens of London who admired the poems of Sándor Petőfi (1823-1849), the ballades of János Arany (1817-1882), and who were delighted by the mystery play of Imre Madách (1823-1864) "The Tragedy of Man". At present time the Hungarian Nobel Prize holder Imre Kertész and other writers are popular among literature liking British people.

The Hungarian public on many occasions enjoyed the concerts of Sir Yehudi Menuhin (1916-1999), who came to us from London. Prior to 1944 he supported Béla Bartók (1881-1945) in New York. Menuhin encouraged Bartók to compose his solo sonatas and Bartók offered his Violin Concert II to Yehudi Menuhin.

The famous conductor György Solti (1912 Budapest – 1997 Antibes) is known all over the world as Sir George Solti. Between 1930 and 1938 he was conductor of the Budapest State Opera. He was conductor of the London Covent Garden from 1961 to 1972, and was artistic director of the London Symphony Orchestra.

We may also note that London's musical life was enriched by the violinist George (György) Pauk (1936 Budapest) and also by the pianist Peter (Péter) Frankl (1935 Budapest), both men were educated in Hungary and both live in London since 1958 and 1962 respectively.

The operas, Albert Herring and Peter Grimes, both composed by Sir Benjamin Britten (1913-1976) ran for an extended period on the stage of the Budapest State Opera and were very much appreciated by the Hungarian audiences.

As for painters and sculptors, names on both sides are too numerous to mention, however, among them was the Hungarian Fülöp László (1869 Pest – 1937 London), a famous portraitist of English high society in the period between the two World Wars. At the head of a list of many important dignitaries, he painted a portrait of King Edward VII and his Queen.

The Hungarian sculptor Zsigmond Kisfaludi-Strobl (1884-1975) was also notable with his many portraits created between 1932 and 1937, among them being that of young Queen

Fig. 9: *William Tierney Clark*

Elisabeth II. Kisfaludi-Strobl held numerous exhibitions in London and a very close connection existed between him and G. B. Shaw.

The internationally acclaimed Hungarian painter László Moholy-Nagy (1895-1946) had exhibitions of his works in the London Art Gallery between 1935 and 1937.

A comprehensive exhibition of the works of sculptor Henry Moore (1898-1986) was held in the Art Gallery of Budapest in 1967 and in the Museum of Fine Arts in 1993. All these illustrate the deep, and hopefully enduring connections between Hungary and Great Britain.

4. CIVIL ENGINERERING AND ARCHITECTURE

4.1 The 19th Century's Outstanding Structures in Hungary by eminent British Engineers

As mentioned in Chapter 2, Count István Széchenyi urged the development of transportation in the third decade of the 19th century. Among the many difficulties facing transport communication Széchenyi sought to solve the deficit in links across the huge Danube river between the two cities of Buda and Pest. These two twin cities developed rapidly but were essentially divided by the wide river Danube.

During his travel in England István Széchenyi became acquainted with an eminent English civil engineer, William Tierney Clark (Bristol 1783 - London 1852) *(Fig. 9)*, who was principally associated with the design and construction of bridges. He was among the earliest designers of suspension bridge structures. Tierney Clark lived in London from 1811 where he designed various buildings and hydraulic engineering works. He was also a Fellow of the Royal Society and a member of the Institution of Civil Engineers.

W. T. Clark designed the first suspension bridge to span

Fig. 10: Széchenyi Chain Bridge

the river Thames, the Hammersmith Bridge (1827) and continued to design suspension bridges in Britain until 1834. At Széchenyi's invitation, in 1839 W. T. Clark designed the bridge across the Danube between Buda and Pest, the bridge which is now known as the Széchenyi Chain Bridge *(Fig. 10)*. This design was in its structure similar to the Marlow Bridge across the Thames in Buckinghamshire, but much larger. The bridge was opened for traffic in 1849.

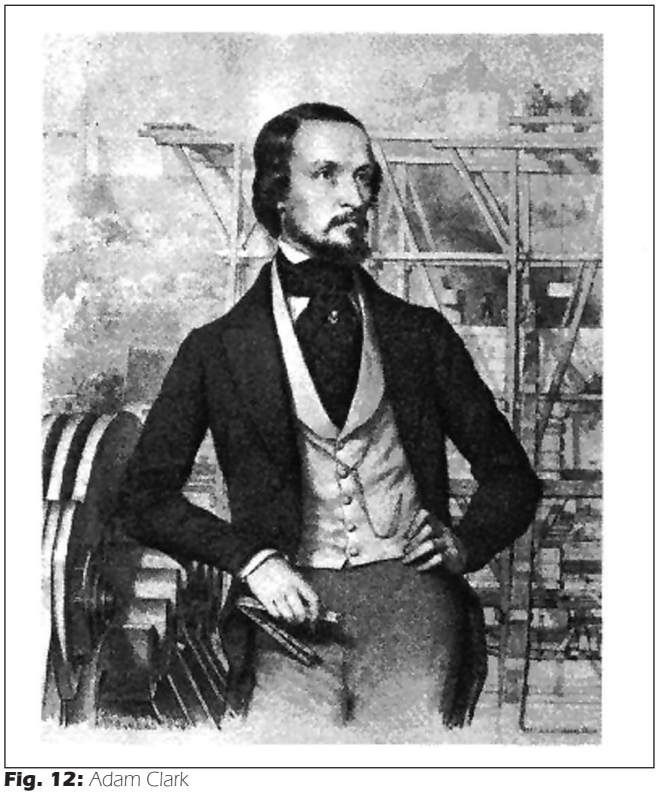

Fig. 12: Adam Clark

The early history of this bridge contains other links to England. While W. T. Clark entered the competition with three designs, another English engineer, George Rennie, also submitted designs for various options. The referees, engineers John Plews and Samuel Slater, were also British. They gave their votes for the three bay suspension bridge not to be built at

Fig. 11: Széchenyi Chain Bridge, Budapest at night

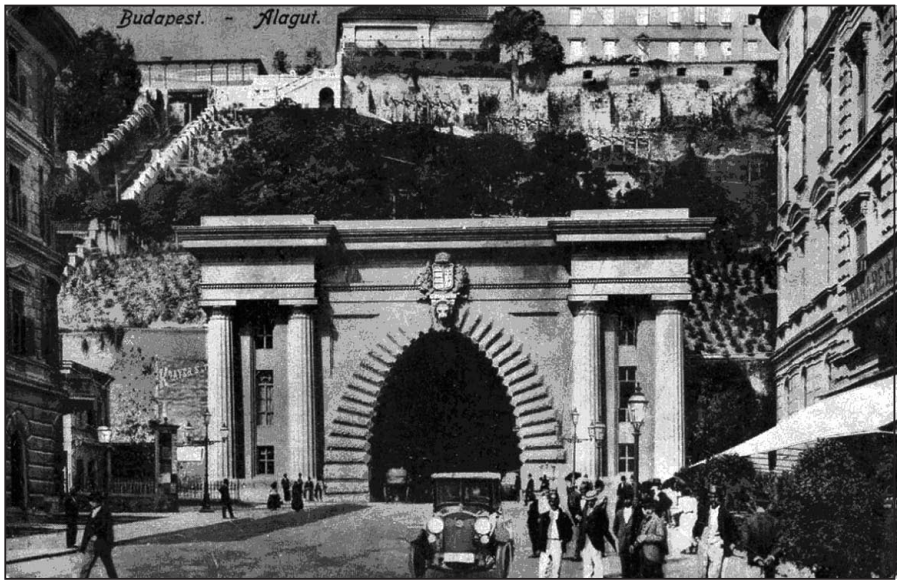

Fig. 13: *Tunnel under the Buda Castle Hill (Completed 1857, Photo 1927)*

the narrowest point of the Danube between Buda and Pest but rather at its to-day existing location. This bridge characterized the future development of these separate cities as one united metropolis now referred to as Budapest.

The full length of this bridge is 380 m; the spans are 88.70+202.62+88.70 m; the carriageway is 6.45 m wide; the sidewalks 2.20 m each; and the full width including the main load bearing structures 14.50 m. The flat foundation level under the lowest water level is to a depth 12.50 m at the Buda abutment. The Mauthausen granite clad pylons rise 60 m above the foundation (Gáll, 1999).

An interesting element of the Chain Bridge is the application of concrete to the foundations of the piers and abutments (1839!). Roman cement, which was manufactured at the very place which later became the plot for central building of the Hungarian Academy of Sciences, was applied. The Hungarian Academy of Sciences building also served as the venue for the ***fib*** Symposium in 2005 in Budapest (Balázs, Borosnyói, Tassi, 2005).

Between 1914 and 1915 refurbishments of the chains resulted in a double system, parallel flange with X diagonals, stiffening truss girders. Today the handrails are of steel, no longer the original wooden ones, and the deck slab is a 15 cm thick reinforced concrete replacing the original lightweight structure. At the time of the reconstruction in 1949 the portals were also widened to enable the meeting of two buses under the tower.

It belongs to the history of the bridge, that refurbishment was required - as mentioned - at the time of WW I, and unfortunately the bridge was destroyed by the withdrawing German troops in January 1945. The reconstructed Széchenyi Chain Bridge was inaugurated on 20th November 1949. The engineer who was responsible for the reconstruction was Professor László Palotás (1905 – 1993), the initiator of foundation of the Hungarian Group of FIP. The Széchenyi Chain Bridge which is internationally acknowledged as one of the most beautiful bridges of its type is still the symbol of the Hungarian capital. It defines the riverside landscape by daylight and gives a splendid appearance when lit at night between the illuminated Buda Castle and the Gresham Palace (presently the Four Seasons Hotel) on the Pest side *(Fig. 11)*.

We may well say that this bridge is the noblest sign of the traditional links between London and Hungary.

The name of W. T. Clark is commemorated by an annual award made by the Association of Hungarian Consulting Engineers, in the frame of Hungarian Chamber of Engineers and Architects as well as the Institution of Civil Engineers, Midland (UK) the Tierney Clark Award for Civil Engineering.

W. T. Clark, acting on behalf of I. Széchenyi searched for a mechanic for the dredger „Vidra" (Otter) working on the

Fig. 14: Miklós Szerelmey

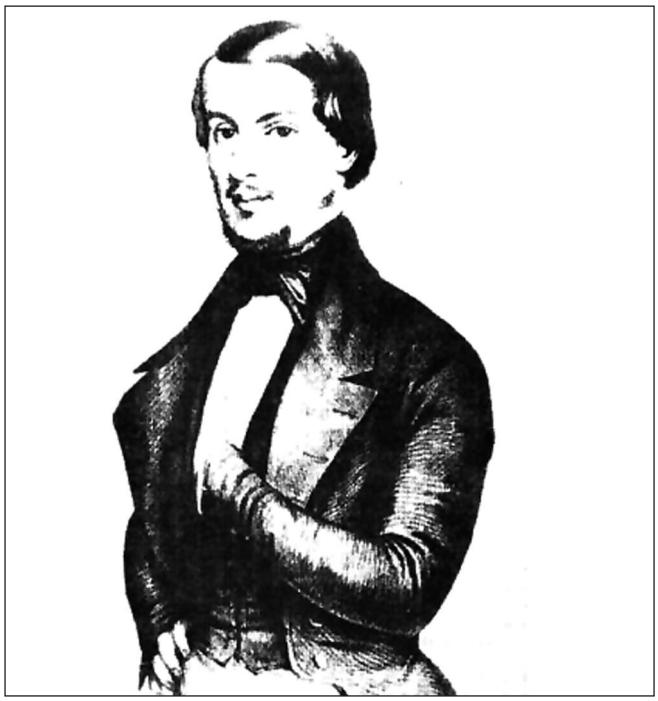

Fig. 15: Ernő Goldfinger

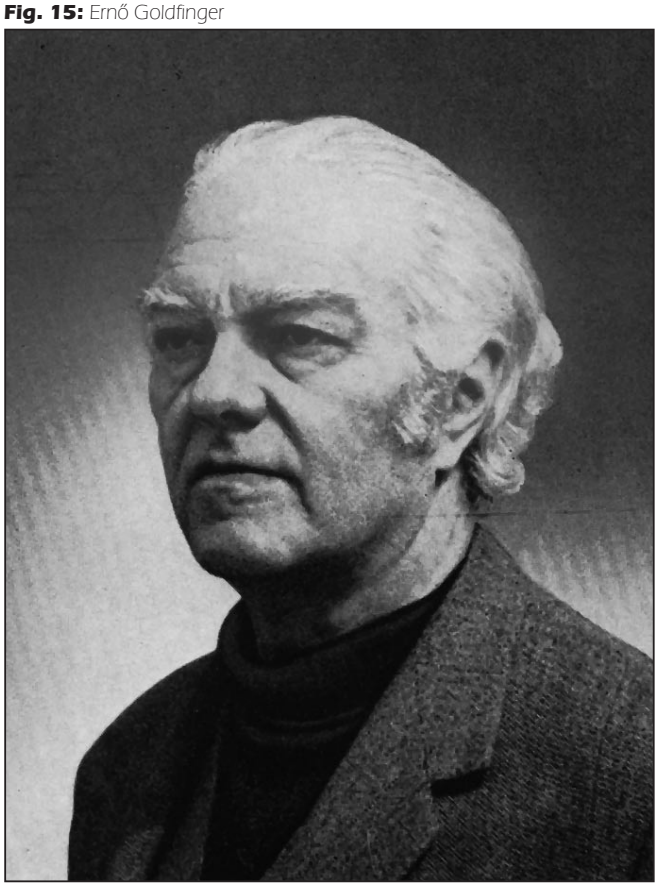

Fig. 16: The Trellick Tower

Danube in 1834. He came together with Széchenyi in the same year in Hungary to assemble the dredger with which it was possible to prepare the riverbed of the Danube for Hungarian navigation.

Adam (Ádám) Clark (Edinburgh 1811 – Buda 1866) *(Fig. 12)* was the leader of the construction works of the Széchenyi Chain Bridge. He was the designer of the tunnel under the Buda Castle Hill. He was appointed by W. T. Clark (no relation) to be the head of contracting of the construction of Chain Bridge in 1839. The laying of the foundation stone took place in 1842 and traffic started on the bridge in November 1849.

The construction of the tunnel under Buda Castle Hill started in 1851. The design was worked out with cooperation of A. Clark with the office of W. T. Clark. The 350 m long tunnel – just along the axis of the Széchenyi Chain Bridge - was completed under the leadership of A. Clark in April 1857 *(Fig. 13)*. Adam Clark continued his activity in Hungary, principally engaging in navigation on the Danube. From 1847 A. Clark was a member of the Hungarian National Transportation Committee. Along side István Széchenyi, he participated as technical adviser in the establishment of the first esplanade square in Pest, the first public fountain, and designed the first water supply system in Buda.

During the fight for freedom 1848-49 the construction work of the Chain Bridge was continued under the leadership of A. Clark. He did his best to hinder the destruction of the bridge by an Austrian general.

A. Clark made his home in Hungary and founded a family there. The square between the Buda abutment of the Chain Bridge and the eastern gate of the tunnel wears the name

Fig. 17: Centre Point

of Ádám Clark. He is buried in the Kerepesi cemetery in Budapest.

4.2 Example of early contribution to the building industry of London initiated by a Hungarian inventor

Walking around in London one can still see today a name posted on scaffolding on renovation or new construction sites: “Szerelmey”. Hungarians recognise this uncommon but nevertheless Hungarian name and so too was it recognised by

a journalist visiting London (Boldizsár, 1965).

Miklós (Nicolas) Szerelmey (Győr, Hungary 1803 - Budapest 1875) *(Fig. 14)* lived a very adventurous life, for a long time in London. Following briefly is a synopsis of his C. V. concentrating principally on his activity in London in the building industry.

Szerelmey was educated at a military technical school in Vienna. He served as an officer of the Austrian-Hungarian army in Italy. In 1830 he was probably the only Hungarian participant of the July 1830 revolution in Paris, and later he was injured in Brussels as a soldier of the Belgian forces fighting for freedom. He then lived in various countries on different continents – including his Hungarian homeland - being active in various fields of trade and art.

In September 1848 he entered the Hungarian army fighting for independence. Szerelmey served as lieutenant colonel of General Klapka. After the fall of Fort Komárom, the collapse of the war for independence, Szerelmey emigrated. He lived in Germany and in France and in 1852 he established himself in London. In Britain Szerelmey continued his work in lithography, publishing his work „Hungary 1848-49". He then turned to his earlier patent for conservation of natural stones (Vajda, 1958). His method was applied at the new Parliament, Saint Paul Cathedral and Bank of England (László, 1975). His „Stone Liquid" survived its inventor and was used for a hundred years in Britain and abroad. The Szerelmey firm exhibited a series of technical construction novelties at the 1862 World Expo in London.

Szerelmey retired in 1874 and returned in poor health to Hungary, where he died in the following year. He is buried in the Budapest Kerepesi cemetery. His name, as mentioned, is still to be seen on many construction works in London.

4.3 Examples from activity of Hungarian born specialists in construction work in London in the 20th century

Ernő Goldfinger (Budapest, 1902 – London, 1987) *(Fig. 15)* was educated in Hungary and from 1921 he studied architecture in Paris. Finishing his course, he designed various buildings along side of his mentor, Auguste Perret (1874-1954), an expert in designing reinforced concrete structures. Perret would later be an inspiration for Goldfinger when designing his own home in 1-3 Willow Road. He designed numerous other interesting single storey residential buildings (Major, 1973).

In the early 1930s Goldfinger moved to London. After the war, he was commissioned to build office buildings. In the 1950s Goldfinger designed two London primary schools from prefabricated concrete.

Among his most notable buildings of the period was the Balfron Tower, a 27 floor building in East London. Another example of his structures is the 31 storey Trellick Tower (North Kensington, *Fig. 16*) built in 1968-72.

Ernő Goldfinger contributed greatly to the activity of different international and British organizations, among them the Union Internationale des Architects and the Royal Academy of Science.

Author[1] was lucky to visit in 1971 the famous architect who contributed so much to concrete construction at his design atelier in the Pall Mall, and in his home in 1975.

Walking along the axis of West End, the eye catches one of London's most famous and best loved building, the Centre Point *(Fig. 17)*.

The building stands 117 m tall, containing 35 floors. Its distinctive concrete pattern makes an instantly recognisable landmark in London. The construction commenced in 1962 and was completed in 1964. The architects were Richard Robin Seifert & Partners.

The building was constructed using prefabricated concrete, H-shaped units. The units were joined to each other and to the concrete floors. The façade becomes the significant feature of this structure. The loads were mainly designed to be carried by two pairs of precast concrete columns in the centre of the building.

Arriving at the London-Hungarian links we reflect on the structural engineer, Dr. Kálmán Hajnal-Kónyi, the consulting structural engineer who contributed much to Centre Point.

K. Hajnal-Kónyi (1898 Budapest – 1973 London) was educated in Hungary. He graduated the Technical University of Budapest. He worked in Hungary and Germany, then he arrived to London where later founded his firm Hajnal & Hajnal.

From among his numerous and various designs, the structural engineering work for Centre Point stands out, e. g. Nr. 5 hangar of Heathrow airport.

There are many other, mainly concrete, structures representing significant designs of K. Hajnal-Kónyi. For example, Author[2] had the opportunity in 1971 to admire his work at Wembley Station in London, which was a relatively early design aimed at the use of the territory above and around the tracks.

K. Hajnal-Kónyi contributed much in developing the theory, materials and technology of reinforced and prestressed concrete. His theoretical and experimental studies were widely published from early 1930's. Here we can only mention some fields which are worked out in his papers:

- Plastic analysis of reinforced concrete members in ultimate state.
- Tests on square twisted steel bars and their application in reinforced concrete.
- Behaviour of steel-concrete composite girders under short time and sustained load.
- Methods for design of statically indeterminate structures.
- Small scale model analysis of engineering structures.

Author[1] was in correspondence with Dr. Hajnal-Kónyi from late 1950s. It was most edifying to meet him during his travel to Budapest, and again in 1971 while visiting him at his London home.

We mentioned here only two examples from among many other Hungarian specialists who contributed to the construction industry in London and to science. There were Hungarian visiting professors and staff members of London universities and colleges who added much value to engineering in the capital of the UK.

There were British architects, structural engineers and firms in the construction industry adding much to the development of design and construction in Hungary, but this paper is limited and so it is impossible to give a complete review of these activities.

5. MUTUAL ACTIVITY IN INTERNATIONAL PROFESSIONAL ASSOCIATIONS

Engineers dealing with concrete have several international associations through which there is opportunity to work together, e. g: IABSE, IUTAM, CIB, RILEM, ISO, IASS and CEB+FIP=*fib*. Here we will concentrate on the latter

federations. The Hungarian engineers interested in concrete construction became aware that an international federation for prestressed concrete had been founded and the first congress of FIP took place in London (1953). Hungary was unable to send delegates there at the time, but the news aroused interest in international works. The possibilities after 1960 improved and in 1962 there was a Hungarian delegation at the FIP Congress in Rome/Naples under the leadership of Prof. L. Palotás and L. Garay (1923-2002) who later served as president of the Hungarian FIP Group from 1970 till 1987. Discussed with colleagues coming from London were held regarding the conditions relating to joining FIP. The procedure lasted a longer time. Meanwhile, the study tour of Author[1] to London gave impulse to the momentum.

Discussions with R. E. Rowe (1929-2008, *Fig. 18*) highlighted the advantages of working in international professional associations, both FIP and CEB (Tassi, 2003, Tassi, Lenkei, 2003). In the following decades Dr. Rowe built up a close friendship with Hungarian colleagues and contributed much to the work of Hungarian engineers over many decades, culminating at the time of his presidency of CEB (1987-1998). To the merit of Dr. Rowe, he was chairman of the session at the VII[th] Congress of FIP where Author[1] presented a paper. Dr. Rowe set the path for us to join a CEB task group at which Author[1] commenced his international scientific activity, leading to his current position of high responsibility. There were many opportunities to work together with colleagues from London. The first significant period of cooperation was during the VIII[th] FIP Congress in London in 1978. Twelve delegates from Hungary attended as well as members of a large group from the Hungarian Scientific Society for Building who visited the exhibition. Eight Hungarian presentations were made at different forums throughout the congress (Tassi 2003).

Fig. 18: R. E. Rowe

In 1981 a FIP Council Meeting was held to which distinguished colleagues came from London: J. Derrington, B. W. Shacklock and W. F. G. Crozier.

There were various meetings of FIP commissions in London, Budapest and other cities where good cooperation developed between concrete engineers of UK and Hungary.

The FIP Symposium 1992 took place in Budapest. During the preparatory period, representatives of FIP headquarters in London visited Hungary. J. W. Dougill provided significant assistance; R. P. Andrew was the chairman of the organising committee. Both displayed their true friendship towards their Hungarian colleagues. D. J. Lee acted as chairman of a session and 12 specialists from UK gave lectures. Ph. Gooding, A. W. Hill, Ch. Spratt and many others from London added greatly to the links forged between London and Hungary.

Another FIP event in London was the symposium in 1996. The Hungarian delegation was comprised of 18 people, some of whom were active at presentations, posters and publications in the Proceedings. This was the first occasion that Author[2] - being at that time the secretary of the Hungarian FIP Group - organized a social event for Hungarian participants in the Sawyers Pub and this meeting enhanced the already very good impression of the London Symposium.

Reflecting on the history of CEB with respect to connections between London and Hungary, we should mention that the outstanding standard bearer of CEB in UK was Andrew Short (1915-1999, *Fig. 19*) whose mother tongue was Hungarian. So, it was unsurprising that we understood each-other well. A. Short was a true representative of the UK together with the international association at all times but particularly from 1971 to 1978, when he was president of CEB. The cooperation between experts of London and Budapest was good. Hungarian specialists paid attention to the CEB Plenary Session London 1973.

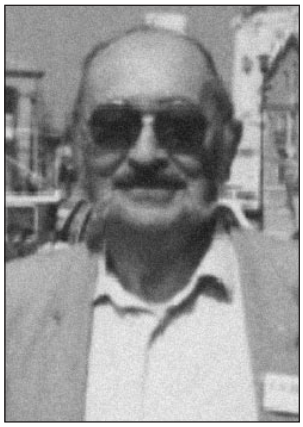

Fig. 19: Andrew Short

The Plenary Session in Budapest 1980 was a successful meeting, and the British delegates added much to the result.

After 1998 the merger of FIP and CEB was realized in the frame of ***fib***. The cooperation between specialists from London and Hungary was continuously good. In this spirit the Hungarian Group of ***fib*** is looking ahead with intense expectation to the ***fib*** Symposium London 2009.

6. CONCLUSIONS

As previously mentioned the occasion of an international meeting is a good time to reflect on the various connections between the participants and the hosts. We hope that these few references will contribute to good impressions of the *fib* 2009 Symposium in London.

7. ACKNOWLEDGEMENTS

Authors express their deep gratitude to Eng. Dr. L. Bajzik who has traditionally contributed to this paper adding very much from his wealth of knowledge in world history. We appreciate the help of Mrs. É. Lublóy PhD, who contributed by completing the data and the figures. Extra thanks are due to Mrs. K. Haworth-Litvai who helped so much in correcting the style and grammar of this paper.

8. REFERENCES

Bajzik, L. (1975): A note from handwritten diary, Kecskemét

Balázs, L. G., Borosnyói, A., Tassi, G, (2005): „Keep Concrete Attractive – towards the *fib* Symposium 2005 Budapest, *Concrete Structures,* p. 2.

Barta, I. (editor) (1953): „*All works of Lajos Kossuth*", Akadémiai Kiadó, Budapest (in Hungarian)

Boldizsár, I. (1965): „*In England with a giraffe"*, Magvető, Budapest, (in Hungarian)

Brown, E. (1673): „*A brief Account of some Travels in Hungaria, Servia*" London.

Cornell, T., Matthews, J. (1982): „*Atlas of the Roman World*", Equinox, Oxford

Feiling, K. (1959): „*A History of England*", Macmillan & Co. Ltd., London.

Gáll, I. (1999): „Construction history of the Széchenyi Chain Bridge", *A Széchenyi Lánchíd és Clark Ádám,* Városháza Publisher, Budapest, pp. 121-154, (in Hungarian)

Hóman, B. Szekfű, Gy. (1936): „*History of Hungary*", (in Hungarian), Királyi Magyar Egyetemi Nyomda, Budapest.

László, M. (1975): „The Hungarian Salvor of Westminster, (in Hungarian). *Múzsák Múzeumi Magazin,* 4.

Lexikon des Mittelalters, (2003) Deutscher Taschenbuchverlag GmbH & KG. München,
Major, M. (1973): „*Ernő Goldfinger*", (in Hungarian) Akadémiai Kiadó, Budapest.
Miklós, I. (1937): „*The Pragmatic History of the Hungarian Railwaymen*", (in Hungarian), Kapisztrán Nyomda, Vác.
Runciman, S. (1995): „*A History of the Crusades*", Cambridge University Press.
Széchenyi, I. (1846): „*Steam Shipping at Lake Balaton*", (in Hungarian), Trattner és Károlyi, Pest.
Tassi, G. (2003): „History of the Hungarian FIP Group from the Beginning to 1998" *Vasbetonépítés*, Special edition.
Tassi, G., Balázs, L. G., Borosnyói, A. (2005): „Benefit of Technical/ Scientific Symposia", *Concrete Structures,* pp. 2-4.
Tassi, G., Lenkei, P. (2003): „Two Antecedents of *fib,* FIP and CEB were founded fifty Years ago", (in Hungarian), *Vasbetonépítés,* pp. 94-97.
Vajda, P. ((1958): "Great Hungarian Inventors", Zrínyi, Budapest, (in Hungarian)

Prof. Géza Tassi (1925), PhD, D.Sc., active (semi retired) in the Department of Structural Engineering of the Civil Engineering Faculty, Budapest University of Technology and Economics. His main fields of interest: Reinforced and prestressed concrete, concrete bridges. He is lifetime honorary president of Hungarian Group of ***fib*** lifetime honorary member of the Hungarian Scientific Society for Building and the Hungarian Chamber of Engineers, FIP Medallist, awarded at the first Congress of ***fib***, holder of Golden Ring and Golden Diploma of the Budapest University of Technology, Palotás László Prize winner (Hungarian Group of ***fib***).

Prof. György L. Balázs (1958), PhD, Dr.-habil, professor in structural engineering, head of Department of Construction Materials an Engineering Geology at the Budapest University of Technology and Economics. His main fields of activities are experimental and analytical investigations as well as modelling reinforced and prestressed concrete, fibre reinforced concrete (FRC), cracking in concrete, durability and fire resistance. he is convenor of ***fib*** Task Groups on "Serviceability Models" and " ***fib*** Seminar". In addition he is a member of several ***fib***, Task Groups or Commissions. He is President of the Hungarian Group of fib. Member of ***fib*** Presidium, deputy president of ***fib***.

THE CABLE-STAYED MEGYERI BRIDGE ON THE DANUBE AT BUDAPEST

Sándor Kisbán

The three span fan-shaped cable-stayed bridge has a symmetric arrangement with a 300 m long middle span and 145 m long side spans. The deck is suspended by two inclined cable planes, each having 44 stay cables, onto two typical, "A"-shaped pylons. The structural depth of the 36.16 m wide orthotropic steel deck is 3.60 m. The height of the prestressed concrete frame pylons is 100 m. A reinforced concrete, box-shaped beam ties the pylon legs at 55.0 m above the top level of the substructure. The pylon legs, which are built in into the substructure, have been built by the use of the climbing formwork technology. The upper triangular part of the pylons bordered by the pylon legs and the horizontal tie beam has been covered by glass walls in order to improve the aesthetical appearance of the pylons.

Keywords: Cable-stayed bridge, steel bridge, bridge construction, concrete frame pylon, climbing formwork technology, free cantilever girder erection

1. INTRODUCTION

The Northern Danube Bridge on the M0 motorway, the Megyeri Bridge, as the longest river bridge in Hungary is situated at the northern border of Budapest, bridging both Danube branches and the southern part of the Szentendre Island. The total length is 1862 m and it consists of five statically independent, consecutive bridge structures. The general description of the whole bridge and its developing process has been published in (Hunyadi,2006).

The span arrangement of the five independent bride structures is the following:

- Flood area bridge on the left river (Pest) side: 37 + 2×33+ 45 m,
- Main bridge over the Wide Danube branch: 145 + 300 + 145 m,
- Flood area bridge on the Szentendre Island: 42 + 11×47 m,
- Bridge over the Szentendre Danube: 94 + 144 + 94 m,
- Flood area bridge on the right river (Buda) side: 43 + 3×44 + 43 m.

In the main Danube branch (Vác side), a three span cable-stayed bridge has been built. River bridge with a cable-stayed main structural system was not built in Hungary so far. The bridge includes two concrete pylons, onto which the steel deck is suspended by two inclined, fan-shaped cable planes at every 12 m. The spans are 145+300+145 m that results in a total length of 590 m. The adjacent structures both on the Pest and Buda sides and above the Szentendrei Island are continuous, post-tensioned concrete bridges with box-girder superstructures.

The M0 highway running through this bridge includes 2×2 traffic lanes with hard shoulders. The hard shoulders are wider than specified giving the possibility to extend the carriageway width up to 2×3 traffic lanes without any structural modification if the future traffic expansion makes it necessary. On the northern side of the bridge a cycle track, which is able also for disabled traffic, on the southern side a footway is added. An asphalt-based surface pavement is laid on the carriageway while the footway and the cycle track are covered by a multilayer, abrasion-resistant, roughened, chloride resisting system. The bridge is equipped by public lighting as well as by ship- and air-traffic navigational signals.

2. FOUNDATION

For the internal bed piers, hydrodynamic flow tests and scouring analyses have been carried out. These simulation tests did not show significant modification in the river flow due to the hydraulically designed piers so their favourable shape could be justified. The bed piers do not adversely affect the safety of the river navigation as well as the stability of the bed and the bank of the river.

The foundation of both the bed and the side piers has been made of large diameter, reinforced concrete bored piles. The piles of all the four piers are bored into the excellent load bearing capacity subsoil, the Oligocene aged, grey marl containing, lean and fair clay. The strength class of concrete was C20/25 for the piles and their pile caps, C30/37 for the solid pier shafts and C35/45 for the load-distributing structural crossbeams at the top of the piers.

The side joint piers, which also support the adjacent bridges, are supported by 16-16 piles. The diameter of the 19.0 m long piles is 1.5 m. The horizontal sizes of the reinforced concrete pile caps are 7.5 m in the longitudinal direction of the bridge and 49.4 m perpendicular to this direction while their depth is 2.0 m. The side face of the pier shafts along the full perimeter has an inclination of 1:20 to the vertical plane. The cross section of the pier shafts has been designed with ogival ends protected by granite nose blocks. The lower 5.5 m high parts of the pier shafts have a thickness of 6.76-6.21 m and a width of 48.36-47.40 m. The upper 7.0 m high parts have a constant thickness of 4.60 m with a variable width between 40.20 m and 36.90 m. The vertical support and the anchorage of the superstructure are realized at the top of the pier shafts, on the load-distributing structural crossbeams. The vertical downward reaction forces transmitted by the bearings are received by two reinforced concrete blocks arranged with 28.83 m centre distance on each pier while the anchorage of the superstructure

Fig. 1: *Positioning of the crib-wall element for the bed pier*

is ensured by other two anchorage points installed with 24.03 m centre distance between the supporting points. The lateral supports of the superstructure on the side piers are positioned to the longitudinal axis of the bridge.

The substructures of the bed piers have been built by the reinforced concrete crib-wall technique *(Fig. 1)*, which was successfully applied for river bridge foundations many times in the past. Due to the big geometrical sizes of the substructures 3-3 crib-wall elements were placed and fixed onto each other to enclose the necessary working space. Onto the top of the upper crib-walls, 5.0 m high, removable steel cutoff walls were fixed whose top level reached the 101.5 m above see level, by which, taking into account 0.5 m high waves, the dry working space could be ensured for water levels up to 101.0 m above see level. Finally, the crib-wall elements together with their inside strutting system were filled with concrete using the outer wall as a formwork.

The bed piers are supported by 46-46 reinforced concrete bored piles. The diameter of the 19.5-20.5 m long piles is 1.5 m. The horizontal sizes of the reinforced concrete pile caps are 16.5 m in the longitudinal direction of the bridge and 70.0 m perpendicular to this direction while their height is 4.5 m including the lower shaft part cast under water. The top level of the pile caps coincide with that of the upper crib-wall elements at 96.5 m above see level. The side face of the pier shafts along the full perimeter has an inclination of 1:20 to the vertical plane. The cross section of the pier shafts has been designed similarly to the side piers, applying ogival ends protected by granite nose blocks against abrasion effects due to floating debris and ice drift. The thickness and the width of the pier shafts varies between 8.0-7.0 m and 64.90-63.16 m respectively while their height is equal to 10.2 m. The pylon legs are fixed into the upper pier shaft parts designed and arranged as load distributing crossbeams. The top surface of these crossbeams has been designed with symmetric, 5% transversal slope for water draining reasons.

3. PYLON

A cable-stayed river bride, the Rheinbrücke Düsseldorf-Flehe (Schambeck et al.,1979) in Germany has been built by the application of inclined pylon legs. The experiences gained from its construction were helpful during the execution of the Megyeri Bridge.

The two pylons of the Megyeri Bridge are "A"-shaped frame structures consisting of partially prestressed, reinforced concrete pylon legs having rectangular, box-shaped cross sections *(Fig. 2)*. Their height is 100 m above the substructures while the outer horizontal distance between the pylon legs at the bottom is 51.0 m. The outer cross sectional sizes of the pylon legs parabolically decrease from 5.0×4.0 m to 3.5×4.0

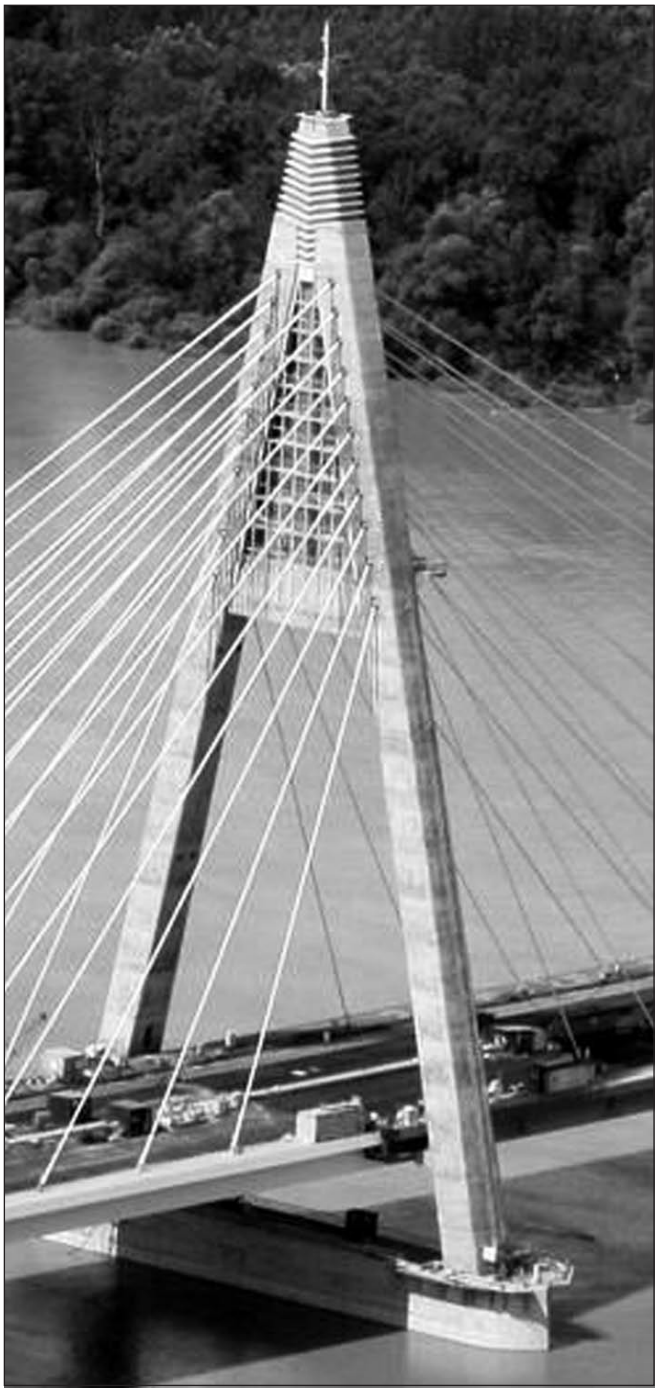

Fig. 2: *The "A"-shaped pylon*

m parallel to the wall thickness decrease from 1.0 m to 0.5 m. The corner edges of the pylon legs are circularly curved along a 300 mm radius in order to reduce the wind turbulence effects. The applied concrete strength class was C40/50.

The bending moments arising in the plane of the pylon frame due to the self-weight of the whole bridge and the internal stay cable force system are eliminated by bonded internal prestressing . For this purpose, prestressing tendon bars having a diameter of 40 mm and a characteristic tensile strength of 1030 N/mm^2 run in the outer walls of the pylon legs. A reinforced concrete, box-shaped beam ties the pylon legs at 55.0 m above the substructure.

The steel units as the upper anchorages for the stay cables are arranged in the upper triangular part of the pylons, above these tie beams. These anchorage units were positioned and fixed simultaneously with the concreting of the anchorage chamber floors. The vertical components of the anchorage forces are transmitted directly to the 0.6 m thick walls of the pylon legs while the horizontal components coming from the two sides are mostly balanced in these steel anchorage units. The anchorage units contain steel shear bolts at their bottom face that are fully embedded in the concrete of the chamber floors and intended to transmit the unbalanced horizontal components of cable forces during the construction stages and the cable replacement phases in the final stage of the bridge.

The inside arrangement of the pylon legs has been arranged according to the requests of the investor. The northern legs contain inner stairs from the bottom up to the lowest stay cable anchorage level while the southern legs are equipped by inner industrial lifts. Vertical panorama lifts starting from the tie beams ensure the accessibility of all structural elements up to the pylon heads. The pylon leg sections, which are equipped by lifts, may alternatively be accessed by inner ladders. The upper triangular space bordered by the pylon legs and the tie beam is covered by glass walls assembled to steel wall columns in order to improve the aesthetical appearance of the bridge.

The steel deck is supported between the pylon legs. The supporting structural elements are the 1.35 m high reinforced concrete corbels projecting out from the pylon legs at 9.0 m above the substructure, to which the reaction forces of the steel deck are transmitted by steel cantilevers as part of the deck itself. The horizontal supports of the deck are arranged also on these corbels using hydraulic devices. These devices behave as rigid supports against the short-term effects such as braking and acceleration forces, wind and earthquake effects but mobilize negligible horizontal reaction forces for the long-term effects such as thermal, creep and shrinkage effects, settlements (Kisbán,2008). During the execution stages the hydraulic devices were substituted by supporting elements fixed by pins to the substructure.

Fig. 3: *Pylon construction using the climbing formwork technique*

The pylon legs have been erected by the climbing formwork technique generally using 4.07 m high units. At the connecting structural elements (supporting corbels, tie beam, stay cable anchorages, pylon head, etc.) additional construction joints had to be arranged. In order to decrease the bending moments in the plane of the pylons due to the long and inclined pylon leg cantilevers during construction, steel auxiliary beams as temporary struts have been installed at 32.0 m and 52.0 m above the substructure. The upper auxiliary beams also supported the formwork of the tie beam.

In accordance with the sequence of the deck assembly, the floors, the vertical elevator shafts and the glass wall covers of the upper triangular parts of the pylons have been built after the vertical and transversal fixing of the deck to its temporary

Fig. 4: *Parallel construction of the pylons and the deck*

supports in the side spans. This was necessary in order to reduce the wind effects on the pylon during these construction phases. The wind analysis of the cable-stayed bridge has been elaborated by I. Kovács (Kovács,2004); the wind tunnel measurements necessary to determine the wind actions on the bridge have been carried out in Aachen (Schwarzkopf,2003).

4. DECK

The deck is a site assembled, welded steel structure having an orthotropic top slab. It has an open cross section together with longitudinal box-shaped side girders due to the two-plane suspension. The distance between the stay cable anchorages measured perpendicular to the longitudinal axis at the top level of the deck is 29.8 m. The carriageways of the two traffic directions are separated by reinforced concrete kerbs and steel safety barriers along the longitudinal axis of the deck. The total width is 36.83 m, the structural depth is 3.63 m. The footway and the cycle track are supported by steel cantilevers fixed to the outer face of the side box girders. The total plan area of the deck is 21,700 m^2. The necessary amount of steel was 8455 t whose strength class was S355 according to the MSZ EN 10025 for the main load bearing structural elements and S235 for the secondary elements.

The deck has been built according to the free cantilever method. In the first step auxiliary, starter assembly scaffolding units had been positioned and fixed to the pylons that were able to support 50 m long parts of the deck in the longitudinal direction. Then the next 12.0 m long and 160 t assembly units were fitted and welded to the starter units while the balance between the cantilevers was strictly fulfilled. Immediately after the welding process of the assembly units had finished, the units were suspended by a pair of stay cables onto the pylon *(Fig. 4)* (Kisbán,2008).

In the side spans, at 60.0 m from the pylons, temporary supports have been installed to ensure the stability of the structure under construction. Thanks to these temporary supports, the internal forces occurring in the construction stages did not exceed the corresponding values in the final stages of the bridge. Thus, the application of these temporary supports made the applied construction process more economic.

The last bed-side unit before the closing unit has been assembled by the use of ballast. The self-weight of the 145 m long bed-side cantilever was insufficient to apply the calculated tensioning force in the connecting stay-cables. The application of ballast made possible that these stay-cables in this temporary construction phase could be stressed by the specified minimum of 20 kN/strand tensioning force.

Before the closing unit was lifted into its final position the ballast loads had been slightly moved in order to get the specified vertical layout of the deck. The distance between the two cantilever ends, which was required to lift the closing unit in between, was produced by shifting the Pest side half bridge by hydraulic jacks along the longitudinal axis of the bridge. Before this operation the fixed supporting elements had been replaced by the final hydraulic supports. After the lifting operation had finished the gap between the closing unit and the cantilever ends, which corresponded to the specified weld size, was adjusted similarly by moving the Pest side half bridge in the opposite direction *(Fig. 5)*.

5. STAY CABLES

The deck is suspended to the pylons by 4×11 stay cables per each cable plane that means a total of 88 stay cables for the whole bridge. The stay cables are bundled from usual 7 wire strands led parallel to the cable axis. The applied strands have a cross sectional area of 150 mm^2 and a characteristic tensile strength of 1860 N/mm^2. Four cable types have been used that consisted of 31, 37, 55 or 61 strands. Their anchorages can be found in the deck and in the pylons.

The cables have been stressed at the deck anchorage points from the inside of the side box girders. During this process each strand has been stressed one by one using the so called "isotension" procedure, which ensured the specified cable force immediately after the stressing process. As a consequence of the above one by one tensioning procedure, stressing of each strand in the cable influences the stress in all previously stressed (and anchored) strands. According to the "isotension" stressing procedure, the stress to be applied to the current strand is determined on the basis of the changes in the stress of the first stressed (so called leader) strand. After stressing the last strand in the cable, this "isotension" procedure results in the same stress in all stands of the cable. The upper anchorage devices in the pylons also contain a rotatable nut, by which the cable force may be adjusted during the service life of the bridge in order to eliminate the long-term effects on the cable forces. Such effects develop especially for the pylons due to the creep and the shrinkage of concrete that results in a change in the distance between the upper and the lower anchorage points of the cables *(Fig. 6)*.

The vibration of cables is controlled by damping devices fitted into the tube against vandalism at 0.85 m above the footway level for all cables. These devices absorb the kinetic energy coming from the cable vibration under service loads in mechanic and hydraulic manner. According to the vibration analyses, not negligible cable vibration can only be expected from the combined wind and rainfall-induced galopping excitation. This is the most frequently observed vibration effect for straight cables of bridges. This self-exciting process can be originated from the changing cross-sectional shape of the cable due to the rainwater flowing around its outer surface. For particular wind velocities and directions, the wind pressure holds the water back from flowing toward the bottom edge of the cable. Due to this, a thin, bulging water stream occurs around the top edge of the cable that – together with the always present bottom water stream – forms a galopping vibration-sensitive, changed cross-sectional shape (Kovács,2004), (Kisbán,2008). The risk of this vibration effect may considerably by decreased by the use of special plastic sheaths ribbed with double helix-shaped ribs on the outer surface. For the Northern Danube Bridge these plastic sheaths are provided by similar shaped ribbing, having a cross section of 1.6×3.0 mm and a pitch of 600 mm.

The adjustment of cable forces was based on the geometrical shape measurements made on the pylons and the unloaded deck being in its final position and as well as the corresponding cable force values. According to the measurement data only small increases and no decrease in the cable forces was necessary. The cable length changes longer than 45 mm were made by applying additional stress in each strand of the cable at the lower (deck) anchorage. The smaller (20-30 mm) length changes were applied by rotating the adjustable nut on the upper anchorage in the pylon and, by doing so, stressing the whole cable in one step.

The free cantilevers of the deck have been assembled under continuous geodetic control made by two independent measuring groups. The measurements have been made early mornings in order to eliminate both the uniform and especially the uneven temperature effects. The deformation of the pylons due to the uneven temperature effects modified the deck shape through the stay cables as an addition to its temperature-change-induced self deformation. In daytime the vertical movement of the cantilever ends fell in between 40 and 80 mm; the vertical movement difference between the two sides of the deck due to the rotation around its longitudinal axis remained between 15 and 20 mm.

The cable replacement is possible if this is deemed necessary for any reason. In these situations the closure of the side traffic

Fig. 5: *Positioning the closing unit of the deck*

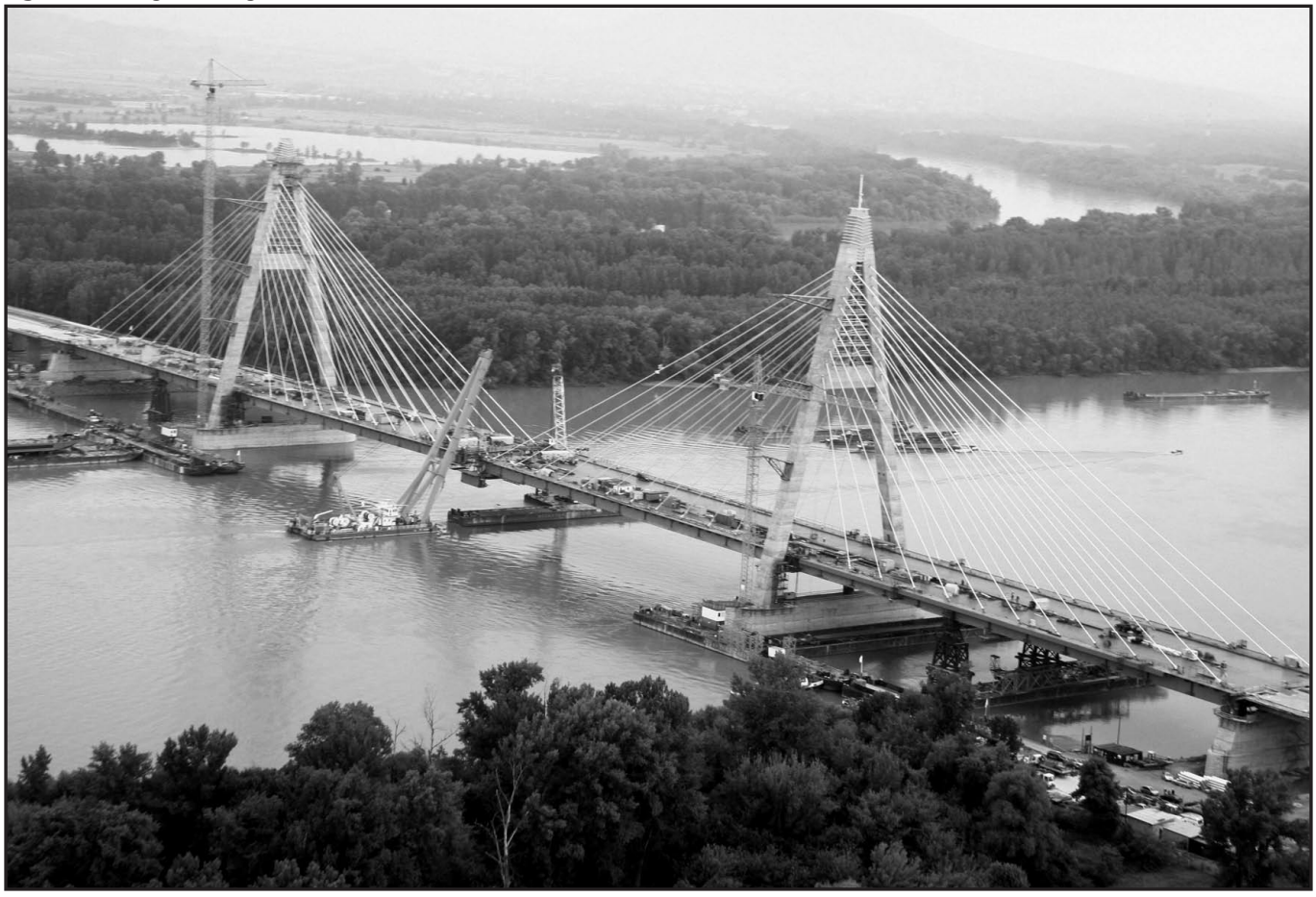

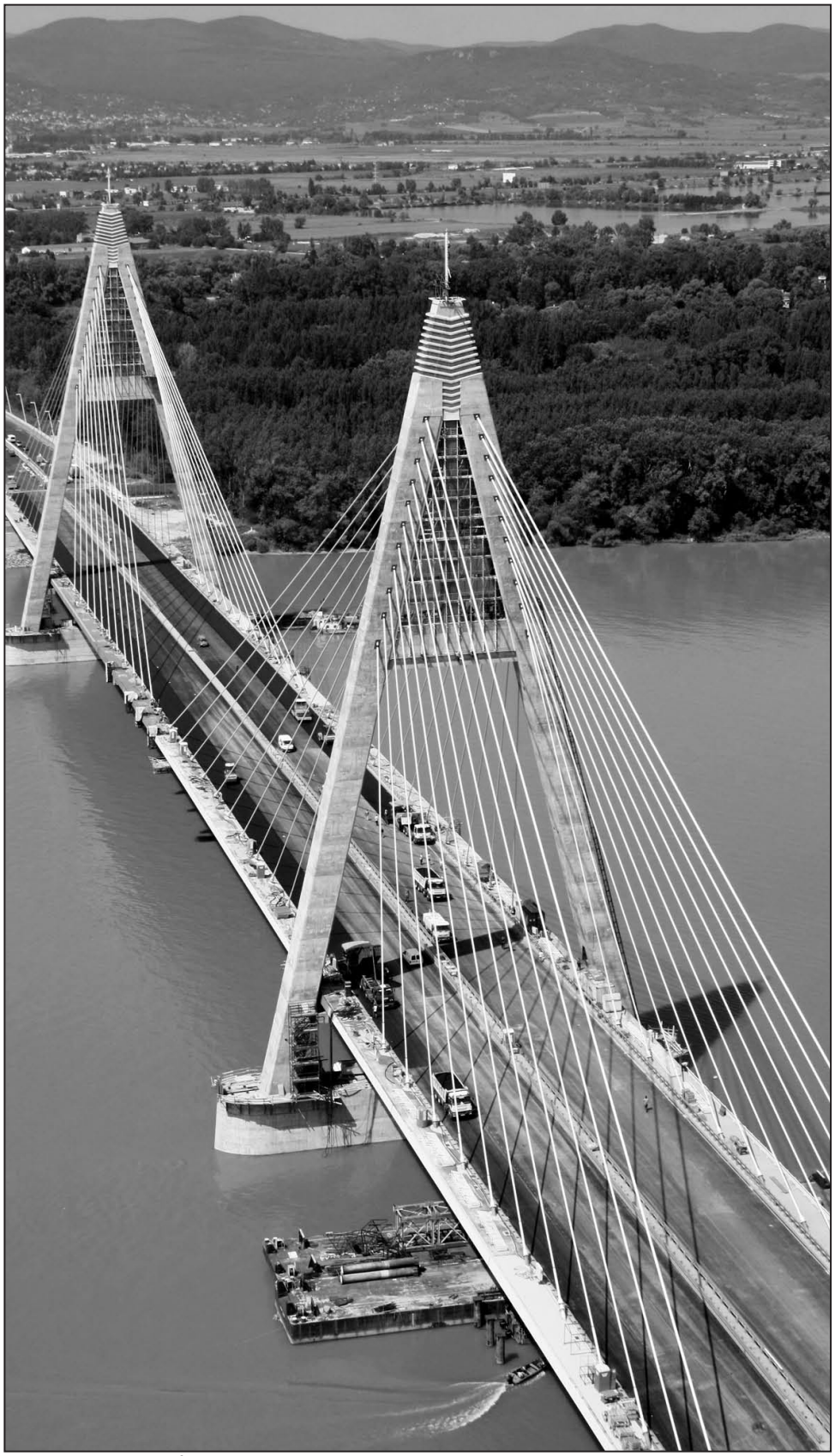

Fig. 6: Arrangement of stay-cables

lane is enough for the simple and safe field working activities, other traffic restrictions are not necessary. The earthquake resistant design of the cable-stayed bridge has been elaborated by Céh Co. with special regards to the behaviour of stay cables. The design was controlled by the Budapest University of Technology (Vigh, Dunai, Kollár, 2006).

6. CONCLUSIONS

6. 1 Environmental and aesthetical considerations

The environmental protection has been a privileged aspect during the full design and construction process. The left bank flood area and the Szentendre Island providing the water supply of the capital are exceptionally protected areas. Therefore, no exit from the bridge to the Szentendre Island has been built and, additionally, noise barriers have been installed on both sides of the bridge above the island in order to protect the existing fauna and the environment of the island. The rainwater is collected and canalled from the bridge in a closed drainage system and transferred into the recipient only after treatment.

The structurally determinant and aesthetically spectacular parts of the cable-stayed bridge over the Wide Danube are the pylons. Due to its harmonic aesthetical appearance, the whole bridge appropriately fits into the variety of bridges of Budapest improving the aesthetical value and increasing the number of the symbols and spectacles of the capital.

6.2 Design and construction

The realization of The Northern Danube Bridge on the M0 motorway has been carried out by The M0 Consortium for The Northern Danube Bridge established by the Hídépítő Co. and the Strabag Co.. The general designer has been the Céh Co.; the construction design has been carried out by the Unitef-Céh Engineering UP. as a contractor of the Consortium. The execution started in 2006, then completely finished and opened for the traffic in September, 2008.

The execution of the substructures and the full piers has been made by the Hídépítő Co. The climbing formworks of the pylons and the associated technological work have been made by the Peri Ltd. The construction period of one bed pier was six months and that for the associated pylon lasted 11 months. The total height of the pylons, measured from the bottom end of the piles up to the top of the pylon heads, is 132 m, out of which the height of the “A”-shaped part of the pylons is 100 m.

The manufacturing and the on-site assembly of the bridge

deck has been made by the Ganz Co. The Pannon Freyssinnet Ltd. supplied and on-site installed the stay cables. The HSP Ltd. carried out the navigation work and the Hídtechnika Ltd. conducted the corrosion protection work.

7. REFERENCES

Hunyadi, M.: The Northern Danube Bridge on the M0 motorway, *Mérnök Újság XIII*. (2006) 2. pp. 4-6. (in Hungarian)

Kisbán, S.: The M0 Northern Danube Bridge. Cable-stayed Bridge in Budapest. *Magyar Tudomány* 2008/4 (in Hungarian)

Kisbán, S.: Free Cantilever Erection of the Cable-stayed Bridge. *The M0 Northern Danube Bridge, Steel Structures*. MAGÉSZ October, 2008. (in Hungarian)

Kovács, I.: The Northern Danube Bridge on the M0 motorway in Hungary. Wind dynamic investigation. Final Report. *Dynamic Consulting.* Weinstadt, Januar 2004. (in Hungarian)

Schambeck, H., Foerst, H., Honnefelder, N.: Rheinbrücke Düsseldorf-Flehe/Neuss-Uedesheim. Der Betonpylon. *Bauingenieur* 54 (1979) 111-117.

Schwarzkopf, D.:Donau Schraegseilbrücke Nord, M0 Autobahnring um Budapest. Windkanaluntersuchung. *Prof. Sedlacek & Partner,* Aachen, September 2003. (in German)

Vigh, L., Dunai, L., Kollár, L.: Experiences on the Earthquake Resistant Design of Two Danube Bridge. *IABSE Symposium,* Budapest, Hungary, 2006.

Dr. Sándor Kisbán (1949) civil engineer (BME, 1973) leading engineer at the Céh Co., managing director of the Céh-Híd Ltd.

His bridge designer carrier started at the Uvaterv in 1975 where he was involved in designing long-span steel bridges (Northern Tisza Bridge at Szeged, highway bridge at Tiszapalkonya, cable-stayed bridge over the Danube in Novi Sad). He received his Dr. techn. degree in the field of cable-stayed bridges in 1986 (Department of Steel Structures, BME)

From 2002 he has been carrying his activity as a leading bridge designer in the Céh Co. where he has completed and managed the design of many domestic river and motorway bridges (M0, M31, M6 motorway bridges and viaducts, M0 Northern Danube Bridge). Member of the Hungarian group of *fib*.

PRESTRESSED CONCRETE FLOOD AREA BRIDGES ON THE NORTHERN DANUBE BRIDGE ON THE M0 RING



Pál Pusztai Ádám Skultéty

The article gives a summary on the prestressed concrete box-girder bridges spanning flood area of the river. The substructures including the abutments and the piers as well as the building technological issues, the auxiliary construction work and the course of the execution will be presented. Information on the applied prestressing system, its consequences in the structural calculation and the consideration of the relevant transient and persistent design situations corresponding to the construction and the final stages of the bridges will be detailed. The special, individually-designed bridge accessories will also be introduced.

Keywords: incremental launching construction technology, post-tensioning, site execution

1. INTRODUCTION

The 1862 meters long Northern Danube bridge on the M0 ring contains five consequetive, different bridge structures. The subject of this article is the presentation of the in-situ cast flood area bridges including both the substructures and the prestressed concrete box-girder-type superstructures. The bridges have been executed by the incremental launching construction technology where the construction units have been prefabricated in a casting yard.

2. GENERAL TECHNICAL DATA

Travelling along the whole bridge from the Pest side towards the Buda side of the Danube, the following flood area bridges are crossed: the left-bank flood area bridge, the flood area bridge over the Szentendre Island, and the right-bank flood area bridge.

The two traffic directions are carried by two, structurally independent superstructures separated by an air gap. These decks have the same structural form and carry the same carriageway. Their total width is equal to 34.60 m and their structural height is equal to 3.29 m. Each carriageway includes two traffic lanes and a side emergency lane. The outer side of the decks is equipped by appropriate lanes for the pedestrian as well as the cycle traffic.

3. SUBSTRUCTURES

3.1 End abutments

The ends of the right-bank and the left-bank flood area bridges are supported by abutments standing behind the embankments. Because the top level of the embankments are situated at a relatively high level above the Danube river, at the left bank a three-storey-high and at the right bank a two-storey-high abutment have been designed, each of them are internally accessible and have a plan area of 44×9 m. The stories contain the necessary rooms for the bridge operation: converter, electric distributor and switch-room, telecommunication room and storage rooms. Additionally, the left-bank abutment includes the bridge caretaker office equipped with a dressing room, a shower and a lavatory. The interior of the decks is accessible through the abutments.

According to the applied incremental launching construction technology for the superstructures, the abutments were built in two phases. In the first phase they were completed up to the top level of the abutment cup, together with the belonging bearing seats. Simultaneously with that, the tie beams foundations of the casting yards installed behind the abutments and their connection to the abutments were built. These connections, which have a favourable effect on the static equilibrium of the abutments by anchoring them back to the soil, remained active after the construction phases. The columns of the provisional

Table 1: Data of the bridges

Name of the structure	Support assignment, m	Length, m
Left-bank flood area bridge	37.15 + 2 x 33.00 + 44.00	149.55
Flood area bridge over the Szentendre Island	41.00 + 10 x 47.00 + 46.25	560.25
Right-bank flood area bridge	39.86 + 3 x 44.00 + 43.50	217.00

launching support were built onto the pile caps and fixed to the front walls by stressing bars. The second phase containing the upstand walls and the back-walls was completed after the launching process of the superstructures.

3.2 Internal piers

The internal piers for the left- and the right-bank flood area bridges have been designed by the Nefer Ltd. managed by Ferenc Németh, and those for the flood area bridge over the Szentendrei Island have been completed by the Speciálterv Ltd.

The foundation of each internal pier includes six bored piles in two rows, each having a diameter of 1.20 m. The length of the pile cap beams in the longitudinal direction of the bridge is 6.0 m and their width in the transversal direction is 9.60 m. Each pier has a solid shaft. When sizing the structural beams, the necessary place for the applied technological auxiliary equipments was also considered.

3.3 Common piers

The end supports No. 5 and 8 of the bridge above the main Danube branch and the end support No. 20 and 23 of the Bridge above the Szentendre-Danube branch have been given the name of common piers, since at these points the ends of two, structurally independent superstructures are supported by a common substructure. Their foundation includes bored piles with a diameter of 1.50 m. The outer surface of the piers is covered by claddings.

4. SUPERSTRUCTURES

The prestressed concrete box-girder-type superstructures were executed in a technically similar way by the incremental launching construction technology. Due to the eccentricity of the box girder to the longitudinal bridge axis and the transition in the transversal slope *(Fig. 1)* for the right-bank flood area bridge the lengths and the height of the clamping sections of side cantilevers differ from those for the other two bridges .

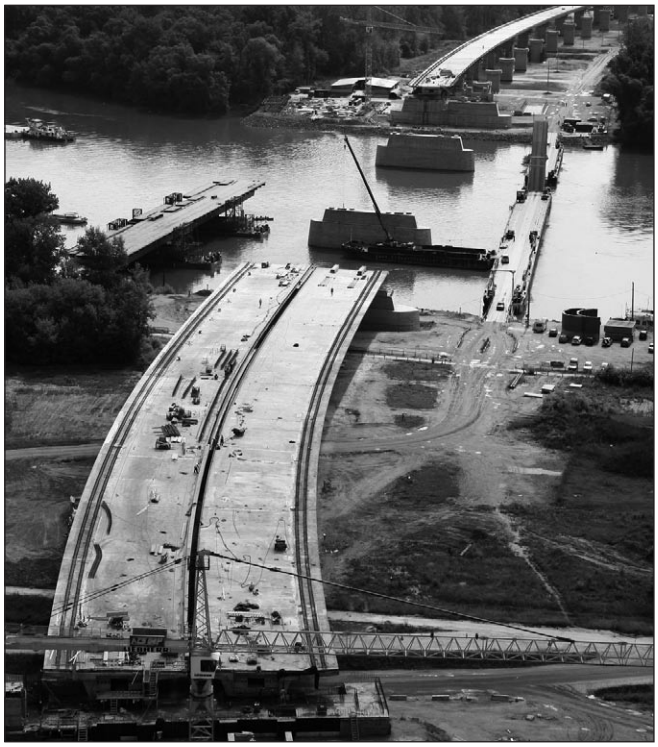

Fig. 1: Right-bank flood area bridge

4.1 Cross-sectional arrangement

The cross-section of the superstructures was formed to fit to the launching technology. The undersides of decks are horizontal in the transversal direction and the top levels are formed with a transversal slope of 2.5%. The total height is 3.00 m measured at the axis of the deck.

Each box is 7.00 m wide at the bottom. The outwardly inclined webs have a thickness of 0.50 m.The deck slab is 0.3 m thick in the middle that is increased up to 0.6 m toward the webs. The total width of the deck slab including the side cantilevers is 16.21 m. The height of cantilevers varies from 0.55 m to 0.25 m. The total area of the concrete cross-section is 10.64 m^2.

Due to the transition in the elevation and the radius

Fig. 2: Cross-section of the right bank flood-area bridge

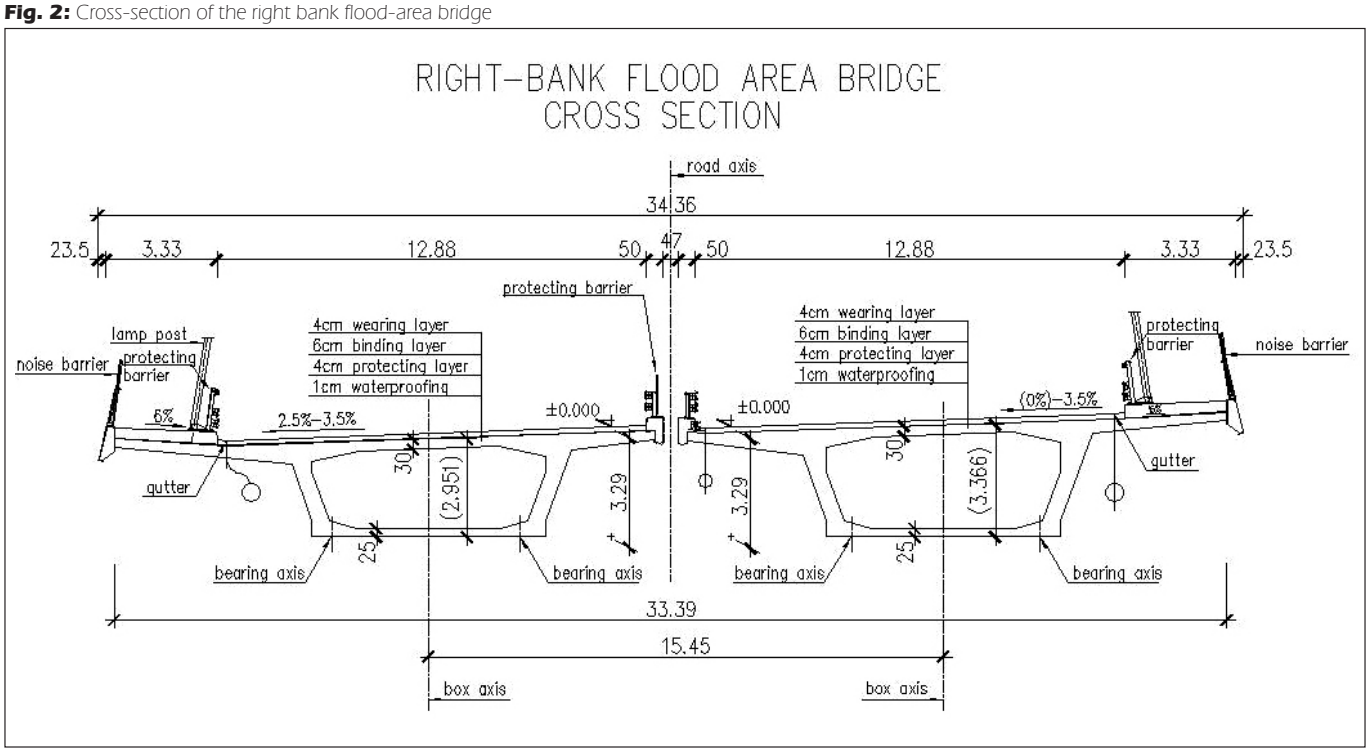

Fig. 3: Cross-section of the construction unit (photo by: György Nyírő)

Fig. 4: Steel launching nose (photo by: György Nyírő)

correction of the launching curve, the cantilever lengths change along the decks in the right-bank flood area bridge. Although the elevation change results in a change in the transversal slope of the deck slab, the level of the bottom slab remains unchanged. As a consequence of this, the structural height in the deck axis grows from 3.00 m to 3.36 m between the abutment and the section of maximum height *(Fig. 2)*.

4.2 Construction technology

The deck was concreted on fix scaffolding then launched longitudinally into its final position. The deck units, which are relatively short compared to the full length of the bridge, called ICL-sections, had been prefabricated in the casting yard. After concrete hardening each unit was post-tensioned to the previously completed unit and then moved forward from the casting yard. The unit lengths vary depending on the span-lengths; they are generally equal to the half of the corresponding span. The longest unit has a length of 23.50 m *(Fig. 3)*.

The manufacturing of ICL-sections including the placing of reinforcement, concreting, prestressing and launching was based on one week cycles. To reduce the cantilever moments in the deck during the launching phases, a 32 m long steel auxiliary launching nose had been fixed to the end of the deck *(Fig. 4)*.

The launching process was conducted on temporary supports placed on the substructures; the continuous side guiding was assured by temporary horizontal supports fixed to the piers.

4.3 Post-tensioning cables

4.3.1 CONSTRUCTION STAGES

In order to provide sufficient bending resistance and appropriate stress limitation in the deck during the launching process bonded prestressing cables were applied.

The bottom and the deck slab cables that are laid along straight lines, connect two ICL-sections. Each cable consists of 0,6”diameter, Fp150/1770-type, 150 mm^2 cross sectional area strands; the number of strands is 12 for the the cables being in the cantilevers and 15 for those in the bottom and the deck slab. The necessary ducts had been previously fixed into the reinforcement cage.

Fig. 5: Casting yard between the piers No. 19 and 20

In a general section of the deck, the applied 18 cables transmit approximately 45000 kN prestressing force to the cross section. These cables are anchored in anchoring beams designed at the ends of the ICL-sections. The cables were stressed from one end in accordance with the stressing instructions.

4.3.2 FINAL STAGE

To carry the live loads in service, external, unbonded Vorspann-type cables were built-in and laid in the interior of the box. Their structurally necessary vertical layout is assured by steel deviators, which are placed below the deck slab at the supports and above the bottom slab in the spans. The length of cables are equal to the full bridge length for both the left-bank and the right-bank bridge. To reduce the frictional loss these cables had been divided into several parts for the bridge above the Szentendre-Island. Each cable contains 16 pieces of 0,6” diameter, Fp150/1860-type 150 mm^2 cross sectional area strands. The total length of the longest cable was 249 m while its total elongation obtained as 1632 mm during stressing it simultaneously from both sides.

4.4 Manufacturing

Considering the local circumstances and the organization plans the casting yard had been installed behind the abutment for the left-bank and the right-bank bridge and between the abutment and the first pier for the bridge above the Szentendre-Island. Their foundation system were rigid tie beams supported by piles. The stiffened formwork panels could be adjusted by threaded supporting bars. The inclination of the webs and the bottom levels of the cantilevers were the same along the whole bridge. The manufacturing process was strictly scheduled into 7-day cycles *(Fig. 5)*.

The completed ICL-sections were launched from the casting yard by lifting and pushing synchronized hydraulic jacks. One pushing jack per web placed in the abutment was applied for the left-bank and the right-bank but for the bridge above the Szentendre Island one jack per web placed at both the abutment and the first pier (four jacks) was required (Fig. 6).

4.5 Structural analysis

The structural analysis of the superstructure can be divided into four parts:

- longitudinal analysis of the deck in construction stages,
- longitudinal analysis of the deck in the final stage,
- analysis of the deck in the transverse direction,
- other additional analyses.

The main girder was analyzed by help of the TDV software using a 3D beam model. This finite element program, specially

Fig. 6: Left-bank flood area bridge

developed for bridge analyses, covered the modelling issues of the following:
- modelling the incremental launching process,
- function approximation of cross sectional properties of elements with varying cross-section,
- geometric definition of prestressing cables,
- stressing of cables according to a given technology,
- calculation of losses of prestress,
- calculation of creep and shrinkage effects according to the Technical Guidance ÚT 2-3.414,
- automatic definition of load cases and combination of actions.

The ability to consider changing cross-sections for the right-bank bridge proved to be very helpful, as here the cross-sectional parameters changed along the whole bridge length due to the changing transversal slope and the applied equivalent launching curve.

For the analysis of the deck slab in the transversal direction, the anchorage zones of the prestressing cables and the deviation zones of the external cables the AxisVM finite element program software was used.

As a consequence of the applied construction technology, the length of the bridge had to be permanently checked. The shortening of the deck from the prestress and the creep effects were followed by in-situ bridge length measurements conducted on each construction unit during the whole execution process.

5. BRIDGE ACCESSORIES

5.1 Curb

Based upon aesthetical considerations, a unique external steel kerb was built along the whole length of the bridge. The part connecting to the edge of the footway was made of steel. The inclination of its outer surface is in full harmony with the inclination of the pylon legs of the cable-stayed bridge above the Main-Danube branch. To the steel decks the curb was fixed by welding, and to the concrete decks it was fixed by using welded steel hooks and additional reinforcing bars. As the inner stress produced by temperature change is radically different between the concrete deck and the significantly thinner steel curb longitudinal and transversal steel stiffeners were applied on the inner side of the steel curbs. The main electric cable and the necessary transformer units as parts of the floodlight system of the curb were fixed to these stiffeners.

5.2 Pedestrain railing

The individually formed, steel pedestrian railing connects to the top level of the steel curb by crews. Its inclination is in accordance with that for the pylons and the outer surface of the curb. The full railing, with the exception of the hand-rail tube, is made of steel profiles. The railing bars run horizontally. The 8 m long assembly units connect with each other by bolts that does not restrain the dilatation movements. Due to its duplex-coated (hot-dip galvanized and painted) surface the joints of the assembly units had to be prepared accordingly by screws without any in-situ welding.

A 2 m high noise barrier designed and manufactured according to a high standard has been fixed to the pedestrian railing on the bridge above the Szentendre-Island and the right-bank flood area bridge.

5.3 Public lighting

The public lighting of the bridge is supplied by 12 m high lamp posts, one per every 24 m on average. Their inclination corresponds to that of the pylons. The individually designed lamp posts have a solid cross section along the bottom 3 m that changes into a built-up section. The upper 180/80 steel hollow section surrounds the lighting unit as a frame.

6. SUMMARY

The bridges were built by Hídépítő Inc. Thanks to the strict time scheduling and the controlled technological processes, the manufacturing of the ICL-sections was conducted within 7-day cycles. The completed bridge became the longest highway bridge built by incremental launching technology in Hungary. A total of 20,000 m^3 concrete was used for the superstructures of the flood area bridges. In the last construction phase for the bridge above the Szentendre Island a ~5,000 t unit had to be moved.

Due to their harmonic structural configuration, the uniquely designed public lighting system and the aesthetic noise barriers, the flood area bridges provide a worthy approach to the cable-stayed bridge above the Main Danube branch.

Pál Pusztai (1974) structural engineer (BME 1998). He started his bridge designer career at the Hídépítő Inc. He took part in designing the prestressed concrete bridge on Zalalövő-Bajánsenye railway line. As a member of the CÉH Inc., beginning from 2000, he took part in the design of the highway bridges in the Northern section of the M0 ring. He was the chief designer of the M31 highway bridges and one of the key persons in the elaboration of the general and final designs of the M0 Northern Danube bridge (Megyeri bridge).

Ádám Skultéty (1979) structural engineer (BME 2003). He has earned his dipl. structural engineer degree at the Budapest University of Technology and Economics in 2003. Since then, he has taken part in designing the bridges of the M0 and M31 highways, preparing the general and final designs of the M0 Northern Danube bridge (Megyeri bridge) as a member of the CÉH Inc.

HOW PORTLAND AND BLENDED CEMENTS RESIST HIGH TEMPERATURES OF TUNNEL FIRES?


Sándor Fehérvári - Salem Georges Nehme

Serious accidents of the last decades have drawn attention to investigate the effect of tunnel fires, tunnelling materials as well as to increase the residual safety of structures after the fire. To moderate the effects of heat on structural materials efficiently, it is necessary to understand the physical and chemical changes of the concrete during and after fire. The change of properties of the hardened cement pastes has been investigated at the Department of Construction Materials and Engineering Geology at Budapest University of Technology and Economics. The aim of our study was to define the change of physical and mechanical parameters of hardened cement pastes caused by thermal shock. Numerous (nearly 4500 pieces) 30 mm cubes have been made with various types of test parameters (e.g. specific surface, water/cement ratio, type and mass of different additives). The specimens have been heat treated in a preheated electrical furnace for 120 minutes. 11 different temperature steps were used (from the base laboratory condition up to 900 °C). Present paper summarises our results of these series of tests.

Keywords: tunnel, fire, fire load, cement, residual properties, blast-furnace slag, limestone filler, dolomite filler, quartz sand, barite

1. INTRODUCTION

One of the basics of the existence of our modern industrial community is the provision of reliable, safe and fast traffic infrastructure, as well as safe and efficient public transport in cities (Haack, 2002). The economical development forced the major part of traffic down into tunnel networks.

Despite of growing and rigorous safety directives, the number of the accidents and the damage in tunnels shows a growing tendency all around the world. These serious accidents turn attention to investigating the effect of tunnel fires as well as to the increase of the residual safety of structures. Some European standards determine the air (gas) temperatures of the tunnel fire based on theoretical assumptions, numerical analysis of real tunnel fires and large-scale tests (Blennemann and Girnau, 2005). Common properties of these derived curves are the fast growing of temperature (1000 °C in 5 minutes).

To moderate effects of the heat on the structural materials efficiently, it is necessary to recognize the physical and chemical changes of the concrete (Khoury, Anderberg, Both, Felinger, Majorana, Høj, 2002). Increasing the temperature, water discharges; first the ettringit and monosulphate dehydrates, followed by the $Ca(OH)_2$, the $CaCO_3$ and the substituents of the concrete dehydrats (e.g. CSH) (Schneider and Horvath, 2002; 2006) as shown in *Fig. 1*.

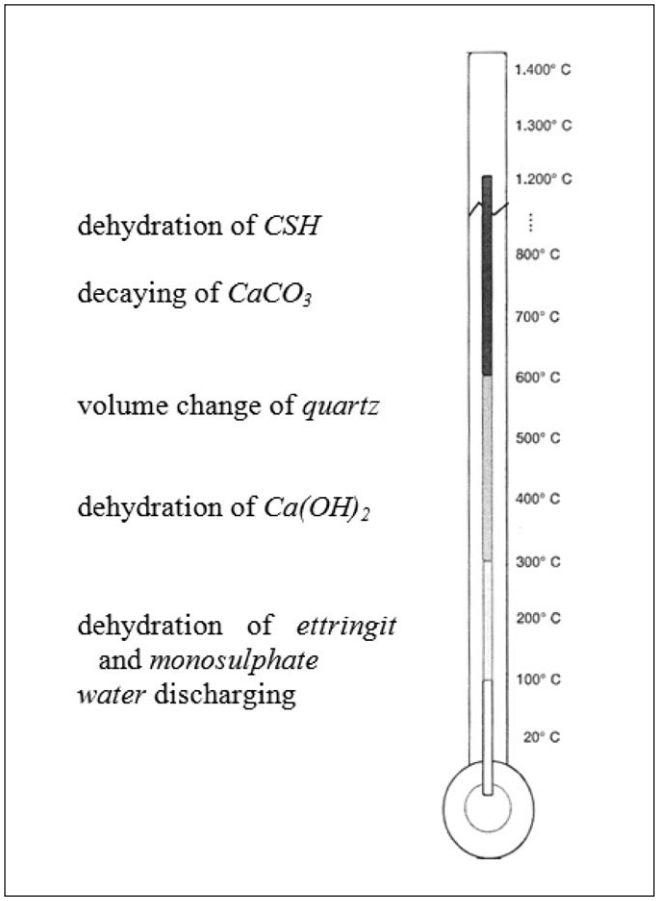

Fig. 1: Chemical changes in the cement (Pflanzl, 2002; Schneider and Horvath, 2002; 2006; Khoury, Anderberg, Both, Felinger, Majorana, Høj, 2002)

2. TESTS ON HARDENED CEMENT PASTES

The change of properties of the hardened cement paste was investigated at the Departement of Construction Material and Engineering Geology at Budapest University of Technology and Economics. The aim of our study was to define the change of physical, chemical and mechanical parameters of the hardened cement pastes due to thermal shock.

2.1 Experimental recipes

Firstly, the effect of different C_4AF contents and specifical surfaces was investigated. Cement types were: CEM I 52.5 N (spec. surf.: 452 m^2/kg; C_4AF content: 0.9 m%); CEM I 42.5 R (353 m^2/kg; 9.6 m%) and CEM I 32.5 R(S) (305 m^2/kg; 18.9 m%). The water/cement ratio of the pastes was 0.3 (constant). Afterwards CEM I 42.5 R and CEM I 32.5 R(S) were tested using 9 different water/cement ratios as shown in *Tab. 1*.

To test the effect of fines, blast-furnace slag (BFS), limestone filler (LS), dolomite filler (DM), quartz sand (QS) and two kinds of barite (barite1, B1 d_{max} = 200 μm; barite2,

B2 d_{max} =50 μm) were used as additive. The applied cement type was throughout CEM I 32.5 R(S). 4 different dosages of fines were used, with constant water/cement (w/c) ratio for all fines and constant water/fines (w/f, fines+cement altogether) ratio (only blast-furnace slag and limestone filler) as shown in *Tab. 2*. In all cases, superplasticizer was used to adjust the consistence.

2.2 Tests

Cube specimens of 30 mm edge length were made. The cubes were in the form for 1 day, then until the 7th day under water. All the tests started on the 28th day.

Before the heat test the specimens' mass and size were measured. Then they were put into a preheated electrical furnace to model the effect of the heat shock. The test duration was 120 minutes in all cases. After the specimens cooled down, their mass and size were measured again, and then the compressive strength was tested. The results were compared to the preheating parameters. 60 (by some cases 120) specimens were used for each series. 10 (20) specimens were stored in laboratory conditions, and sets of 5 (10) pieces were heated to 10 different temperatures (50, 100, 150, 200, 300, 400, 500, 600, 750 and 900 °C).

To compare each other the temperature vs. relative strength curves, the *TE,* i.e., temperature endurance, the definite integral of the curve (i.e. area below them), was inducted.

Tab. 1: *Water/cement ratios of Portland cement pastes (CEM I 52.5 R; CEM I 42.5 R and CEM I 32.5 R(S))*

water/cement	*0.120* *0.160* *0.195* *0.240*	*0.300*	*0.375* *0.462* *0.545* *0.750*
tested cement types	42.5 32.5	52.5 42.5 32.5	42.5 32.5

Tab. 2: *Experimental recipies of the dosage of fines*

Dosage of fines of the total mass	*water/fines* ratio, if w/c = 0.3 (additives: BFS, LS, BM, QS, B1,B2)	*water/cement* ratio, if w/f = 0,3 (additives: BFS , LS)
20%	0.240	0.375
35%	0.190	0.462
45%	0.160	0.545
60%	0.120	0.750

2.3 Results

2.3.1 Portland cements

Comparison of the relative residual strength of different types of cements with ***w/c= const.***

Fig. 2 shows the strength of the specimens heated to 50 °C exceeds the strength of the reference value (unheated specimens compressive strength). It was followed by a decline in the range of 100-150 °C. A second major strength increase was experienced in the range of 200-400 °C with the maximum level of 120-130% at 300 °C by each series. *Fig. 3* shows the temperature endurance (TE) in the function of the specific surface area.

The reason of this increment is the posthydration effect of the discharging crystal waters (see later). If the temperature is over 400 °C a significant drop of strength is noticeable due to the dehidaration of $Ca(OH)_2$. The cement with smallest specific

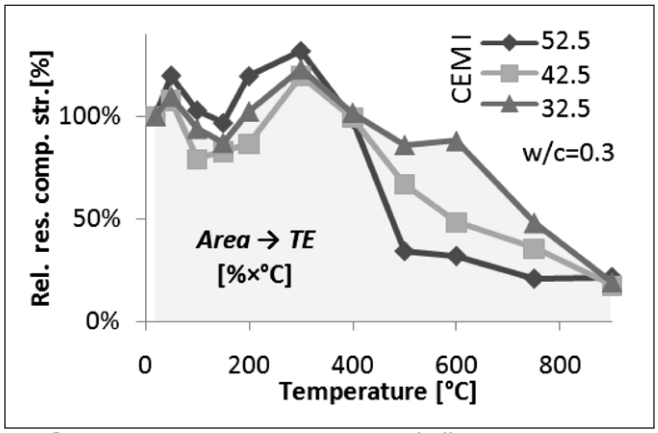

Fig. 2: *Relative residual compressive strength of different types Portland cement pastes*

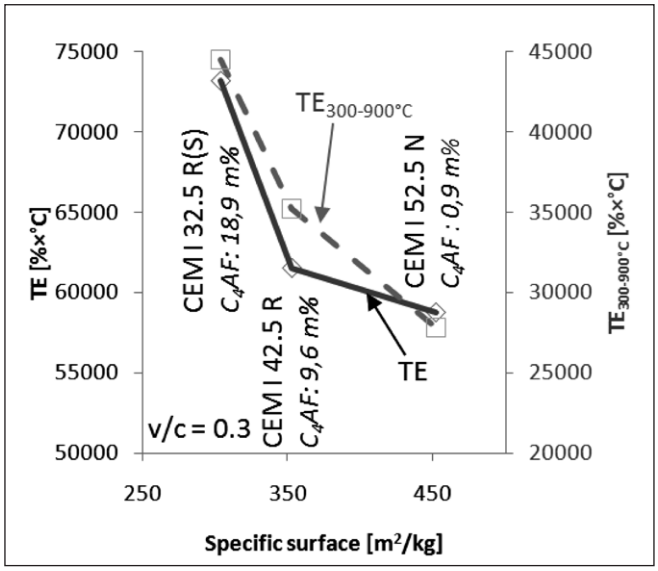

Fig. 3: *Temperature endurance (20-900°C and 300-900°C) of different types of Portland cement pastes in function of specific surface*

surface is CEM I 32.5 R(S) which has the lowest degradation. Its curve crosses the 50% relative strength level at 700 °C. Although, the specifical surface area is important for the behaviour of the hardened cement pastes's result in the range of 400-800 °C, at the highest temperature step (900 °C) each series pastes have nearly the same results (cca. 20%). Both of the integrals (20-900°C or 300-900°C) show that the less the specific surface area the better the temperature endurance is.

The TE, temperature endurance is also connected to the quantity of C_4AF in the Portland cement, higher C_4AF content brings with higher (better) TE.

Comparison of the strength of hardened cement pastes specimens with different water/cement ratios

Both cements CEM I 42.5 R, and CEM I 32.5 R(S) have nearly the same character of behaviour for all water/cement ratios as discussed in the previous paragraph.

Analysing our experimental results, shown in *Figs. 4 and 5*, it has been determined that the rule of the relationship between strength and water/cement ratio, without reference to the actual temperature level, is immutable, especially below 500 °C. Thus, above 500 °C the residual strength decrease due to the character of the curves are affine to unheated specimens curve.

The temperature endurance of CEM I 32.5 R(S) cement is better than CEM I 42.5 R by all water/cement ratios, as shown in *Fig. 6*.

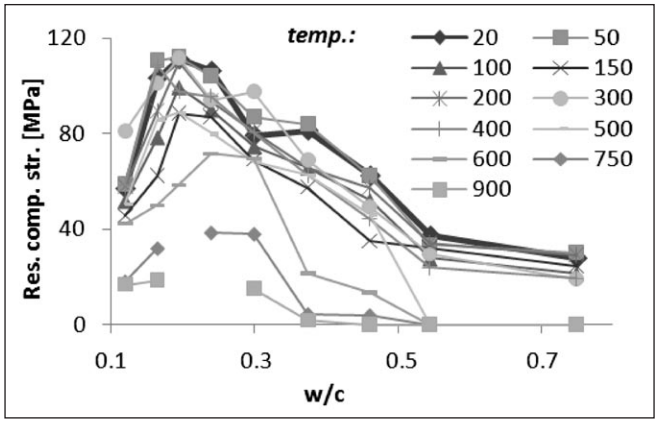

Fig. 4: Residual strength of CEM I 32.5 R(S), different water/cement ratios and temperatures

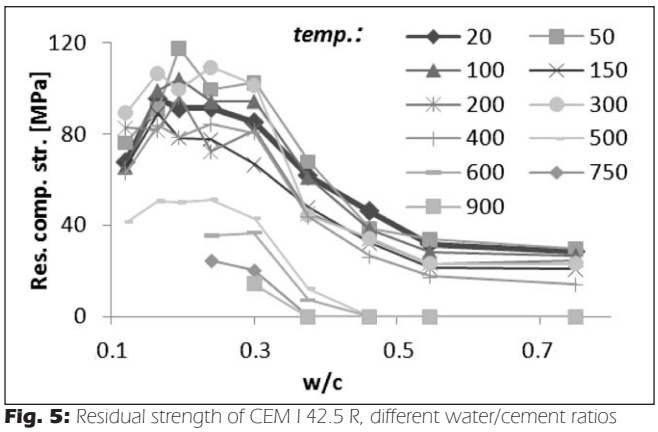

Fig. 5: Residual strength of CEM I 42.5 R, different water/cement ratios and temperatures

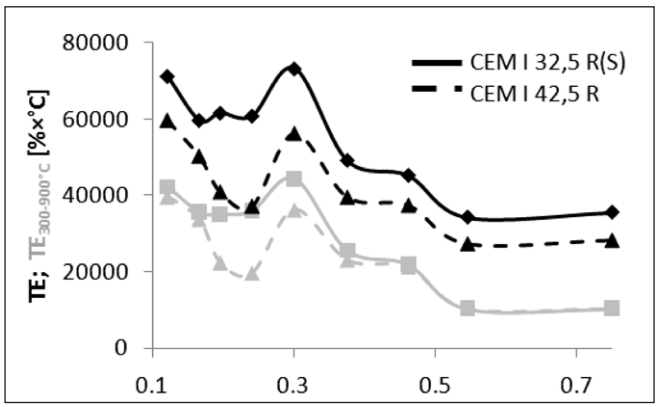

Fig. 6: Temperature endurance (TE) of CEM I 32.5 R(S) and CEM I 42.5 R, different water-cement ratios

Comparison of the mass of Ca(OH)$_2$ to the compressive strength and temperature

To determine the mass of the Ca(OH)$_2$ in postheated specimens, DTA tests were made. The mass of the Ca(OH)$_2$ in the unheated specimens are shown in *Tab 3*.

The Ca(OH)$_2$ derives from the chemical reactions of the clinkers. The masses of the Ca(OH)$_2$ in the cooled down specimens are shown in *Figs. 7 and 8*. The mass of the Ca(OH)$_2$ shows growing tendency up to a maximum of about 400 °C. This increment (if the maximal temperature was below the dehydrating level of Ca(OH)$_2$) shows that at elevated temperatures, the *discharged hydrate water reacts with unbounded clinkers* resulting increment of the strength.

The increase of relative compressive strength and increase of relative level of Ca(OH)$_2$ is shown in *Fig. 9*. It has been proved that the posthydration of unbounded clinkers effects strength increment (except at high water/cement where no strength maximum could be observed).

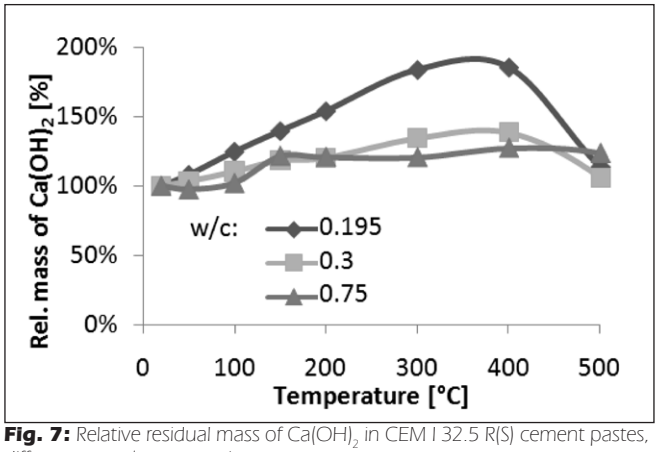

Fig. 7: Relative residual mass of Ca(OH)$_2$ in CEM I 32.5 R(S) cement pastes, different water/cement ratios

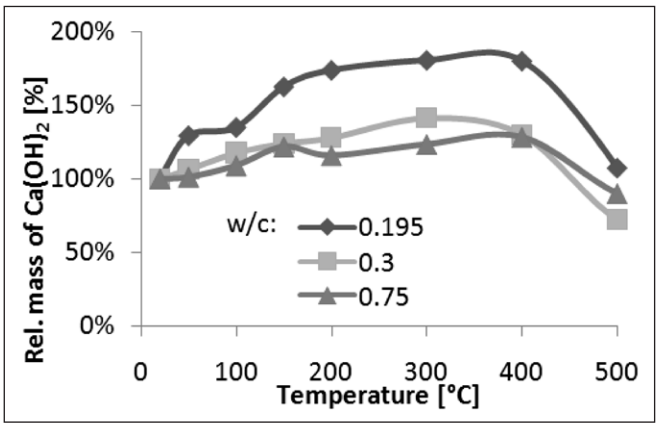

Fig. 8: Relelative residual mass of Ca(OH)$_2$ in CEM I 42.5 R cement pastes, different water/cement ratios

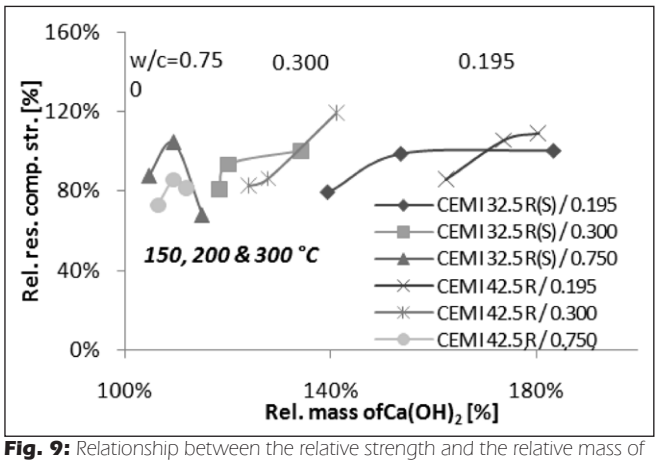

Fig. 9: Relationship between the relative strength and the relative mass of Ca(OH)$_2$

Tab. 3: Mass of Ca(OH)$_2$ in the unheated specimens [m%]

type of cement w/c	CEM I 32,5 R(S)	CEM I 42,5 R
0,195	7.2	7.3
0,300	11.6	11.8
0,750	17.1	18.0

2.3.2 Effect of dosage of fines with constant water/fines ratio (limestone filler, blast-furnace slag)

By adding *limestone filler* a part of cement was replaced with an inert material. Over the decaying temperature of the *limestone filler* (LS) 700 °C, fast change of properties was expected. By adding *blast-furnace slag (BFS)* to the cement, a reactive material with high specific surface was added to the matrix. The blast-furnace slag additive results in higher

compactness and higher compressive strength by the same water/cement(fines) ratio.

Figs. 10 and 11 show the *residual relative strength* of the series with limestone filler and blast-furnace slag using constant water/fines ratio. The reference values of the CEM I 32.5 R(S) series were also indicated. In *Fig. 12* the temperature endurance of our hardened paste specimens is shown.

According to our results the strength increase of Portland cement with the same water/fines ratio at 50 °C and 200 °C diminish and disappear because of the lack of unhydrated clinkers. The curves straighten in the range of 200-500 °C. Nevertheless, the real strength values of the *limestone filler* containing specimens show adverse properties. The base laboratory strength decreases from 80 MPa (without fines) to 40 MPa (with 60% fines) (100% in *Fig. 8*). Total disintegrating at laboratory temperature because of the swelling effect of CaO rehydration at high dosages, was also noticed. It was determined that using constant water/fines ratio the *maximum dosage of limestone filler is 20 m%.*

Adding *blast-furnace slag*, the behaviour of the curves are nearly the same as the reference curve but *usually below that*. However, the base laboratory strength slightly increases from 80 MPa (without fines) to 90 MPa (with 60% fines) (100 % in *Fig. 9*). The first local minimum at 150 °C is significant. The strength increase around 300 °C is also visible. The results of the relative postheating strength parameters shows that the dosage is optimal around 35-45%, when relative results between 600-750 °C were slightly higher than the reference values. Analysing the temperature endurance (*Fig. 11*) it has been also observed, that TE decreases parallel to the increment of the mass of the addings.

It should be marked, that the cements with blast-furnace slag additive using constant water/fines ratio did *not give us significant benefit*, but in contrary, it results *lower relative strength in the middle temperature levels than the reference value*.

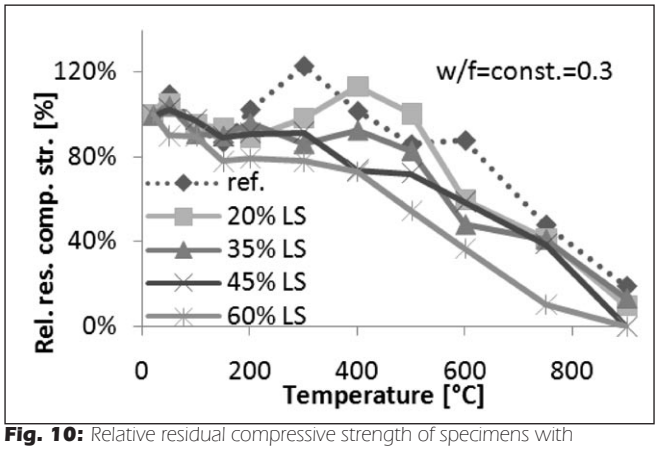

Fig. 10: Relative residual compressive strength of specimens with limestone filler, constant water/fines ratio

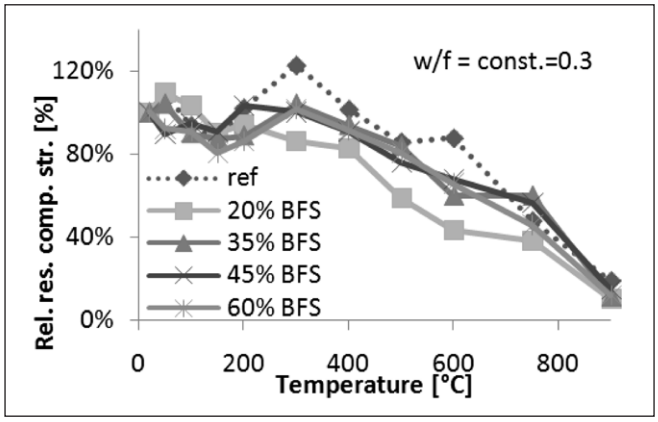

Fig. 11: Relative residual compressive strength of specimens with blast furnace slag, constant water/fines ratio

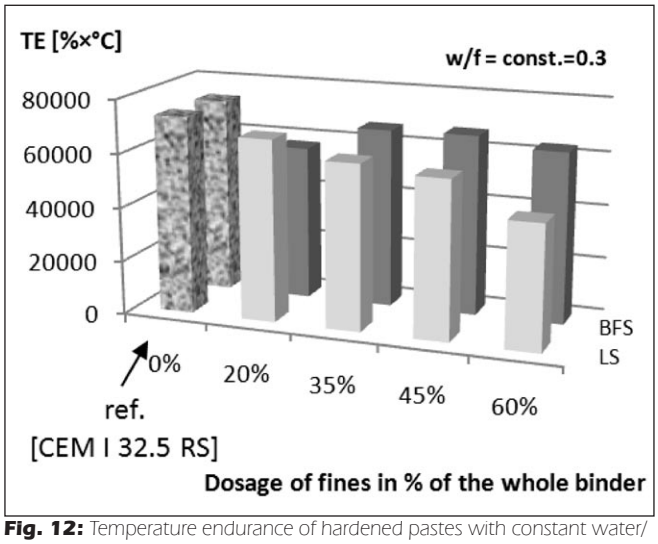

Fig. 12: Temperature endurance of hardened pastes with constant water/fines ratio

2.3.3 Effect of dosage of fines with constant water/cement ratio (six types of additvies)

The material properties of the *limestone filler* (LS) and the blast-furnace slag are explained in 2.3.2. The *dolomite filler's* (DM) behaviour is nearly the same as that of the limestone filler, but has a lower decaying level. The decaying of the limestone filler and the dolomite filler produce CO_2 gas, which causes explosion of the specimens at high dosages. The behaviour of the *quartz sand* (QS) is different. The quartz is also an inert material, it changes its structure effecting volume growth at 573 °C. The restructuring quartz effects structural changes in the cooled down specimens.

The last examined additive was *barite* which is a remaining material of roasting at 730-740 °C of siderite ($FeCO_3$) with high $BaSO_4$ content. Two different fineness of barite (barite1 d_{max} = 200 µm B1 and barite2 d_{max} =50 µm B2) were used. The barite additive behaves during the process more stable then the cement, thus the structural integrity of the specimens was better.

Following diagrams, *Figs. 13 to 16* show the comparative result of the different dosages. The reference values of the CEM I 32.5 R(S) series were indicated, too. The temperature endurance of the specimens is shown in *Fig. 17*, the reference values were also figured.

By analysing the curves and the temperature endurance levels, it has been determined, that *neither the limestone filler nor the dolomite filler series could produce better behaviour than the reference*. It has been also determined, that the *limestone filler and dolomite filler*, especially at high dosage (above 35%), are *disadvantageous* to the residual compressive strength properties. As expected, the base strengths of blast-furnace slag additive were higher than the reference values. At higher dosages at middle temperature level (400 °C) higher relative strength than the reference were measured. Nevertheless, the decrease of relative strengths over 500 °C was extremely fast, so the temperature endurances (TE) are lower than the reference values. At all dosages, the end strengths (900 °C) of the hardened cement pastes containing *quartz sand* were auspicious. The reason of the high strength values at high temperature is the expressum of small particles (compressive self stress) and restructuring effect of the quartz during its cooling down. Mixtures containing barite had an altering

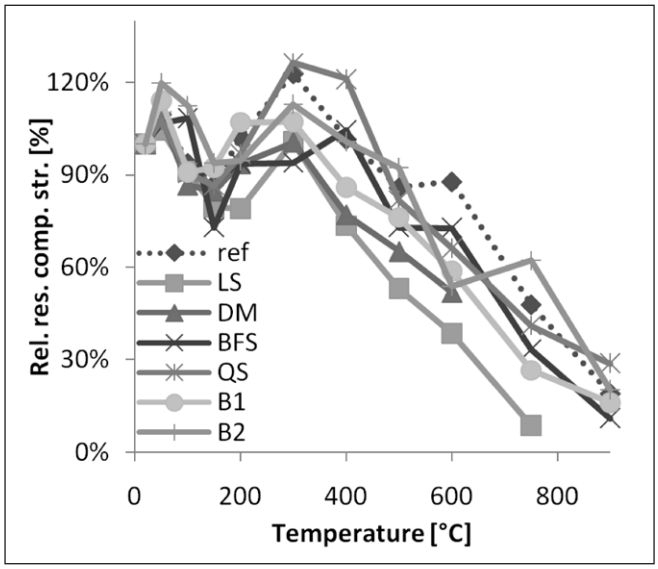

Fig. 13: Relative residual compressive strength of cement containing 20% of different additives

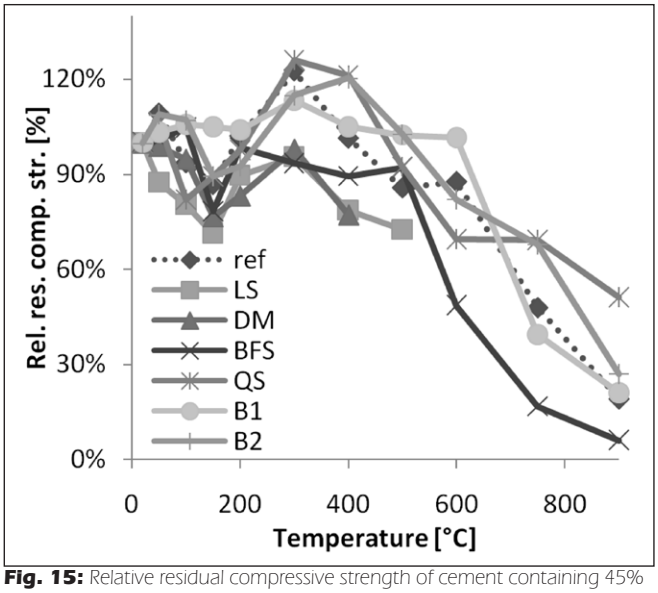

Fig. 15: Relative residual compressive strength of cement containing 45% of different additives

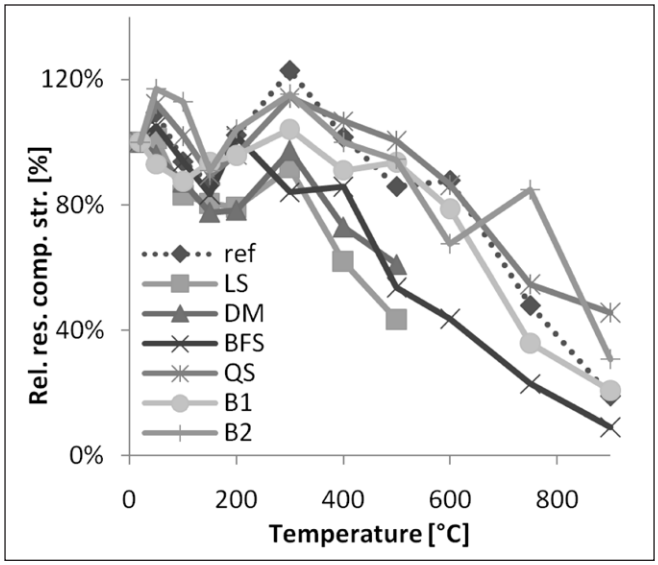

Fig. 14: Relative residual compressive strength of cement containing 35% of different additives

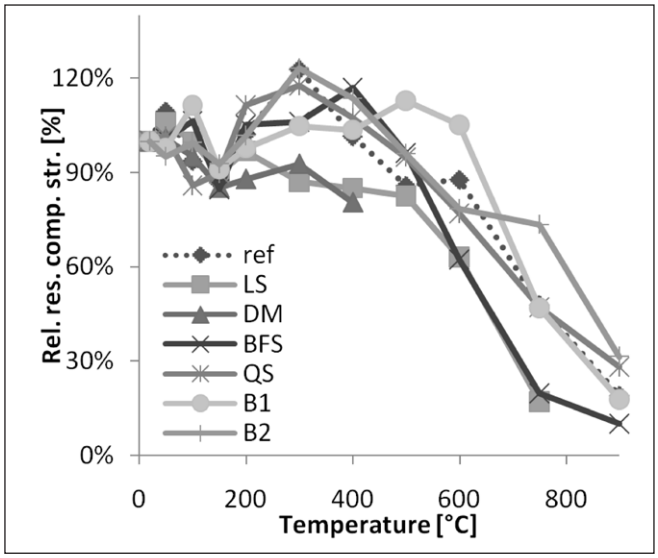

Fig. 16: Relative residual strength of cement containing 60% of different additives

behaviour compared to the tested materials. Depending on the fineness, the behaviours show constant or nearly constant compressive strength up to 600 °C.

Analysing the comparative strength results as well as the temperature endurance the *quartz sand and the barite have auspicious influence* on the temperature endurance of the hardened cement pastes. However, it should be noticed that the positive effect is not radical.

3. CONCLUSIONS

In this paper our experimental results of the temperature endurance of hardened cement pastes consisting *different kinds of Portland cements*, moreover hardened cement pastes of Portland cements with *different water/cement ratios*, and different dosages of limestone filler, dolomite filler, blast-furnace slag, quartz sand, barite1 and barite2 (making essentially well defined blended cements) were summarised. The results of almost 4500 specimens were evaluated in this research.

It has been assessed that the relative residual strength of Portland cements (CEM I 52.5 R; CEM I 42.5 R; CEM I 32.5 RS) is min. 90-100% up to 400 °C. It is a special result that the strength change of the hardened Portland cement pastes is *reciprocally proportional to the specific surfaces*, and *directly proportional to the mass of C_4AF of the whole clinkers*. The most advantageous cement type among the tested three ones was the CEM I 32.5 RS. It has been determined that the change of the *water/cement ratio does not influence significantly the shape of the relative strength function*, neither the relationship of the strength with water/cement ratio. Using DTA tests a *correlation of the strength increment of the specimens and the mass development of $Ca(OH)_2$* was indicated. The posthydration of unbounded cement causes strength increment in the range of 200-300°C.

Using *constant water/fines ratio* (fines = additive+cements altogether) limestone filler and blast-furnace filler were tested with 4 different dosages. It has been determined the *maximum dosage of limestone filler is 20 %*. The result of the relative postheating compressive strength parameters of blast-furnace slag shows that the *dosage is optimal at 35-45%*. In this range, relative results between 600 and 750 °C were slightly higher than the reference values.

Limestone filler, dolomite filler, blast-furnace slag, quartz sand, barite1 and barite2 were used to determine the temperature endurance of the cement pastes with *constant water/cement ratio*. It has been determined, *neither* the series consisting *limestone filler nor dolomite filler* could produce

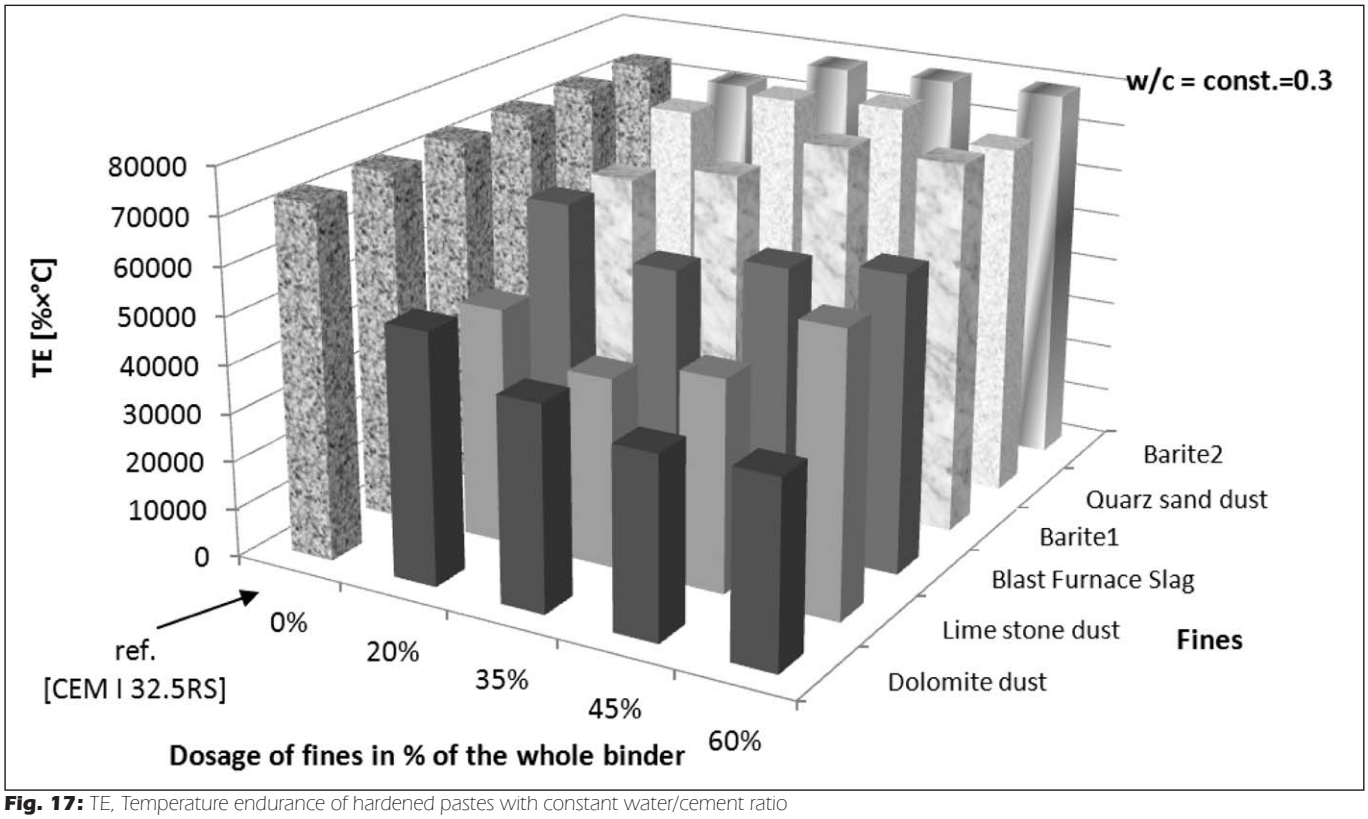

Fig. 17: *TE, Temperature endurance of hardened pastes with constant water/cement ratio*

better or equal behaviour than the reference strength and by high dosage, these additives are *disadvantageous for the residual compressive strength properties*. Though, relative strength of *blast-furnace slag* containing specimen's was higher than the reference value at some temperatures and some dosages, the total *trends were equal or worse results than the reference*. The *quartz sand* had the *highest final strength* in our tests because of the restructuring effect and compressive self stress of quartz. *The mixtures containing barite had a different behaviour*. Depending on the fineness, the behaviours show *constant or nearly constant strength up to 600 °C*. Both barite and the quartz sand additive had a *very advantageous effect* on the temperature endurance, equalling or even superpassing the reference value.

As a comprehensive result of our tests using ordinary Portland cement it is suggested to use the cement with lower specific surface to improve the temperature endurance of the structures. The advantageous effect of barite and quartz sand additive argues to use them for blended (heterogeneous) cements.

4. ACKNOWLEDGEMENTS

Authors wish to express their gratitude to Holcim Hungária Co., Danubius Betonkészítő Kft., BASF Hungária Ltd. and PólusKincs Co. for research materials, for proof-reading of present papers to Dr. Attila *Erdélyi* and Dr. István *Sajtos*; and last but not least for the important help in the laboratory works to Ms. Erika *Csányi*, Ms. Viktória *Rónaky*, Ms. Anikó *Demján*, Ms. Veronika *Gál*, Ms. Csilla *Szabó*, and Mr. Dávid *Diriczi*, Mr. András *Eipl*, Mr. Gábor *Kovács*, Mr. Patrik *Tóth*.

5. REFERENCES

Blennemann, F., Girnau, G. eds. (2005): "Brandschutz in Fahrzeugen und Tunneln des ÖPNV" (Fire Protection in Vehicles and Tunnels for Public Transport), *Alba Fachverlag*, Düsseldorf

Haack, A. (2002): „Current Safety Issues in Traffic Tunnels", STUVA, Cologne

Khoury, G. A.; Anderberg, Y.; Both, K.; Felinger, J.; Majorana, C. and Høj. N. P. (2002): „Fire design of concrete - Materials, structures and modelling" *Proceedings of the 1st fib Congress*; pp 99-118, Osaka

Pflanzl, Harald (2002): "Passiver Brandschutz im Tunnel- und Tiefbau" (Passive Fire Protection at Construction of Tunnels and Deep Foundations); *Zement + Beton*; Sonderheft 2002; pp 38-40

Schneider, U. and Horvath, J. (2002): „Behaviour of Ordinary Concrete at High Temperature", Vienna University of Technology, Institute of Bulding Material, Building Physics and Fire Protection, Vienna, Austria in Khroustailev, B. M.; Leonovich, S. N. and Schneider, U.: „Behaviour of Concrete at High Temperature and Advanced Design of Concrete Strucures" *Proceedings of the International Conference „Construction and Architecture",* Minsk, 2003

Schneider, U. and Horvath, J. (2006): „Brandschutz-Praxis in Tunnelbauten" (Fire Protection at Buildings of Tunnels), Bauwerk Verlag GmbH, Berlin

Sándor Fehérvári (1981), MSc. in civil engineering (BME 2006). PhD Student at BME (Budapest University of Technology and Economist) Dep. of Construction Materials and Engineering Geology. Main fields of interest are the effect of the tunnel fires on structures, structural and curtain grouting, building and repair techniques of underground and tunnel structures. Member of the Hung. Group of ***fib***, the Hung. Chamber of Engineers, the Hung. Tunnelling Assoc., the Hung. Sci. Assoc. for Transport, the Sci. Soc. of Silicate Industry (Concrete Div.) and the Hung. Sci. Soc. for Building. Activities: ITA (International Tunelling Assoc.) WG 6 (Maintenance and Repair).

Salem G. Nehme (1963), MSc. civil engineer (BME 1992); reinforcement construction engineer (BME 1996), PhD (BME 2005). Assoc. professor at BME Department of Construction Materials and Engineering Geology. Main fields of interest: concrete technology, testing of concrete, quality controlling of building materials. Member of the Hungarian Group of ***fib***.

PROBABILISTIC APPROACH FOR THE DURABILITY DESIGN OF PREFABRICATED CONCRETE MEMBERS


Kálmán Koris – István Bódi

Durability design of structures is an important part of the design process. A possible method for the durability design is the probabilistic approach considering changes of structural resistance and the load effect during the service life of the structure. In order to determine stochastic parameters of structural resistance as a function of time, deterioration of materials and the decrease of structural sizes due to environmental effects must be predicted. In this paper the probability of failure of prefabricated concrete members are analysed as a function of time. The effect of creep, shrinkage, relaxation, carbonation induced corrosion and the deterioration of cross-sectional sizes were considered during the analysis. Results of the calculations can be used for the durability design of the appropriate prefabricated members. The introduced calculation method is illustrated by numerical example on a prefabricated, prestressed concrete beam.

Keywords: durability, service life, probabilistic approach, prefabricated concrete, prestressed concrete

1. INTRODUCTION

The importance of durability became an important aspect of the design process recently (Balázs, 2008). In order to perform proper durability-design, the rheological changes of material properties and the decrease of structural sizes due to environmental effects must be considered during the determination of structural resistance. Rheological processes are usually affected by the environmental conditions, such as average temperature, ambient humidity and presence of aggressive agents, as well as by the initial material properties of the structure. The aim of the research was, on one hand, to determine the decrease of load carrying capacity in time due to slow deformations and aging of materials, on the other hand to calculate the probability of failure of the structure by means of varying load carrying capacity and external loads. The relationship between elapsed time and the probability of failure was finally used for the purposes of durability design of appropriate structural members. The probability of failure was determined by the Stochastic Finite Element Method. In frames of this paper, the applied stochastic finite element formulation, the determination method of input parameters and the calculation of the probability of failure as a function of time are briefly introduced.

During the research, bending moment capacity of prefabricated, prestressed concrete beams was analysed. These types of beams are used for the construction of floors in houses or industrial buildings and they are usually not subjected to aggressive environmental effects or freeze-thaw actions, therefore these effects were neglected during the analysis. Creep and shrinkage of concrete, relaxation and carbonation induced corrosion of steel bars and tendons as well as the decrease of material properties and cross-sectional dimensions were considered. The probability of failure of analysed members was evaluated as a function of time elapsed since manufacture, the relative ambient humidity and the initial value of imposed load. The humidity was selected for a variable parameter since it is one of the most important environmental factors to influence the process of carbonation and its value can be measured or even controlled during the service life of the structure. Results of the presented analysis can be used to reduce the maintenance costs or to schedule the necessary repair work, as well as to determine the service life of appropriate concrete members under given circumstances.

2. CALCULATION METHOD

The durability of a structural member is satisfactory if the probability of failure does not exceed a certain value during the lifetime (Bolotin, 1970; Lawrence, 1989; Koris, 1996; Mistéth, 2001). Failure of the structure can be defined by different limit states such as ultimate or serviceability limit state. The probability of reaching such a limit state is the function of different stochastic parameters and the values of these parameters are changing in time due to the deterioration of materials and structural sizes as well as due to changes of the load effect. The purpose of the presented method is to predict the value of process parameters in any given point of time and to evaluate the probability of failure using the appropriate quantities. The adequacy of the structure is decided by the comparison of calculated and expected probability of failure. During the calculations the probability of failure was analysed in ultimate-limit state only.

2.1. Evaluation of the probability of failure

The failure probability of structural members can be usually obtained by means of the first two parameters of the distributions of structural resistance and acting loads (Lawrence, 1989; Koris, 2007). During the research, mean value and standard deviation of structural resistance were calculated by stochastic finite element method (Augusti et al., 1984; Belytschko et al., 1986; Eibl – Schmidt-Hurtienne, 1996; Koris, 1996) in function of time while the distribution of load effect was assumed as proposed by Mistéth (2001). The probability of failure of examined pre-cast structural members was calculated in dif-

ferent points of time using the probability density function of normal distribution (Bolotin, 1970; Mistéth, 2001).

2.2. Mean value of structural resistance

Mean value of structural resistance in case of the analysed prestressed concrete beams was determined by finite element method (Bojtár – Gáspár, 2003) considering non-linear behaviour of concrete and steel (Koris, 1996 and 2004). Mean values of input parameters (structural geometry, material properties) were used for the analysis. Shear deformations were neglected in the calculation since they are significantly lower than the flexural deformations in case of reinforced concrete. The method of load increments was used and for each load increment, the chord of the stiffness matrix was evaluated (Koris, 2004). Failure of the structure was specified by a damage indicator, consisting of the eigenvalue of stiffness matrix in case of structural damage and the eigenvalue of current stiffness matrix at the given load level.

2.3. Scatter of structural resistance

The deterministic finite element system of equations in a displacement format can be written as:

$$\underline{\underline{K}}\,\underline{u} = \underline{q} \tag{1}$$

where $\underline{\underline{K}}$ is the stiffness matrix of the structure, $\underline{q}$ is the vector of external loads and $\underline{u}$ is the vector of unknown nodal displacements. A single-parameter load was applied during the analysis, which means that the load vector was expressed as product of the load-intensity (F) and a load-distribution vector (Φ). The displacements of the structure are influenced by the variation of stiffness properties and the scatter of load-intensity so they can be split up into its mean and fluctuating components:

$$\left(\underline{\underline{K}} + \delta\underline{\underline{K}}\right)\cdot\left(\underline{u} + \delta\underline{u}\right) = \left(\underline{q} + \delta\underline{q}\right) \tag{2}$$

Equation (2) can be rearranged to the following form:

$$\underline{\underline{K}}\cdot\underline{u} + \underline{\underline{K}}\cdot\delta\underline{u} + \delta\underline{\underline{K}}\cdot\underline{u} + \delta\underline{\underline{K}}\cdot\delta\underline{u} = \underline{q} + \delta\underline{q}$$

The product of the fluctuating components can be neglected from equation (2) since its influence on the results is expected to be insignificant. Considering equation (1), the fluctuating components can be separated into an independent system of equations:

$$\delta\underline{\underline{K}}\cdot\underline{u} = \delta\underline{q} - \underline{\underline{K}}\cdot\delta\underline{u} \tag{3}$$

If we assume that the variation of the displacement (δu_i) is zero at the node i where the structure fails in ultimate limit state, we are able to transform expression (3) into the following equation (Eibl – Schmidt-Hurtienne, 1996; Koris, 1996):

$$\delta\underline{q}_F = -\underline{\underline{K}}_F^{-1}\cdot\delta\underline{\underline{K}}\cdot\underline{u} \tag{4}$$

where $\delta\underline{q}_F$ is a vector including variation of displacement and the variation of load intensity at row i and $\underline{\underline{K}}_F$ is the stiffness matrix including the load-distribution vector at column i. The variation of the load-intensity (δF) can be expressed from equation (4), however, the variation of the stiffness matrix ($\delta\underline{\underline{K}}$) is still not known. Assuming that the stiffness matrix $\underline{\underline{K}}$ is a function of an α random input variable, $\delta\underline{\underline{K}}$ can be approximately expressed by its Taylor's series:

$$\delta\underline{\underline{K}} = \frac{\partial\underline{\underline{K}}}{\partial\alpha}\delta\alpha \tag{5}$$

where $\delta\alpha$ is the variation of α. This approximation is reasonable if the variation of the stiffness matrix is less than about 15%. According to the results of the calculations, this limitation does not apply to analysed prefabricated members. Substituting equation (5) into equation (4) and forming the covariance matrix we get (Eibl – Schmidt-Hurtienne, 1996; Koris, 1996):

$$\underline{\underline{C}}_q = \delta\underline{q}_F\cdot\delta\underline{q}_F^T = \underline{\underline{K}}_F^{-1}\cdot\frac{\partial\underline{\underline{K}}}{\partial\alpha}\cdot\underline{u}\cdot\delta\underline{\alpha}\cdot\underline{\underline{C}}_\rho\cdot\delta\underline{\alpha}^{\mathrm{T}}\cdot\underline{u}^{\mathrm{T}}\cdot\frac{\partial\underline{\underline{K}}^{\mathrm{T}}}{\partial\alpha}\cdot\underline{\underline{K}}_F^{-T} \tag{6}$$

where $\delta\underline{\alpha}$ includes the standard deviations of random input variables (structural dimensions and material properties) and $\underline{\underline{C}}_\rho$ is the correlation matrix. The correlation between different elements was described by an exponentially decaying function of the distance between two elements and the length of correlation. The standard deviation of structural resistance can be obtained as square root of the diagonal elements in the covariance matrix $\underline{\underline{C}}_q$. Using equation (6), the standard deviation of structural resistance can be evaluated on structural level instead of cross-sectional level.

3. EXPERIMENTAL AND ANALYTICAL DETERMINATION OF INPUT PARAMETERS

3.1. Initial values of material properties and structural geometry

Initial mean values and standard deviations of input parameters (strength of materials, geometry of the structure) were determined from material test results and measurements on existing prefabricated beams. Products of 7 different Hungarian companies were considered during the analysis (company names are not mentioned upon request so they will be referred

Fig. 1: Concrete cube specimen after compression test

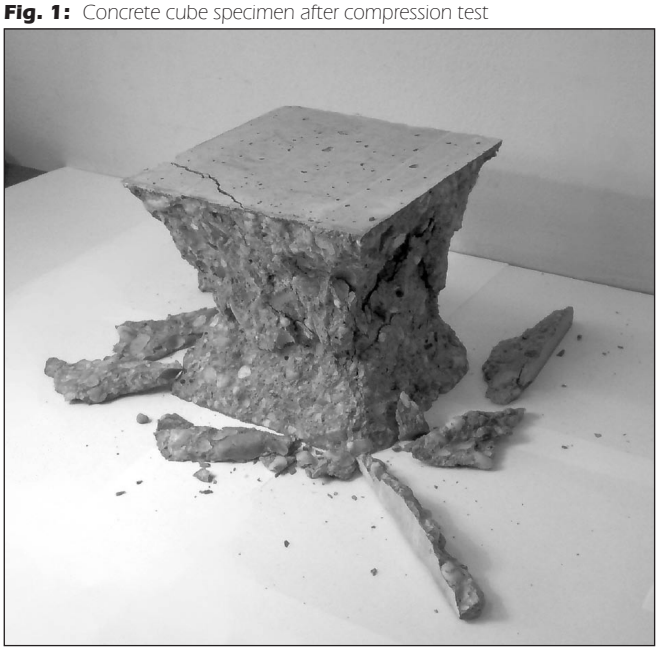

as M1, M2, etc.). Material tests and geometrical measurements were carried out at the laboratories of these companies. Concrete strength was obtained from uniaxial compression tests carried out on 150×150×150 mm cubes (*Fig. 1*). Test results of altogether 810 specimens were considered.

Laboratory tensile tests were carried out to determine material properties of reinforcing steel. Modulus of elasticity, strength and ultimate strain of different steel bar types were measured. Steel products of 3 different manufacturers were analysed on altogether 291 specimens. Mechanical properties of prestressing strands were also measure by laboratory tensile tests. The modulus of elasticity, strength and the ultimate strain were measured on 23 specimens. The complete list of tested materials and prestressed beams is displayed in *Table 1*.

Table 1: List of tested materials and prestressed beams

Type of material or beam		Manufacturer	Characteristic strength [N/mm^2]	Number of tested / measured specimens
Concrete	C40/50, 28 days	M1	40	54
	C50/60, 28 days	M1	50	42
	C30/37, 7 days	M2	30	9
	C35/45, 7 days	M2	35	12
	C40/50, 7 days	M2	40	54
	C60/75, 7 days	M2	60	3
	C50/60, 28 days	M3	50	636
Steel bar	BHB55.50, Ø6	M4	500	3
	BHB55.50, Ø8	M4	500	4
	BHB55.50, Ø12	M4	500	5
	BST 500 KR, Ø8	M5	500	52
	BST 500 KR, Ø10	M5	500	28
	BST 500 KR, Ø12	M5	500	5
	B60.50, Ø12	M6	500	20
	B60.50, Ø14	M6	500	15
	B60.50, Ø16	M6	500	20
	B60.50, Ø20	M6	500	89
	B60.50, Ø25	M6	500	45
	B60.50, Ø28	M6	500	5
Prestressing tendon	Fp 38/1770-R2	M7	1770	3
	Fp 100/1770-R2	M7	1700	20
Prestressed concrete beam	EE-42 (l=4.4 m, h=19 cm)	M2	-	7
	EE-48 (l=5.0 m, h=19 cm)	M2	-	11
	EE-54 (l=5.6 m, h=19 cm)	M2	-	5
	EE-66 (l=6.8 m, h=19 cm)	M2	-	4
	4000 (l=28.78 m, h=1.45 m)	M1	-	11
	4700 (l=6.06 m, h=74.9 cm)	M1	-	10

3.2. Evaluation of process parameters as a function of time

Due to different deterioration processes, the input parameters described above are not constant but they are changing in time. Possible deterioration mechanisms of reinforced concrete structures are presented in *Table 2* according to the fib bulletin 34 (2006).

In frames of the research, the collapse of the structure due to carbonation induced corrosion was analysed. The process of carbonation is getting slower as the concrete strength is increasing. For concrete classes higher than C40/50 (which is common for prefabricated concrete members) the carbonation induced corrosion first evolves after 40-50 years only. However prefabricated beams can also used for structures with a service life of 50-150 years (e.g. bridges) so it is important to consider

Table 2: Possible deterioration processes of reinforced concrete structures

Type of deterioration	Limit states
Carbonation induced corrosion	depassivation corrosion induced cracking corrosion induced spalling **corrosion induced collapse**
Chloride induced corrosion	depassivation corrosion induced cracking corrosion induced spalling corrosion induced collapse
Frost induced internal damage	local loss of mechanical properties cracking scaling and loss of cross section
Frost and salt induced surface scaling	surface scaling deflection and collapse

the effect of carbonation as well. Determination method of time-dependent parameters is described below.

The initial value of prestressing stress (σ_{p0}) is usually determined so that plastic deformations of tendons are avoided (Koris, 1998). The usual value for this stress is around 1200-1300 N/mm^2 depending on the actual conditions. For the analysed beam types σ_{p0} = 1300 N/mm^2 was used by the manufacturer. The loss of prestressing stress was determined according to the relevant Eurocode 2 standard, considering the effect of creep, shrinkage, relaxation and the elapsed time since manufacture (t). The shrinkage strain and the creep coefficient were, of course functions of the relative ambient humidity (RH). Depending on the humidity level, the stress loss after 100 years was about 10-15% in case of the tested beams.

Stochastic parameters of height and width of the cross section as well as the effective depth of rebars and prestressing tendons were considered during the analysis. Distribution of these parameters was approximated by normal distribution (Mistéth, 2001) therefore mean value and standard deviation of the parameters were evaluated. Change of the mean values of geometrical sizes is usually insignificant in case of concrete structures, thus a constant value was assumed during the calculation. Change of the standard deviation of a given geometrical parameter (W) in time was considered by the Gauss-process as (Mistéth, 2001):

$$s_W(t) = \sqrt{\sum_{i=0}^{n}\left\{\left[\frac{\partial W(t)}{\partial u^{(i)}(t)}\right]_{u^{(i)}(t)=\bar{u}^{(i)}(t)} s^{(i)}(t)\right\}^2} \cong \sqrt{{s_{W,0}}^2 \cdot \left(1 + f\frac{t}{t_1}\right)}$$

where $s_{w,0}$ is the initial value of standard deviation for the given geometrical parameter, t_1 is the time needed to reach the maximum deterioration. The value of t_1 can vary between 50 and 1000 years depending on the type of material, on the conditions of usage and on the rate of maintenance. During the analysis t_1 = 1000 years was used. The value of f is equal to 1.2 under normal circumstances for reinforced concrete.

The strength of concrete, steel bars and prestressing tendons are the most important material properties to affect the structural resistance in ultimate limit state. Mean value of concrete strength reaches its maximum in about 2 years after manufacturing because of afterhardening, later this value starts to decrease due to fatigue of the material. Same decrease can be observed in case of mean values of steel bar and prestressing tendon strengths. This effect can be described by the following equation (Mistéth, 2001):

$$f_m(t) = f_{m0} \cdot \beta(t)$$

where $f_m(t)$ is the mean value of strength at the time t, f_{m0} is the initial mean value of strength and $\beta(t)$ is the function describing

the decrease of the strength. Assuming a time period t_0 in which the strength of the material decreases to zero, $\beta(t)$ can be expressed by the first few terms of its Taylor-series:

$$\beta(t) \cong 1 - \frac{1}{3}\left(\frac{t}{t_0}\right)^2 - \frac{1}{3}\left(\frac{t}{t_0}\right)^3 - \frac{1}{3}\left(\frac{t}{t_0}\right)^4$$

The value of t_0 can usually vary between 50 and 1000 years depending on the type of material, on the conditions of usage and on the rate of maintenance. During the analysis, t_0 = 500 years was assumed. Standard deviation of material strength also changes during time. This effect can be again described by the Gauss-process (Misteth, 2001):

$$s_f(t) = \sqrt{s_{f0}^2 \cdot \left[1 + b\left(\frac{t}{t_0}\right)^r\right]}$$

where $s_f(t)$ is the standard deviation of strength at the time t, s_{f0} is the initial value of standard deviation, b and r are constants describing the increase of standard deviation. The exact values of constants b and r can be usually determined empirically. In case of concrete, the values b = 1.5 and r = 1 were used, for steel bars and tendons the values b = 1.4 and r = 1.2 were applied during the analysis based on the recommendations of Misteth (2001).

Decrease of steel bar and tendon diameter due to carbonation induced corrosion was also considered in the calculation. The carbonation depth at the time t can be expressed from the following equation (fib bulletin 34, 2006):

$$x_c(t) = \sqrt{2 \cdot k_e \cdot k_c \cdot \left(k_t \cdot R_{ACC,0}^{-1} + \varepsilon_t\right) \cdot C_s} \cdot \sqrt{t} \cdot W(t) \qquad (7)$$

where k_e is the environmental function, k_c is the execution transfer parameter, k_t = 1.25 is the regression parameter, $R_{ACC,0}^{-1}$ is the inverse effective carbonation resistance of concrete derived from accelerated test (ACC), ε_t = 315.5 (mm^2/years)/(kg/m^3) is the error term considering inaccuracies which occur conditionally when using ACC test method, C_s is the CO_2 concentration and $W(t)$ is the weather function that takes the effect of rain events on the concrete carbonation into account. The environmental function can be expressed as a function of the relative humidity of the carbonated layer. During the analysis, the relative humidity of the carbonated layer was assumed to be same as the relative ambient humidity (RH), which is one of the most important factors to influence the process of carbonation and its value can be measured or controlled during the service life of the structure. The execution transfer parameter was calculated by the consideration of a curing period t_c = 7 days. The inverse effective carbonation resistance of concrete can be obtained from the ACC test. There was no test data available for the analysis, so recommended values from *Table 3* were used.

The cement type CEM I 42.5 R and the value w/c = 0.4 were assumed in the calculations. For the calculation of the CO_2 concentration, the CO_2 concentration of the atmosphere and the CO_2 concentration due to emission sources were considered. The actual CO_2 content in the atmosphere has been detected to be in a range of 350-380 ppm. This corresponds to a CO_2 concentration of 0.00057 to 0.00062 kg/m^3. The increase of CO_2 concentration is about 1.5 ppm ($1.628 \cdot 10^{-6}$ kg/m^3) per year according to fib bulletin 34 (2006). The additional CO_2 concentration due to emission sources was $C_{s,emi}$ = 0.00082 kg/m^3. According to these values, the CO_2 concentration was calculated from the equation below:

$$C_s(t) = 0{,}00139 + t \cdot 1{,}628 \cdot 10^{-6} \text{ [kg/m}^3\text{]}$$

where t is the elapsed time in years. Assuming interior structural elements, a constant weather function $W(t) = 1$ was used in the analysis. After the concrete cover (a) is completely carbonated, steel bars and tendons may begin to corrode. Using equation (7), the time of carbonation (t_c) of concrete cover can be calculated from the following equation:

$$a = x_c(t_c)$$

The process of corrosion is an electrochemical reaction. The relation between the diameter of rusted steel bar and corrosion time under normal atmospheric conditions is outlined as (Zhao – Fan, 2007):

$$\varnothing(t) = \varnothing_0 - 0{,}0232 \int_0^t i_{corr}(t)dt$$

where t is the time of corrosion measured from the time point t_c, $\varnothing_0$ [mm] is the diameter of steel bar before corrosion and $i_{corr}(t)$ represents current corrosion density at time t:

$$i_{corr}(t) = 37{,}8 \frac{(1 - w/c)^{-1{,}64}}{a} \cdot 0{,}85 \cdot t^{-0{,}29}$$

where w/c is the water/cement ratio of the concrete. The area of steel bars or tendons in a certain point of time can be obtained from:

$$A_{s,p}(t) = \varnothing(t)^2 \cdot \frac{\pi}{4}$$

where t is the elapsed time since the time point t_c as described above. Steel bars are usually closer to the surface of the concrete than the prestressing tendons; therefore they start to corrode earlier.

4. APPLICATION OF THE IMPLEMENTED DESIGN METHOD

4.1. Verification of the method by bending tests

Table 3: *Inverse effective carbonation resistance of concrete obtained from accelerated test*
(Notations: I – Portland cement, III – Fly ash portland cement, R – rapid cement, FA – fly ash, SF – silica fume)

Inverse effective carbonation resistance [10^{-11} (m^2/s)/(kg/m^3)]	**w/c ratio**					
Cement type	**0.35**	**0.40**	**0.45**	**0.50**	**0.55**	**0.60**
CEM I 42.5 R	-	3.1	5.2	6.8	9.8	13.4
CEM I 42.5 R + FA	-	0.3	1.9	2.4	6.5	8.3
CEM I 42.5 R + SF	3.5	5.5	-	-	16.5	-
CEM III/B 42.5	-	8.3	16.9	26.6	44.3	80.0

Bending tests were carried out on prefabricated concrete beams (*Fig. 2*) to verify stochastic characteristics of the ultimate load. Altogether 26 beams of type "EE" in 4 different sizes (L_b = 4.20–6.60 m) were tested in laboratory. The test arrangement and the simplified cross-section of beams are presented in *Fig. 3*. Length of beam, height of the cross-section, width of the top and bottom flange and the concrete cover of the prestressing wires were measured before the bending tests (*Table 4*). Beams were loaded until failure in steps by four forces of equal value. The loading force and the corresponding deflection of the midspan were recorded for each load step. The ultimate load was also documented (*Table 4*) for each beam.

Test results on ultimate load of "EE" beams were compared to the numerical results. Calculations were performed by the implemented stochastic finite element method. Mean values and standard deviations of structural sizes were obtained from measurements on the tested beams. Mean value and standard deviation of concrete and steel strengths were obtained from material test results described in Chapter 3. The calculated and the measured relative standard deviations of ultimate load are compared in *Fig. 4*. According to the comparison, the calculated standard deviations are in correspondence with the test results. In case of the analysed beams, the maximum difference between them is about 8.8 %.

The effect of the standard deviation of different input parameters on the standard deviation of ultimate load was also analysed for each type of "EE" beam. The calculation was carried out by changing the standard deviation of a single input parameter (s_i) between $0{,}25 \cdot s_i$ and $3 \cdot s_i$ while values of other parameters remain constant. The effect of the width and height of the cross-section, the effective height and the strength of concrete and prestressing wires were examined. An example to this analysis in case of beam "EE-42" is presented in *Fig. 5*.

4.2. Application of the method on a long-span prestressed concrete beam

Fig. 2: Beams of type "EE" after manufacture

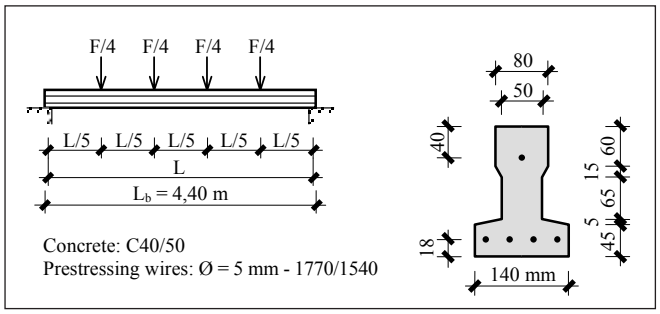

Fig. 3: Bending test arrangement and cross-section of beam type EE-42

Fig. 4: Measured and calculated standard deviations of ultimate load

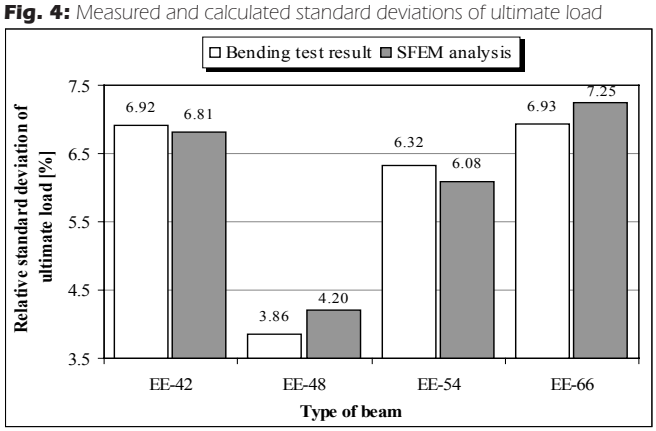

Fig 5: Effect of the standard deviation of different input parameters on the standard deviation of ultimate load in case of beam type "EE-42"

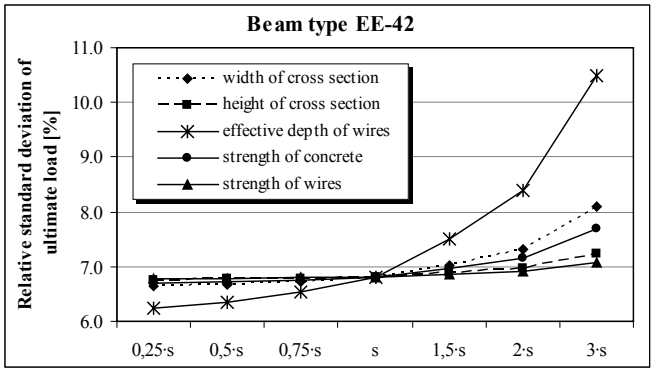

Table 4: Mean values and standard deviations of geometrical sizes and ultimate load (F_u) in case of tested "EE" beams

Type of beam	L [m]	Number of wires	L_{bm} [m]	h_m [mm]	$b_{f,m}$ [mm]	$b_{a,m}$ [mm]	$a_{p,m}$ [mm]	$d_{p,m}$ [mm]	$F_{u,m}$ [kN]
EE-42	4.27	1+4	4.40	189.8	80.8	144.1	37.8	168.5	49.28
EE-48	4.87	1+6	5.01	195.2	80.6	145.4	30.8	175.4	53.93
EE-54	5.47	1+6	5.64	196.1	81.7	144.4	39.5	176.5	51.60
EE-66	6.67	1+6	6.85	197.1	79.8	142.3	45.7	175.3	47.50

Type of beam	L [m]	Number of wires	v_{Lb} [%]	v_h [%]	v_{bf} [%]	v_{ba} [%]	v_{ap} [%]	v_{dp} [%]	v_{Fu} [%]
EE-42	4.27	1+4	0.171	1.60	3.13	1.59	18.21	1.73	6.92
EE-48	4.87	1+6	0.224	1.86	1.30	1.49	19.48	0.86	3.86
EE-54	5.47	1+6	0.119	2.72	1.96	1.98	11.32	2.07	6.32
EE-66	6.67	1+6	0.084	2.27	0.48	0.23	4.42	0.92	6.93

Fig. 6: Reinforcement of the beam type "4000"

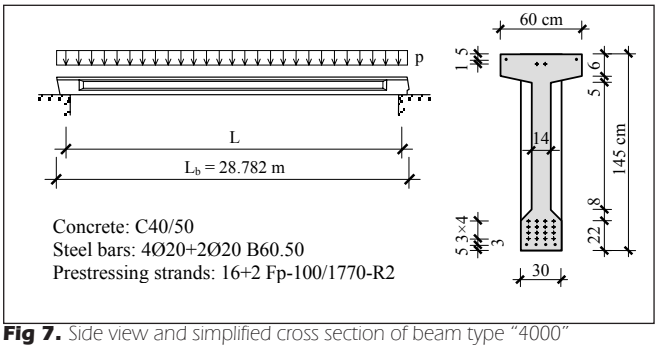

Fig 7. Side view and simplified cross section of beam type "4000"

Long-span, prefabricated concrete beams were also analysed by the implemented method. Results of the analysis are demonstrated in case the beam type "4000", which is a L_b = 28.782 m long and h = 1.45 m high prestressed main girder that is used for the construction of industrial buildings and halls. The armature of this beam is presented in *Fig. 6*, the side view and cross-section of the beam is displayed in *Fig. 7*. Height and width of the cross-section as well as the length was measured on 11 beams after manufacture. Mean value and standard deviation of structural geometry were calculated from these data.

During the analysis of the above girder, width and height of the cross section, effective height of steel bars and prestressing strands as well as strength of concrete, steel bars and strands

Fig. 8: Calculated bending moment – curvature diagrams for beam type "4000" at different ages and humidity levels

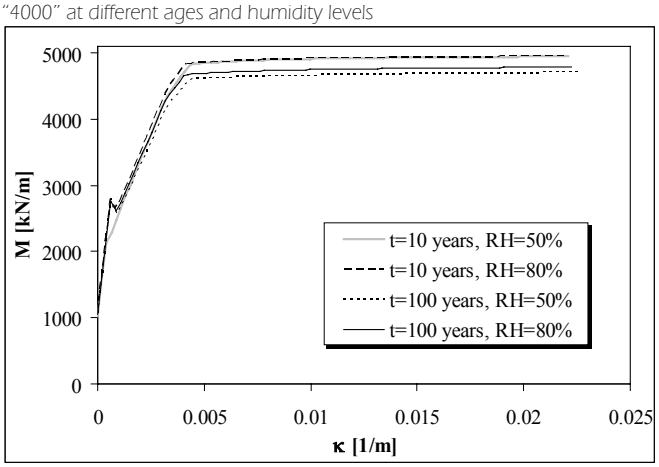

were considered as random quantities. Failure probability was calculated in different points of time. Selected times for the analysis were t = 10, 25, 50, 75 and 100 years. In each point of time, 3 different values of the ambient relative humidity were considered. The examined cases were: RH = 50%, 65% and 80%. The initial value of imposed load (q_0) acting to the structure was also changed during the analysis. Values q_0 = 16, 18, 20, 22 and 24 kN/m were used for beam "4000". Current values of input parameters and the load effect were calculated as a function of time, relative humidity and initial imposed load. To perform the calculations, the computer software *PFEM2008* was developed using the *Matlab*® software package. Using mean value and standard deviation of structural resistance and current load effect, the probability of failure was calculated in each case. Considering 5 different times, 3 humidity levels and 5 different values for initial imposed load, the number of runs was 5×3×5 = 75.

The flexural capacity of the beam was evaluated for each configuration of process parameters using the relevant Eurocode 2 standard. The effect of elapsed time and humidity level on the flexural behaviour of the cross-section is demonstrated by the corresponding bending moment-curvature (M-κ) diagrams on *Fig. 8*. It can be stated that the mean value of structural resistance decreases with the decrease of humidity level and progress of time, the rate of the decrease

Fig. 9: Change of the probability of failure in time in case of different initial imposed loads and different humidity levels

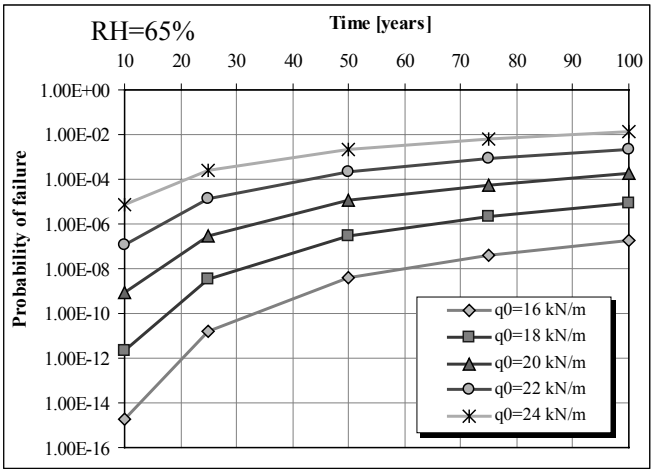

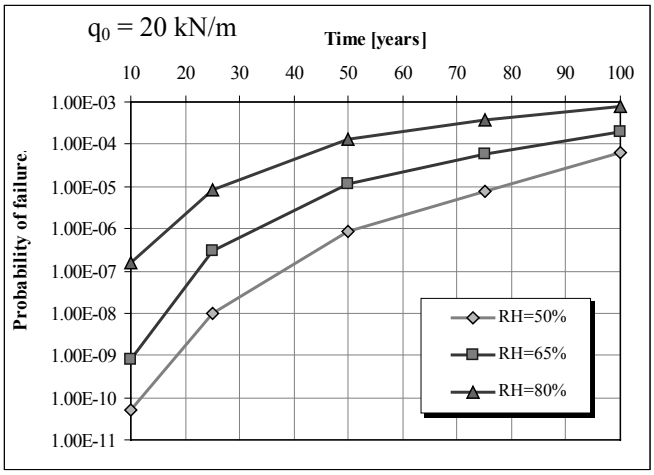

after 100 years was around 4-6%. The changes of mean value and relative standard deviation of load effect in case of beam "4000" over a period of 100 years were also evaluated. The standard deviation of load effect is increasing due to the increasing variation of geometrical sizes; however, relative standard deviation is decreasing in time because the growth

rate of mean value is higher. The probability of failure as a function of time, relative humidity and initial imposed load was calculated for the beam "4000" considering the effects mentioned above. Results of this analysis is presented in *Fig. 9*. The horizontal axis of the diagrams refers to the time elapsed since the manufacture of the beam, while the probability of failure is displayed on the vertical axis. In the first diagram, different curves refer to different levels of initial imposed load while the relative ambient humidity level was $RH = 65\%$. In the second diagram, different curves refer to different humidity levels by a constant initial imposed load $q_0 = 20$ kN/m. It can be stated that the probability of failure is increasing as time is passing by; it is increasing as the level of relative humidity is increasing, and it is increasing as the initial value of imposed load is increasing. The rate of increase is presented in the corresponding diagrams.

4.3. Application of the method for the purposes of durability-design

Results on the beam "4000" were also compared to the Eurocode 2 standard. The bending moment resistance calculated by the principles of Eurocode 2 (prEN 1992-1-1) was $M_{Rd} = 3611.3$ kNm. According to this bending moment resistance, the mean value of corresponding imposed load – assuming normal distribution and a relative standard deviation $\nu_q = 5\%$ – was: $q_{m.EC} = 16.37$ kN/m. The maximum applicable imposed load according to the introduced probabilistic method was $q_m = 18.13$ kN/m. This value was about 10% higher than the result obtained from calculation according to Eurocode 2. It can be stated that more economical design can be achieved by the use of the implemented durability-design method compared to Eurocode 2.

Besides the durability-design of new structural members, the implemented method is also suitable for the analysis of existing structural elements. The expectable service life or the necessary strengthening of old or damaged structural members can be designed by measuring the current values of structural geometry and strength of materials and by applying the described design method.

5. CONCLUSIONS

A design method based on probabilistic approach was presented. The introduced method is considering the creep and shrinkage of concrete, relaxation and carbonation induced corrosion of steel bars and tendons as well as the decrease of material properties and cross-sectional dimensions were considered during the calculations. The effect of standard deviations of different input parameters (height and width of cross-section, effective depth of tendons, strength of concrete and tendons) on the standard deviation of load carrying capacity were examined in case of several prefabricated, prestressed beams. The influence of the standard deviations of effective depth and concrete strength were the most significant, while change of the standard deviation of tendon strength had the least influence on the standard deviation of load carrying capacity in case of all examined beam types. Results of these comparisons can be used to assist the efforts on improving the durability of pre-cast concrete structural members. It was demonstrated that the failure probability of pre-cast, prestressed concrete beams is increasing as time is passing by; it is increasing as the level of relative humidity is increasing and it is increasing as the initial value of imposed load is increasing. Results on the analysis of the failure probability as a function of different parameters (time, relative humidity, initial imposed load) were presented graphically. Durability design or service life estimation of examined girders can be performed by the presented charts. In the case of the examined structural members, the application of this method results in a more economic design (higher load carrying capacity or smaller member sizes) than the use of the relevant Eurocode 2 standard.

7. REFERENCES

Augusti G. – Baratta A. – Casciati F. (1984), "Probabilistic Methods in Structural Engineering" *Taylor & Francis.*

Balázs, Gy. (2008), "Durability and methods for its improvement" (in Hungarian) *Betonszerkezetek tartóssága*. (Szerkesztők, Balázs Gy., Balázs L.Gy.) Műegyetemi Kiadó, Budapest, pp. 7-19.

Belytschko T. – Liu W. K. – Mani A. (1986), "Random Field Finite Elements" *International Journal for Numerical Methods in Engineering* 23, pp. 1831-1845.

Bojtár, I. – Gáspár, Zs. (2003), "Finite Element Method for engineers" (in Hungarian) *TERC Kft*, Budapest.

Bolotin V. V. (1970), "Statistical methods in structural mechanics" (in Hungarian) *Műszaki Könyvkiadó*, Budapest.

Eibl J. – Schmidt-Hurtienne B. (1996), "Grundlagen für ein neues Sicherheitskonzept", *Bautechnik* 72(8), pp. 501-506.

fib bulletin 34 (2006), "Model Code for Service Life Design", Sprint-Digital-Druck, Stuttgart.

Koris, K. (1996), "Safety of reinforced concrete beams subjected to combined stress" *Proceedings of the 1st International PhD Symposium*, (Ed. Balázs, Gy. L.) Budapest, pp. 7-11.

Koris, K. (1998), "Controlling of a prestressed concrete beam according to EC2" (in Hungarian) *Beton évkönyv 1998/1999*, főszerkesztő, Szalai Kálmán, 5.5 fejezet, p.88-116, Magyar Építőanyagipari Szövetség, Budapest.

Koris, K. (2004), "Durability-design of reinforced concrete traffic infrastructure" *Proceedings of the Second International Conference on Structural Engineering, Mechanics and Computation*, (Ed. Zingoni A.) Capetown, South Africa, 5-7 July, pp. 182-186.

Koris, K. (2007), "Durability-design of pre-cast concrete members" *Proceedings of the 3rd Central European Congress of Concrete Engineering "Innovative materials and technologies for concrete structures"*, (Eds. Balázs, Gy. L, Nehme, S. G.) Visegrád, Hungary 16-18 September, pp. 407-412.

Lawrence M. (1989), "An Introduction to Reliability Methods" *Computational Mechanics of Probabilistic and Reliability Analysis*, edited by Belytschko T. and Liu W. K., Department of Mechanical Engineering, Northwestern University, Elmpress International, Evanston.

Mistéth, E. (2001), "Design theory" (in Hungarian) *Akadémiai kiadó*, Budapest.

Zhao D. – Fan L. (2007), "Numerical analysis of carrying capacity deterioration and repair demand of existing reinforced concrete bridge" *Proceedings of the Fifth international conference on current and future trends in Bridge design, construction and maintenance*, Beijing, 17-18 September 2007, pp. 173-179.

Kálmán Koris (1970) civil engineer, MSC. Senior Assistant Professor at the Department of Structural Engineering, Budapest University of Technology and Economics. Research fields: safety of reinforced concrete structures, analysis of prefabricated, prestressed concrete structures, strengthening of structures. Member of the standardization subcommittee "NAD MSZ ENV 1992 Eurocode 2, Design of concrete structures". Member of the Hungarian Group of *fib*.

Dr. István Bódi (1954) civil engineer, post-graduate engineer in mathematics, PhD, Associate Professor at the Department of Structural Engineering, Budapest University of Technology and Economics. Research fields: Reconstruction and strengthening of reinforced concrete and conventional structures, modelling of timber structure joints. Has over 80 publications. Member of the ACI and the ACI Subcommitte#423 „Prestressed Concrete". Editorial member of the journal "Reinforced concrete structures". Member of the Budapest and Pest County Chamber of Engineers. President of the standardization committee Eurocode 5 - MSZ NAD. Member of the Hungarian Group of *fib*. Member of the „Schweizerische Arbeitgemeinschaft für das Holz" organisation and the Wood Industry Scientific Association.

PRESTRESSED AND NON-PRESTRESSED STRENGTHENING OF RC STRUCTURES WITH CFRP STRIPS


András Molnár – István Bódi

The use of CFRP (Carbon Fibre Reinforced Polymer) materials in the building industry is the result of international research of the past 20 years. Previously steel plates were used for the tension-side flexural strengthening of RC (Reinforced Concrete) beams. Nowadays the use of CFRP strips is predominant due to their beneficial properties: they may have higher modulus of elasticity and higher strength than steel, they are corrosion resistant and lightweight. The development of the technology for tensioning the CFRP strips makes the new material competitive in the field of prestressed strengthening as well. This paper gives details and discussion on the prestressing methods, equipments, and provides a parametric comparison which shows the benefits of the application of prestressed CFRP strips.

Keywords: carbon fibre, CFRP, prestressing, strengthening, RC

1. INTRODUCTION

The properties and possibilities of FRP (Fibre Reinforced Polymer) materials were discussed in several papers (Kollár, Kiss, 1997; Balázs, 1999), and Hungarian practical examples were also presented (Balázs, 1994; Kiss, Sapkás, 1999a). The Hungarian version of this journal (*Vasbetonépítés*) also reports continuously on the research results on the application of CFRP rods as normal or prestressing reinforcement (Majorosné, Balázs, Borosnyói, 2004). The in-situ application of CFRP strips is getting more and more wide-spread in Hungary, due to the ease of application, the low self-weight, and beneficial mechanical properties of CFRP strips. The effectiveness and feasibility of the prestressed strengthening is proven among many international examples by the in situ tensioning of a precast RC industrial floor in Győr: The RC plates had to be tensioned against each other because of the vibration-sensitivity of production technology.

CFRP materials may not only be used for flexural strengthening of RC structures, but also for increasing the shear, torsional and compressive capacity of load bearing elements of any construction material (steel, wood, glass).

Fig. 1: Comparison of σ–ε diagrams

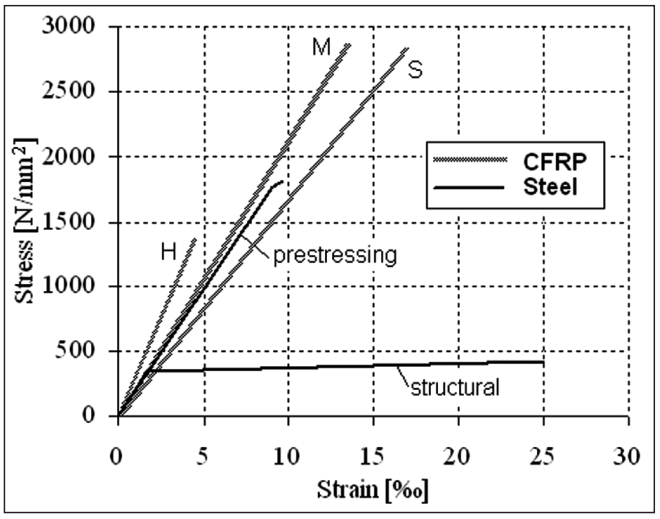

This paper aims to present the application of prestressed CFRP strips, which results in increased flexural capacity and stiffness, and reduced crack-width. In the further subsections only the flexural stiffness and capacity will be analysed in detail thus we will omit the word "flexural", while the stiffness of the CFRP strips ($\Sigma E_f A_f$) means their stiffness in tension. The strengthening method will be called *prestressed* strengthening throughout the paper, because the CFRP strips get used more efficiently by the application of a tension force prior to permanent anchoring to the structure.

After an introduction on the materials (*Section 2*) we give a short summary (*Section 3*) on the mechanical, constructive and environmental aspects of the design based, on international regulations (***fib*** Bulletin 14, 2001; DIB, 2002). In *Section 4* we give an overview on the different anchorage concepts. The second part of the paper (*Sections 7* to *9*) provides a parametric comparison of different strengthening methods based on their effect on the flexural stiffness and capacity.

2. MATERIALS FOR STRENGTHENING

Various types of CFRP (Carbon Fibre Reinforced Polymers) may be used for structural strengthening. In CFRP strips the carbon fibres (∅=6-10 μm) are arranged parallel in one direction, and they are embedded in epoxy resin. The longitudinal properties of strips are mainly influenced by the quality of fibres and the fibre volume content (usually about 60-70 V%). The embedding matrix positions, binds together and protects the fibres. The epoxy resin is a thermosetting polymer, which means that the change of shape of the strip after curing is impossible (unlike steel, which might be bended on-site).

The modulus of elasticity of CFRP strips may be higher than that of steel. The strip's linear-elastic behaviour lasts up to failure. A comparison of elastic and strength properties of different types of fibres can be found in *Tab. 1* and in *Fig. 1*. Other types of FRP and CFRP materials are reported in ***fib*** Bulletin 14 (2001) and Kollár, Kiss (1998).

The density of CFRP strips is 1.7 g/cm^3, which is less than one fourth of the density of steel (7.8 g/cm^3). The elastic

Tab. 1: Comparison of material properties

	Modulus of elasticity	Limit strain of elasticity	Ultimate tensile strain	Ultimate tensile strength
Types of FRP strips (Sika, 2005)	kN/mm^2	‰	‰	N/mm^2
CarboDur S	165	-	17	2805
CarboDur M	210	-	13.5	2835
CarboDur H	300	-	4.5	1350
Constructional steel (S350GD) (Dunaferr, 2008)	210	1.67	160	420
Tensioning steel (VT, 2007)	195	-	35	1770

behaviour of strips and their low weight facilitate their transportation and on-site application.

The following properties of CFRP materials justify their use in structural strengthening (***fib*** Bulletin 14, 2001):
- resistance to galvanic corrosion,
- no reduction in load bearing capacity under long-term loads,
- practically no creep,
- better fatigue-resistance than that of steel,
- no stress-corrosion.

3. GENERAL DESIGN ASPECTS

The design should consider all the factors that influence the durability of the RC structure, the CFRP strip and the bond and anchorage of the strips.

The health of the *RC structure* may be endangered by the corrosion of reinforcing bars, the carbonization of concrete, and the wide cracks. Before the structural strengthening work, all these defects have to be investigated and the needed repairs and protective interventions must be done.

The service life of *CFRP strips* should be investigated with extra care if exposition to UV light is present or the strengthened member is under extreme climatic conditions (***fib*** Bulletin 14, 2001; DIB, 2002). The CFRP strips are sensitive to physical damage, and they are located on the surface of members thus they should be protected against accidents and vandalism.

The bond quality is influenced by many parameters. In practice the most important ones are:
- high service temperature,
- moisture diffusion and pore pressure,
- freeze-thaw cycles,
- fire.

The design guideline for externally bonded FRP reinforcement (***fib*** Bulletin 14, 2001) gives a detailed analysis of these factors, and discusses the possible protection methods.

4. APPLICATION METHODS OF CFRP STRIPS FOR FLEXURAL STRENGTHENING

4.1 Bonded CFRP strips

The "traditional" way of structural strengthening with CFRP strips is the bonded application: the strips are applied parallel to the member axis on the tension side of the cross-section, glued on the pre-treated surface of the member with a special (in most cases epoxy-based) adhesive. In most cases the strips end up near to the supports, where the curvature of the member is small. This results in low interfacial stresses, which can be resisted by the bond.

The Near Surface Mounted (NSM) application of the strips is also an emerging technique: the stripes are glued in pre-cut grooves in the concrete cover. This offers protection for the strips against mechanical and thermal effects, and also has the advantage of a higher surface to force ratio, which means a higher safety against debonding (Szabó, Balázs, 2007).

4.2 Prestressed CFRP strips

The use of prestressed CFRP strips in flexural strengthening has two types, differing in the presence of bonding: the strips may be bonded to the RC structure after tensioning, or they may be only fixed at their both ends. The strengthening system is composed by:
- the structure to be strengthened,
- the CFRP strip,
- the connection of these (anchorage device, bonding).

The most sensitive detail of the system is the anchorage. The difficulties are much higher than in case of steel tensioning systems because of the special structure of the strip. The tensile forces are carried by the carbon fibres, which are embedded in epoxy resin, thus:
- the anchorage of the single fibres is practically impossible,
- the transversal compression may damage the CFRP strip.

The problem of the anchorage is present in both cases (bonded and non-bonded application), because while the tensile force is applied by the hydraulic jack, the strip is only clamped at its ends. The bonding of the strip is made after the application of the full tensile force.

The gradiented anchorage of the prestressing force is also possible. That means that the tensile force is gradually decreased to the strip end, and thus the peak values of interfacial stresses are avoided at strip end. There are attempts to develop devices for this type of anchorage, but by now, no commercially available solution exists (Stöcklin, Meier, 2001).

The role of the anchorage is to transfer the tensile force from the strip to the strengthened member. This happens usually in two steps. In the first step the anchorage device takes the force from the strip: this can be realised by clamping the strip (that means shear stresses on the interface), or by widening the end of the strip. In the second step the anchorage device transfers the force to the strengthened member.

4.2.1 Anchorage by active compressive force

To be able to anchor high tensile forces high shear stress values are needed – adhesion and friction or their combination may provide it (Andrä, König, Maier, 2001). For the development of friction the two influencing factors are roughness of the surfaces and transversal compressive force.

The company Sika Ltd. developed an anchorage device called LeobaCarboDur (Sika, 2004) (*Fig. 2*). The CFRP strip (**e**) is clamped between the steel anchor plates by high strength stressed screws (**a**). This method is called anchorage with *active* transversal force. Beside the screws, the anchorage is glued too, which has two main reasons: the bond contributes to the load bearing capacity, and the adhesive layer levels the

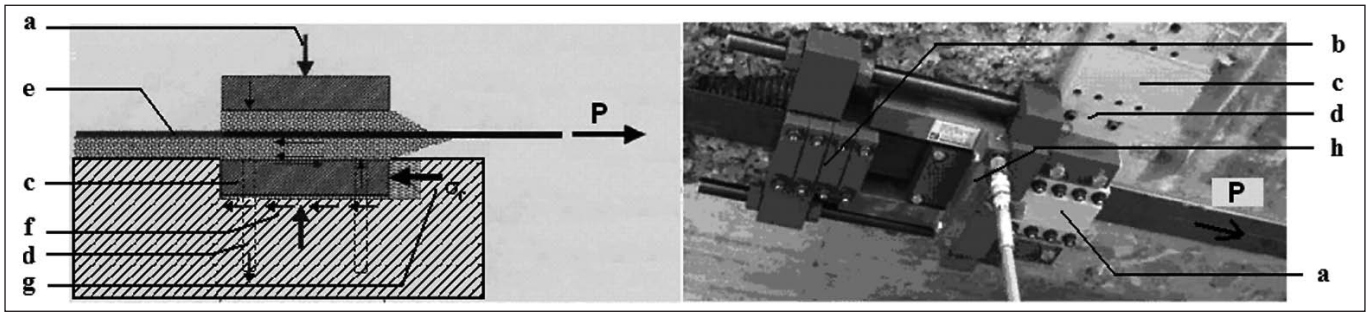

Fig. 2: *Sika Leoba CarboDur LCII anchorage, tensioning*

unevenness of the surfaces, so that constant compressive force may develop.

The base plate (**c**) is recessed into the concrete. It is glued to the ground material by adhesive mortar (**f**), and since the gaps are filled with low-shrinkage mortar, the contact stress (**g**) of the base plate on the concrete contributes to the load bearing capacity. Since the axis of the stripe is shifted from the concrete surface a small tilt-up moment occurs, which is balanced by bolts drilled into the concrete (**d**).

The process of the mounting has the following steps. After the surface preparation, the base plates are installed. Both ends of the CFRP strip are clamped: the fixed end is clamped and glued to its position, and the other end is clamped to the tensioning anchor (**b**). After completion of the tensioning with the hydraulic jacks (**h**) the end anchorage is glued and fixed with screws. Then after the curing of the adhesive, the force is transferred to the end-anchorages by releasing the force of the hydraulic jacks. The tensioning anchor and the hydraulic jack are demounted and used for the next CFRP strip.

4.2.2 Anchorage by passive compressive force

The company S&P Reinforcement also developed an anchorage device (Suter, Jungo, 2001). The first step of the strengthening process is the laying on of the adhesive, and the positioning of the CFRP strip. This is followed immediately, within the open time of the adhesive, by the tensioning of the strip by hydraulic jacks. Than the strip ends are covered by steel plates, which are bolted to the concrete structure. After the curing period the hydraulic jacks are released, which causes a crack in the concrete in the strip-end zone. The opening of the crack is withstood by the bolted steel plate, thus a passive compressive force occurs, which develops a sufficient amount of friction to hinder the withdrawal of the CFRP strip. To improve the sustainability, the latest versions of this anchorage use stressed screws at the end-anchorage. This way of anchorage transfers the strip force to the concrete structure in one single step.

4.2.3 Anchor head on the strip end

The Swiss company StressHead together with Sika Ltd. developed this technology (StressHead, 2005). The CFRP strip is cut to its specified length in the factory, and non-metallic (CFRP) anchor heads are formed at both ends, with a maximum load bearing capacity of 220 kN. This device was originally developed for prestressed strengthening without bond, but the bonded application is possible as well. The force transfer might be resolved by steel anchorages offered by the manufacturer (see *Fig. 3*), but in case of special projects, the designer may choose the place and art of anchorage freely. The CFRP strips may be bended, so the prestressing force might change its direction with the help of appropriate structural details.

The fixed end is anchored first, than they apply the tensioning force by hydraulic jacks, and they fasten the free end at its final position. Screw bolts may ensure that the displacement during the tensioning process can take place, and the anchorage is adjustable.

5. REQUIREMENTS ON THE STRUCTURE TO BE STRENGTHENED

For a good bonding, the suitability of concrete substrate has to be checked: the tensile strength of the concrete has to be 1.5 N/mm^2 at least. The permissible unevenness of the concrete surface is 10 mm on a 2.0 m base and 4 mm on a 0.3 m base (***fib*** Bulletin 14, 2001).

To ensure reliable transfer of the prestressing force, appropriate anchorage solution has to be chosen. Local failure modes (splitting, shear failure) of the RC structure must be avoided by appropriate structural detailing (StressHead, 2005).

Fig. 3: *Anchorage solutions type StressHead: adjustable and fixed (StreesHead, 2005)*

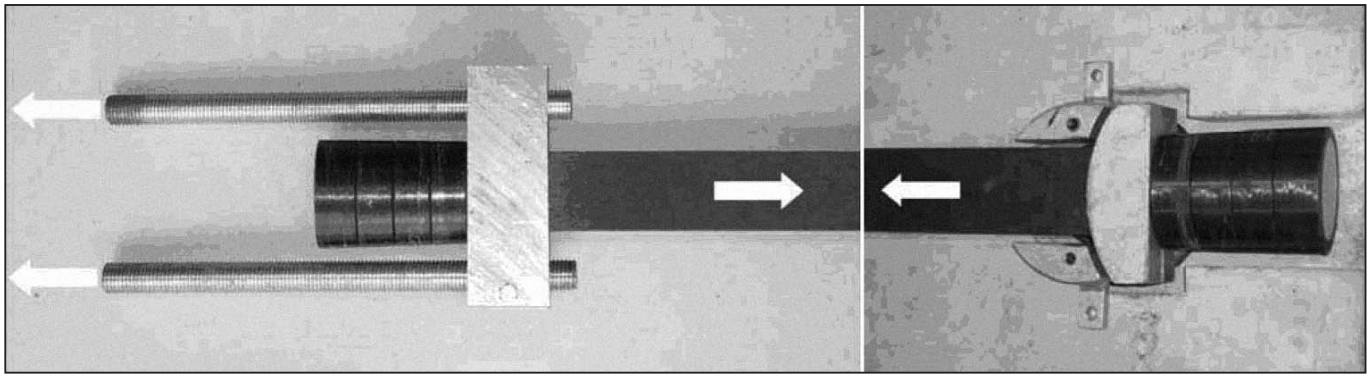

6. MAIN ASPECTS OF DESIGN OF STRUCTURAL STRENTHENING

During the service life of a structure the change of use may cause growing loads, or it may require the altering of the static system. The aging of materials and the environmental conditions may lead to decreasing structural value. These are possible causes of insufficient load bearing capacity, stiffness and too wide cracks of RC structures. Structural strengthening aims to resolve these problems. Bonded CFRP strengthening of RC members can easily raise the load-bearing capacity, thus the requirements of serviceability tend to become determining. Application of an eccentric prestressing force by the means of CFRP strips may overwhelm the excessive deformations and crack-widths.

It is of high importance to keep the ductility of failure when strengthening a structure, which means the prediction of failure by large deformations. To ensure this, the design of the strengthening of RC structures should comply with the regulation of EC 2: in order to enable high plastic strains in the rebars in tension, the location of neutral axis at failure should fulfil the $\xi < 0.45$ requirement (***fib*** Bulletin 14, 2001). The ***fib*** Bulletin (2001) says that if the design load bearing capacity of the strengthened member is at least 1.2 times higher than the design action, the requirement on the failure ductility might be passed by. This may easily happen, if the governing design criterion is one of the serviceability limit states.

An important governing design rule is that the strengthened structure should not have higher load bearing capacity than twice of the original (***fib*** Bulletin 14, 2001).

At the design of structural strengthening the full loading history and the loads at the time of the strengthening works must be considered:

– at the time of strengthening, the strain in the CFRP strip differs from that of the RC structure, and this strain-difference is conserved by the bond,
– the RC member may have flexural cracking due to pre-strengthening loads.

7. FAILURE MODES OF STRENGTHENED MEMBERS

The failure modes of RC beams, strengthened by bonded CFRP strips can be grouped in two main categories:

a) There is an ideal bond between the CFRP strip and the RC beam until the failure. Possible failure modes are the crushing of concrete, the rupture of rebars in tension and the rupture of CFRP strips in tension.

b) The connection between the CFRP strip and the RC member brakes partly or fully. This is called *delamination* or *debonding* of the CFRP strips. The debonding may occur at different positions of the cross-section (at strip-glue or glue-concrete interface, or inside the strip or glue or concrete layer) and at different positions in longitudinal direction (e.g. at strip end or at flexural cracks). The experimental study and the development of appropriate design models is still not a fully resolved topic (***fib*** Bulletin 14, 2001; DIB, 2002; Kishi, Mikami, Kurihashi, Sawada, 2006; Neubauer, Rostásy, Budelmann, 2001). The calculations presented in this paper take in consideration the debonding of the CFRP strips by limiting the strain of the strips after bonding up to 8 ‰. By this, we define a limit for the opening of the cracks, since they might serve as initiation for the debonding (***fib*** Bulletin 14, 2001).

An important question is the integrity of the CFRP strip itself: the proper composite action of the carbon fibres and the epoxy matrix. The bending design of the strengthened member is only part of the work has to be done: the shear and torsional capacity has to be checked as well. If it turns out to be necessary, appropriate strengthening has to be planned for these actions too. As mentioned earlier, this paper only deals with the flexural design of the strengthening.

8. COMPARATIVE STUDY OF STRENGTHENING METHODS

We calculated the flexural capacity, the bending stiffness and the M-κ diagram for CFRP striped RC cross-sections with usual assumptions for RC structures: plain strain profile of cross-section, neglecting the concrete in tension. The equations for bonded strengthening are presented and discussed in the ***fib*** Bulletin 14 (2001) and by Kiss and Sapkás (1999b) in detail. Their calculation method was extended to take the eccentric tensioning force in consideration, and instead of using the branching analytical calculation method we developed a numerical approach, with the location of the neutral axis as main variable.

The compared strengthening *methods* are:

„***B***" – bonded CFRP strips without prestressing,
„***PB***" – prestressing CFRP strips bonded to the member on full length,
„***P***" – prestressing CFRP strips without bond.

In the following parts of the paper we will refer to the *method* of application with the above notations.

8.1 Cross-sectional and material data

The aim of the calculations is the comparison of different strengthening methods. It has been done by comparative calculations on a normally reinforced T-cross-section. The investigated cross-section is shown in *Fig. 4*. In the RC cross-section there are 6 Ø20 rebars on the tension side and 2 Ø16 rebars on the compression side.

The material models and data comply with the MSZ EN standards for the concrete and rebars (Farkas, Huszár, Kovács, Szalai, 2006), and with the ***fib*** Bulletin 14 (2001) for the CFRP

Fig. 4: The investigated cross-section

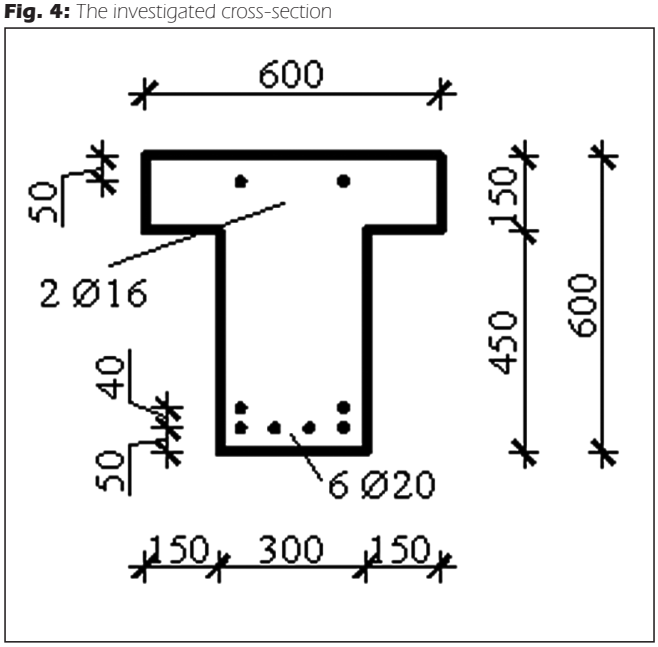

strips. The calculations apply the following material grade and material-models:
– concrete: C25/35, bilinear material model,
– rebars: B.60.50, elastic-plastic bilinear material model,
– CFRP strips - elastic-brittle material model

Sika® CarboDur® "S" (E_f=165 GPa) in case of prestressed strengthening (***P*** or ***PB***),

Sika® CarboDur® "M" (E_f=210 GPa) in case of bonded strengthening (***B***).

8.2 Parameters of the comparative calculations

The strengthened cross-section remains the same in all cases. We vary the following parameters of the strengthening:

(all parameters are defined exactly in *Section 12 – Notation*)
– number of applied strips (n),
– sum of the stiffness of applied strengthening strips ($\Sigma E_f A_f$),
– the magnitude of applied prestressing force (P_f).

The applied strengthening influences the following parameters:
– the moment-curvature diagram,
– the flexural capacity of the cross-section (M_{ult}),
– relative value of the flexural capacity increase (μ_{ult}),
– the flexural stiffness of the cross-section (EI_{ser}),
– the relative value of flexural stiffness increase (λ_{ser}),
– the ductility of failure (δ_t and δ_a).

We calculate the moment-curvature diagram and the flexural stiffness with the characteristic value of material parameters, and the ultimate value of bending moment is calculated with the design values of material parameters.

In case of prestressed strengthening, the moment-curvature diagram is "shifted" (see *Fig. 5*, ***P***) thus the effective stiffness is not well described by the gradient of the diagram. Therefore we use the bending moment (M_{ref}) value corresponding to a characteristic curvature (κ_{ref}) in order to compare the flexural stiffness reached with different strengthening methods (see *Fig. 8*). The characteristic curvature is set to represent the curvature of the non-strengthened cross-section in serviceability limit state.

In the following sections we analyse strengthening *cases* (***a*** to ***i***) leading to a prescribed change in a selected parameter, thus the changes in other parameters can easily be compared. The prescribed parameters are:
– the increase of flexural capacity (*Section 8.3*),
– the sum of the stiffness of strengthening strips and the prestressing force (*Section 8.4*),
– the increase of flexural stiffness (*Section 8.5*).

At the beginning of *Section 8* the strengthening methods (***B*** – ***PB*** – ***P***) were defined. With the above listed three types of comparison we get 9 *cases*. Every *case* is defined by the *method* and the *layout* data, which consist of the amount of CFRP strip and the magnitude of prestressing force (see *Tab. 2-4*).

8.3 Strengthening cases with prescribed increase of flexural capacity

The possible increase in flexural capacity is (among technological aspects) limited by the flexural capacity of the cross-section for negative bending moments. The possible maximum of prestressing force (P_f=337.8 kN) for the prestressed, non-bonded strengthening (***P***) is determined by this limit, and it defines the reached flexural capacity increase in *case* ***c***. The layout of the other strengthening cases (***a*** and ***b***) is calibrated to reach the same increase. For the *cases* ***a*** to ***c*** the layout and the resulting cross-sectional parameters are listed in *Tab. 2*, the corresponding moment-curvature diagrams are plotted in *Fig. 5*.

The values of *Tab. 2* show, that to reach a prescribed increase of flexural capacity, the pre-stressed and bonded (***PB***) type of strengthening gives the most favourable material consumption. If the reached effective flexural stiffness values are compared, significant differences may be found:
– the ***P*** (only prestressed) strengthening (*case* ***c***) yields the highest increase: 41%,
– the ***PB*** (prestressed and bonded) and ***B*** (only bonded) strengthening (*cases* ***b*** and ***a)*** yield significant lower increase in effective flexural stiffness: 24% and 13% respectively.

When designing a strengthening, the fact that the limit states of serviceability tend to become governing should always be considered. The comparison presented in *Section 8.5* aims to compare the strengthening methods from this point of view.

To be able to compare the above presented strengthening methods (***a-b-c*** *cases*), the moment-curvature diagrams are plotted in *Fig. 5*. The difference between the strengthening methods and the effect of strengthening on the ductility of failure is clearly visible on the diagrams.

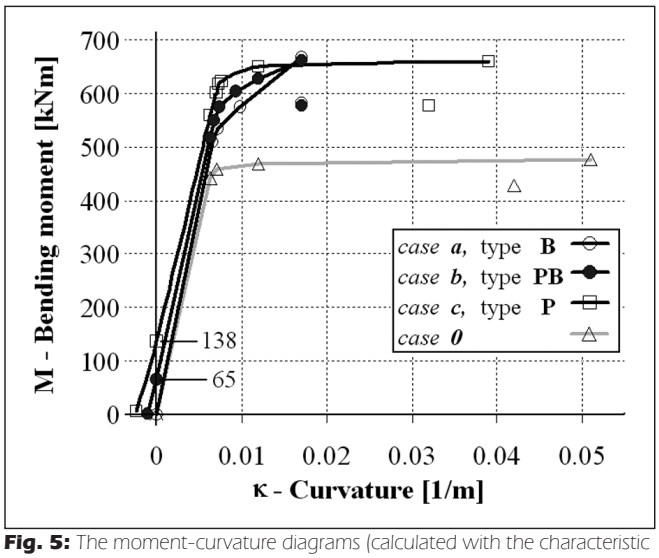

Fig. 5: The moment-curvature diagrams (calculated with the characteristic value of material parameters) and points corresponding to flexural failure (calculated with the design value of material parameters) of the cross-section with layouts of Tab. 2.

8.3.1 Type of flexural failure

The numerical analysis of the cross-sections established the following failure modes:
case ***0*** – crushing of concrete in compression,
case ***a, (B)*** – reaching the limit value of 8‰ in the CFRP strip,
case ***b, (PB)*** – reaching the limit value of 8‰ in the CFRP strip,
case ***c, (P)*** – crushing of concrete in compression.

8.3.2 Effect of strengthening methods on the moment-curvature diagram

In this subsection, the moment-curvature (M-κ) diagrams are analysed and compared with the M-κ diagram of the non-strengthened cross-section (*case* ***0***), separately for the *cases*

Tab. 2: Prescribed increase of ultimate flexural capacity (layout and resulting cross-sectional parameters)

case		Type of strengthening	Strengthening strips			Force	Fl. capacity		Fl. stiffness		Ductility	
			n	A_f (1pcs)	$\Sigma E_f A_f$	P_f	M_{ult}	μ_{ult}	M_{ref}	λ_{ser}	δ_{cap}	δ_{def}
			[pcs]	[mm^2]	[MN]	[kN]	[kNm]	[%]	[kNm]	[%]	M_{ult}/M_y	κ_{ult}/κ_y
a	***B***	Only bonded	3	72	47.5	-	582.1	36	343.9	13	1.25	2.39
b	***PB***	Prestressed and bonded	1	144	23.8	160	576.7	35	377.3	24	1.20	2.52
c	***P***	Only prestressed	2	144	45.4	337.8	575.7	35	429.1	41	1.05	5.15
0		Non-strengthened	none				427.4		305.3		1.04	7.36

Tab. 3: Strengthening cases with equal stiffness of strips and equal prestressing force (layout and resulting cross-sectional parameters)

case		Type of strengthening	Strengthening strips			Force	Fl. capacity		Fl. stiffness		Ductility	
			n	A_f (1pcs)	$\Sigma E_f A_f$	P_f	M_{ult}	μ_{ult}	M_{ref}	λ_{ser}	δ_{cap}	δ_{def}
			[pcs]	[mm^2]	[MN]	[kN]	[kNm]	[%]	[kNm]	[%]	M_{ult}/M_y	κ_{ult}/κ_y
d)	***B***	Only bonded	1	144	23.8	-	506.8	19	325.5	7	1.15	2.27
e)	***PB***	Prestressed and bonded	1	144	23.8	210	598.0	40	396.0	30	1.10	2.49
f)	***P***	Only prestressed	1	112	23.5	210	474.1	11	380.6	25	1.02	4.43
0)		Non-strengthened	none				427.4		305.3		1.04	7.36

a to ***c*** (*Tab. 2*).

*case **a**, **(B)*** – The stiffness of the tension zone is enlarged by the bonded CFRP strips, thus the bending moment corresponding to the yielding of rebars in tension grows. The gradient of the diagram after the yielding point of rebars remains much higher than in *case **0***. The bending moment is increasing until failure, because the CFRP strips remain elastic to the failure.

*case **b**, **(PB)*** – The prestressing force has different effects. Firstly, a bending moment of 65 kNm corresponds to the 0-curvature deformation state (see *Fig. 5*, intersection of diagram and vertical axis). Secondly, the M-κ diagram is non-linear on its full length. Thirdly, the M-κ diagram runs similarly to the diagram of the only bonded (***B***) *case **a***, but it is shifted in vertical direction.

*case **c**, **(P)*** –The M-κ diagram runs similarly to the diagram of the non-strengthened *case **0***, but it is shifted in vertical direction so, that a bending moment of 138 kNm corresponds to the 0-curvature deformation state (see *Fig. 5*, intersection of diagram and vertical axis). However, the alteration of the diagram is not a simple shifting, because the prestressing force is balanced by compressive stresses of concrete and that leads to a change in shape of the diagram at the limit of elasticity (see *Fig. 5*). On the other hand the curvature corresponding to the point of failure is lower than in *case **0*** (the increased compressive stress leads to earlier failure).

8.3.3 Ductility of failure

The ductility of the flexural failure is defined through the characteristics of the plastic section of the moment-curvature diagram. In *Tab. 2* two representative parameters are listed: the plastic deformation capacity (δ_{def}) and the plastic flexural capacity (δ_{cap}). The values, and the moment-curvature diagrams (*Fig. 5*) show that in case of bonded strengthening methods the delamination causes much higher cut in plastic deformation capacity (δ_{def} = 2.39 for *case **a**,* type ***B***, and δ_{def} =2.52 for *case **b***, type ***PB***) than in case of only prestressed (***P***) strengthening (δ_{def} = 5.15 for *case **c***) compared to the non-strengthened *case **0*** (δ_{def} = 7.36). At the same time the development of load-bearing capacity is more favourable in case of strengthening methods with bond: the relation of failure moment to yielding moment (δ_{cap}) is in case of the bonded strengthening (***B***, *case **a***) 1.25 and in case of the bonded and prestressed strengthening (***PB***, *case **b***) 1.20. This parameter has a value of 1.04 in case of non-strengthened *case **0*** and 1.05 in case of only prestressed (***P***) *case **c***. The requirements (see *Section 6*) prescribed in the design guideline (***fib*** Bulletin 14, 2001) are fulfiled by all strengthening methods.

8.4 Strengthening cases with equal stiffness of strips and equal prestressing force

In this comparison each strengthening *case* (***d*** to ***e***) has the same total normal stiffness of strips (ΣEA) and both prestressed strengthening layouts have the same magnitude of prestressing force (P_f). For these cases the layout and the resulting cross-sectional parameters are listed in *Tab. 3*, the corresponding moment-curvature diagrams are plotted in *Fig. 6*.

The moment-curvature diagrams show clearly the superposition of the load-bearing capacity increasing components: the only bonded (***B***) strengthening method increases the flexural stiffness (*case **d***), the only prestressed (***P***) strengthening method "shifts" the diagram upwards (*case **f***), the prestressed and bonded (***PB***) strengthening method superposes these two effects (*case **e***).

The increase in flexural capacity and effective flexural stiffness also follows the previous logic: they reach their highest value in case of the prestressed and bonded (***PB***) strengthening (*case **e***) (see *Tab. 3*). If the strengthening methods with tension (***P*** and ***PB***) are compared, it can be seen, that the difference between the increase in flexural capacity (40% and 11%, respectively) is much higher than the difference between the increase in effective flexural stiffness (30% and 25%, respectively) (see μ_{ult} and λ_{ser} values of *Tab. 3*).

The analysis of moment-curvature diagrams (*Fig. 6*) and that of failure modes might happen the same way as it had been done in *Section 8.3* for the diagrams in *Fig. 5*.

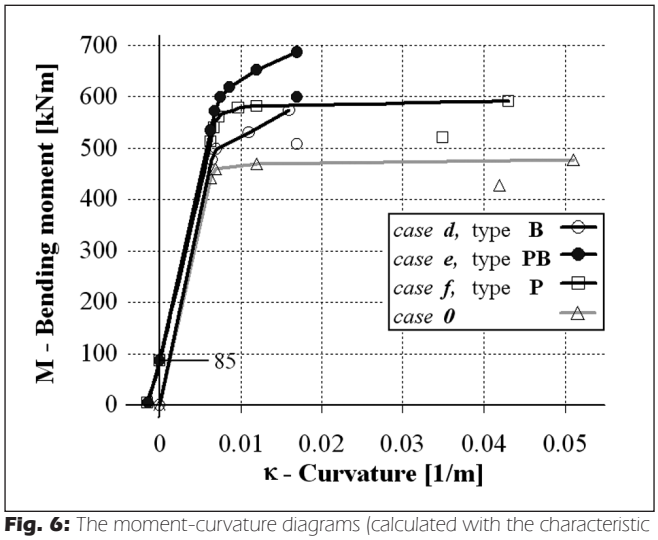

Fig. 6: *The moment-curvature diagrams (calculated with the characteristic value of material parameters) and points corresponding to flexural failure (calculated with the design value of material parameters) of the cross-section with the layouts of Tab. 3.*

8.5. Strengthening cases with the same increase in effective flexural stiffness

This comparison aims to show the difference in needed strengthening amount of different strengthening types, if a prescribed increase of the effective flexural stiffness is defined. For *cases* ***g*** to ***i*** the the layout and the resulting cross-sectional parameters are listed in *Tab. 4*, the corresponding moment-curvature diagrams are plotted in *Fig. 7*.

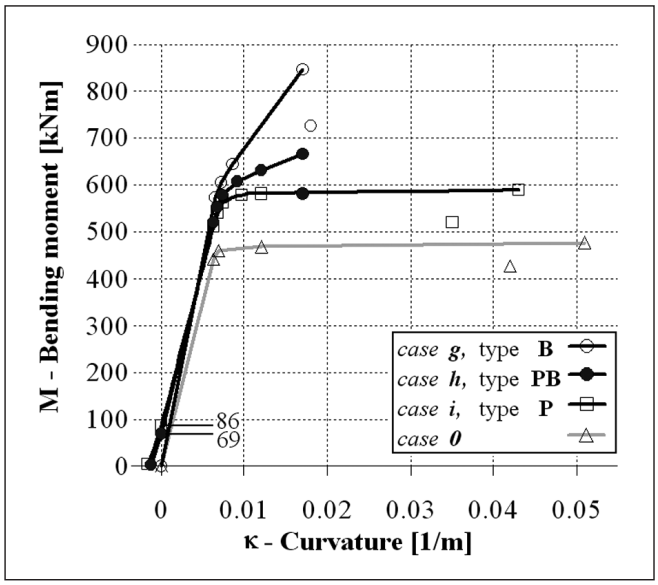

Fig. 7: *The moment-curvature diagrams (calculated with the characteristic value of material parameters) and points corresponding to flexural failure (calculated with the design value of material parameters) of the cross-section with layouts of Tab. 4.*

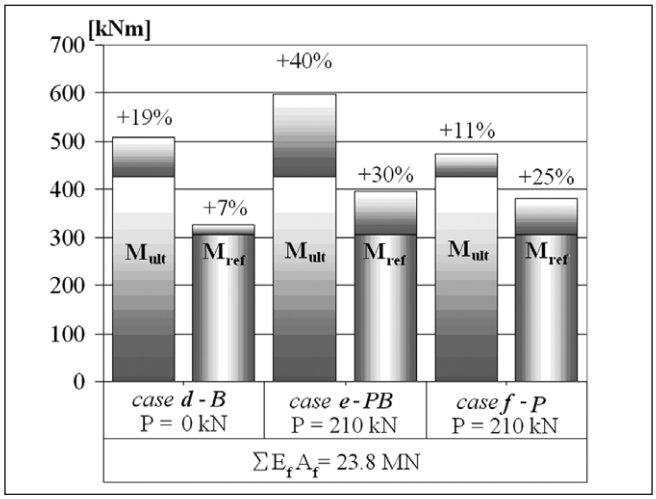

Fig. 8: *Effect of the same amount of CFRP strips and same magnitude of prestressing force, applied by different methods (Section 8.4, Tab. 3)*

In *Tab. 4* it is worth to compare the needed amount of strips and the magnitude of prestressing force. To reach an effective stiffness increase of 25% of the given cross-section by only bonded (***B***) strengthening (*case* ***g***), approximately 4 times more CFRP strips are needed than in the cases that apply prestressing force (***PB*** and ***P***, *cases* ***h*** and ***i***). The difference between the prestressed strengthening methods is not that high: if the same amount of strips is applied, a prestressing force of 170 kN is needed in case of prestressed and bonded (***PB***) strengthening (*case* ***h***), and a prestressing force of 210 kN is needed in case of only prestressed (***P***) strengthening (*case* ***i***).

When the cross-section is strengthened to reach a defined effective stiffness, the flexural capacity might be increased in excess. In *case* ***h*** the bonded and prestressed (***PB***) strengthening leads to a 24% increase of effective flexural stiffness. If we consider the design criterion of unchanged deflections, a load increase of app. 24% would be possible. At the same time, we reached a 70% increase of flexural capacity which would remain mainly unused.

9. SUMMARY OF RESULTS

In this section a short summary of the results of the comparative calculations referred to the given normal reinforced T cross-section is given:

- If we apply a CFRP strip with 144 mm² cross-sectional area, prestressed with a force of 160 kN and bonded (***PB***) to the RC member (*case* ***b***), the other methods (***B*** and ***P***) need twice as much amount of CFRP strips (*case* ***a***), and prestressing force (*case* ***c***) to reach the same increase in flexural capacity (*Section 8.3, Tab. 2.*),
- If the same amount of CFRP strips and the same magnitude

Tab. 4: *Prescribed effective flexural stiffness increase (layout and resulting cross-sectional parameters)*

case		Type of strengthening	Strengthening strips			Force	Fl. capacity		Fl. stiffness		Ductility	
			n	A_f (1pcs)	$\Sigma E_f A_f$	P_f	M_{ult}	μ_{ult}	M_{ref}	λ_{ser}	δ_{cap}	δ_{def}
			[pcs]	[mm²]	[MN]	[kN]	[kNm]	[%]	[kNm]	[%]	M_{ult}/M_y	κ_{ult}/κ_y
g)	***B***	Only bonded	4	105	88.2	-	726.0	70	379.0	24	1.39	2.34
h)	***PB***	Prestressed and bonded	1	144	23.8	170	580.9	36	381.3	25	1.20	2.51
i)	***P***	Only prestressed	1	144	23.8	210	520.3	22	380.6	25	1.02	4.43
0)		Non-strengthened	none				427.4		305.3		1.04	7.36

of prestressing force are applied to the cross-section by different strengthening types, we obtain the results summarized in *Fig. 8*. The difference between the effect on flexural capacity and effective flexural stiffness in case of different strengthening methods (***B***, ***PB***, ***P***) is clearly visible. The only bonded (***B***) strengthening (*case **d***) gives the smallest increase in effective flexural stiffness, and the highest difference between the increase in flexural stiffness and flexural capacity. The bonded and prestressed (***PB***) strengthening (*case **e***) gives the highest increase for both parameters (M_{ult} and M_{ser}), while in case of the only prestressed (***P***) strengthening (*case **f***) the increase in effective flexural stiffness is higher than the increase in flexural capacity (*Section 8.4*, *Tab. 3*).

– If a 25% increase of effective flexural stiffness is prescribed then a CFRP strip of 144 mm^2 cross-section and a prestressing force of 170 kN is needed in case of prestressed and bonded (***PB***) strengthening (*case **h***). To reach the same effect on effective flexural stiffness in case of the only bonded (***B***) strengthening, 4 times higher total stiffness of CFRP strips is needed (*case **g***), and in case of the only prestressed (***P***) strengthening the applied CFRP strip may remain the same, but it should be prestressed at 210 kN (24% higher) (*case **i***) (*Section 8.5*, *Tab. 4*).

10. CONCLUSIONS

The paper discussed the special requirements on anchorage systems for CFRP and presented the commercially available systems (*Section 4.2*) whose suitability has been shown by experiments and practical applications.

In case of the studied T cross-section we have shown, that the most efficient material consumption is provided by the prestressed and bonded strengthening. The growth of flexural capacity of the cross-section is promoted mainly by the normal stiffness of bonded CFRP strips. The effective flexural stiffness of the cross-section may be increased foremost by the prestressed application of the strips (see *Section 8* and *9*).

In case of over-reinforced cross-sections the tension-side-strengthening and the applied prestressing force contribute to the increase of compressive stresses and thereby speed up the crushing of the concrete. Therefore, in case of over-reinforced cross-sections the compression-side strengthening should be preferred and applied. The available prestressing technologies are not economically suitable for strengthening of thin (< 25 cm) slabs, since the anchorage systems are designed for high tension forces, and the slabs only have a low negative bending moment capacity.

Section 3 points out that the design should not only consider the requirements of ULS and SLS, but also the environmental effects, the accidental case of fire and the practical feasibility.

The prestressed applications of CFRP strips may be competitive with steel tendons at strengthening tasks, thanks to their lower self-weight, high tensile strength, low creep and favourable fatigue properties. The prestressed CFRP strips may be bonded as well. In case of prestressed and bonded application the bond is a very sensitive point of the system: mechanical and temperature effects might damage the strengthening. On the other hand, the bond between the strip and the member contributes effectively to the increase of flexural capacity and stiffness.

11. ACKNOWLEDGEMENTS

The authors wish to express their gratitude to András Berecz (senior manager of Sika Hungary Ltd.). He provided the authors up-to-date technical data and valuable information on structural strengthening methods and shared experiences of practical applications. The authors whish to express thanks to Dr. László Erdélyi (English language reviewer) on behalf of his efforts and valuable advices, which contributed to the finishing of the English version of this paper.

12. NOTATION

n	Number of applied strips: pcs
A_f	Cross-sectional area of one strip: mm^2
$\Sigma E_f A_f$	Total normal stiffness of applied strengthening strips: kN
EI_{ser}	The effective flexural stiffness, which is defined as the tangent of the line connecting the origin of moment-curvature plane with the point corresponding to the reference curvature (κ_{ref}, M_{ref}): kNm^2
M_{ref}	The bending moment value corresponding to the κ_{ref} reference curvature: kNm
M_{ult}	Value of bending moment at failure of cross-section: kNm
M_y	Value of bending moment at the yielding of rebars in tension: kNm
P_f	The magnitude of total prestressing force: kN
δ_{def}	Parameter for the plastic deformation capacity, defined by the quotient of curvature at failure and curvature at yielding of rebars in tension.
δ_{cap}	Parameter for the plastic flexural capacity, defined by the quotient of bending moment at failure and bending moment at yielding of rebars in tension.
κ_y	Value of curvature of cross-section at yielding of the rebars in tension: 1/m
κ_{ref}	Reference curvature for comparison of effective bending stiffness values, defined as 80% of the κ_y value for non-strengthened cross-section: 1/m
λ_{ser}	The increase of effective bending stiffness reached by the actual strengthening case in percentage of the effective bending stiffness of the non-strengthened cross-section
μ_{ult}	The increase of bending moment at failure reached by the actual strengthening case in percentage of the bending moment at failure of the original cross-section.

13. REFERENCES

Andrä, H-P., König, G., Maier, M. (2001), „Einsatz vorgespannter Kohlenfaser-Lamellen als Oberflächenspannglieder“, *Beton- und Stahlbetonbau* 96 2001 Heft 12, pp. 737-747.

Balázs, L. Gy. (1999), „Strengthening with carbon fibres – Hungarian experiences“ (In Hungarian), *Vasbetonépítés* 1999/4, pp. 114-122.

Balázs, L. Gy. (1999), „Sika CarboDur CFRP structural strengthening system – design and application manual“ (In Hungarian), Sika Hungária Kft.

Borosnyói, A., Balázs, L. Gy. (2002), „Bond of non-steel (FRP) reinforcing bars in concrete“ (In Hungarian), *Vasbetonépítés* 2002/4, pp. 114-122.

Borosnyói, A. (2006), „FRP reinforced concrete – brittle or ductile behaviour?” (In Hungarian), *Vasbetonépítés* 2006/3, pp. 71-80.

DIB (2002) „Allgemeine Bauaufsichtliche Zulassung, Nr.: Z-36.12-29: Verstärkungen von Betonbauteilen durch schubfest aufgeklebte Kohlefaserlamellen Sika CarboDur”, Deutsche Institut für Bautechnik, 33 p.

Dunaferr (2008), „Products of ISD Dunaferr Zrt.” (In Hungarian), http://www.dunaferr.hu/02-termekek/termekeink21.htm, 2008.05.02.

Farkas, Gy., Huszár, Zs., Kovács, T., Szalai, K. (2006), „Eurocode-based design of concrete structures” (In Hungarian), Terc Kft., Budapest

fib Task Group 9.3 (2001) „Externally bonded FRP reinforcement for

RC structures", EBR working party of ***fib,*** 138 p.
Kishi, N., Mikami, H., Kurihashi, Y., Sawada, S. (2006), „Experimental study of debond-controlling method for FRP sheet of flexural reinforced RC beams", IABSE Report Vol. 92., Responding to Tomorrow's Challenges in Structural Engineering, IABSE Symposium Budapest, 13-15 September 2006, pp. 286-287
Kiss, R. M., Sapkás, Á. (1999a), "Strengthening of a RC slab with CFRP stripes" (In Hungarian), *Magyar Építőipar* 1999/3-4., pp. 113-116.
Kiss, R. M., Sapkás, Á. (1999b), „Strengthening of RC beams using the system Sika CarboDur®" (In Hungarian), *Magyar Építőipar* 1999/9-10., pp. 292-298.
Kodur, V. (2004), „Fire researchers report breakthrough on FRP-strengthened concrete columns", *Construction innovation*, Vol. 9., No. 3., September 2004, pp. 5-8.
Kollár, L. P., Kiss, R. M. (1998), „FRP composites in the building industry I. – materials of composites" (In Hungarian), *Közúti és Mélyépítési szemle* 1998./9. pp. 331-338.
Majorosné, L. É., Borosnyói, A., Balázs, L. Gy. (2004), „Bond of CFRP tendons under elevated temperatures" (In Hungarian), *Vasbetonépítés* 2004/4, pp. 108-113.
Neubauer, U., Rostásy, F. S., Budelmann, H. (2001) „Verbundtragfähigkeit geklebter CFK-Lamellen für die Bauteilverstärkung", Bautechnik 2001, Heft 10, 681-692.
Sika (2004), „Prestressing Systems for Structural Strengthening with Sika® CarboDur® CFRP Plates", Sika Services AG, Zürich, 2004.
Sika Product Data Sheet (2005), „Sika® CarboDur® Plates, Sika Services AG, Zürich, 2005.
StressHead (2005), „Innovative Bauwerksverstärkung mit vorgespannten CFK-Lamellen – Technische Dokumentation" StressHead AG, CH Luzern
Stöcklin, I., Meier, U. (EMPA) (2001), „Strengthening of concrete structures with prestressed and gradually anchored CFRP strips", Proceedings of the 5th International Conference on FRP Reinforcement for Concrete Structures, FRPRCS-5, 15-17 July 2001, Cambridge, ed. Chris Burgoyne, Thomas Telford, pp. 291-299.
Suter, R., Jungo, D. (2001), „Vorgespannte CFK-Lamellen zur Verstärkung von Bauwerken", Beton- und Stahlbetonbau 2001, Heft 5, 350-358.
Szabó, K. Zs., Balázs, L. Gy. (2007), „Near surface mounted FRP reinforcement for strengthening of concrete structures", Periodica Politechnica, Civil Engineering, Vol l51/1, 2007, 33-38.
Vorspann-Tecnik (2007), Litzen-Spannverfahren, intern, ohne Verbund, für das Vorspannen von Tragwerken, Europäische Technische Zulassung ETA-06/0165

András Molnár (1983) MSc structural engineer, PhD student at the Departement of Structural Engineering at the Budapest University of Technology and Economics. His main field of interest is the structural application of fibre reinforced polymers at upgrading structures and structural members, and strengthening of existing reinforced concrete and wooden structures with special regard to prestressed applications.

Dr. István Bódi (1954) civil engineer, post-graduate engineer in mathematics, PhD, associate professor at the Department of Structural Engineering, Budapest University of Technology and Economics. Research fields: Reconstruction and strengthening of reinforced concrete and conventional structures, modeling of timber structure joints. Has over 80 publications. Member of the ACI (American Concrete Institute) and the ACI Subcommitte#423 „Prestressed Concrete". Editorial member of the Hungarian Version of the journal "Concrete Structures" (Journal of the Hungarian group of ***fib***). Member of the Budapest and Pest County Chamber of Engineers. Former president of the standardization committee Eurocode 5 - MSZ EN 1995 (Timber Structures). Member of the Hungarian Group of ***fib***. Member of the „Schweizerische Arbeitgemeinschaft für das Holz" organisation and the Scientific Association of Hungarian Wood Industry.

50 YEARS OF EXPERIENCE WITH THE SCHMIDT REBOUND HAMMER


Katalin Szilágyi – Adorján Borosnyói

The Schmidt rebound hammer has the most widespread use in the non-destructive surface hardness testing of concrete. Compressive strength of structural concrete can be estimated by empirical relationships that can be found between rebound index (readings on the Schmidt rebound hammer) and compressive strength. Empirical formulae based on laboratory tests can be used only within their limits of application. Extension of the validity of the curves is usually not possible. The expected error of the strength estimation by the Schmidt rebound hammer under general service circumstances is about 30 percent. If users are not skilled well usually overestimate the reliability of the Schmidt rebound hammer. Present paper gives a summary of experiences with the Schmidt rebound hammer in the last more than 50 years. Detailed literature review reflects to the sensitive nature of the testing method. Authors' intention is to give a general review to practitioners and engineers, to highlight special scientific questions in the field, and to help maintaining the widespread use of the Schmidt rebound hammer in the future.

Keywords: Schmidt rebound hammer, surface hardness, rebound index, strength estimation

1. INTRODUCTION

History of non-destructive testing (NDT) of concrete strength in structures goes back more than 70 years (Carino, 1994). Researchers adopted the Brinell method to cement mortar and concrete to find correlations between surface hardness and strength of concrete in the four decades following that Brinell (1901) introduced his ball indentation method for hardness testing of steel (Crepps, Mills, 1923; Dutron, 1927; Vandone, 1933; Sestini, 1934; Steinwede, 1937). The first NDT device for in-place testing of concrete strength was introduced in Germany in 1934 which also adopted the ball indentation hardness testing method, however, dynamic load was applied with a spring impact hammer (Gaede, 1934). Similar device was developed in the UK in 1936 (Williams, 1936). In the following decades several other NDT instruments were introduced adopting the same method (e.g. pendulum hammer by Einbeck, 1944) or different methods (e.g. pull-out testing and firearm bullet penetration testing by Skramtajew, 1938; drilling method by Forslind, 1944; ultrasound pulse velocity method by Long et al., 1945).

Fig. 1: The Schmidt rebound hammer
a) Original Schmidt hammer
b) Silver Schmidt hammer

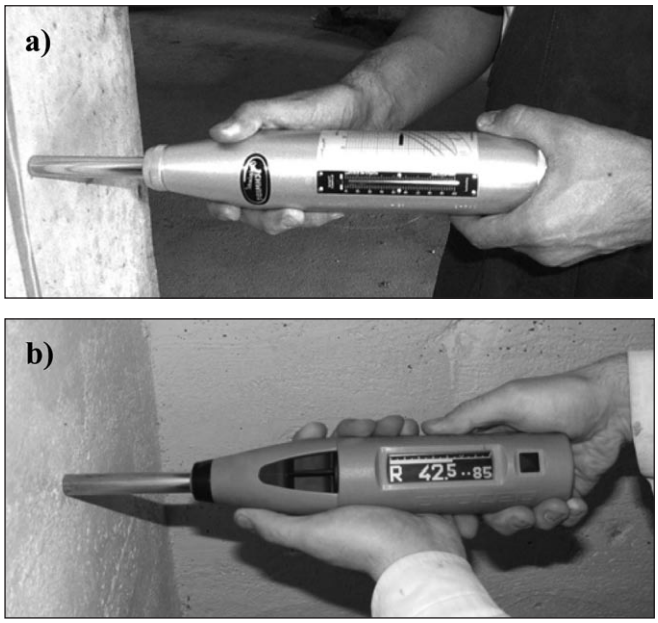

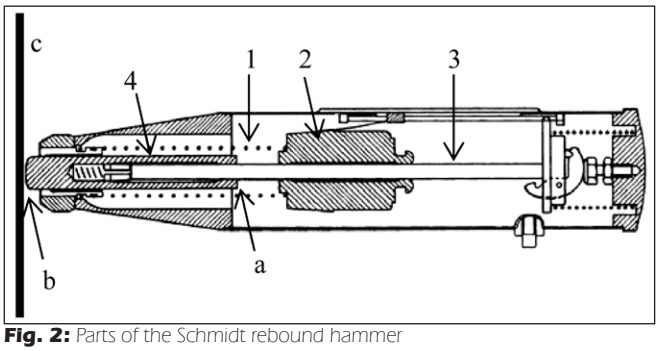

Fig. 2: Parts of the Schmidt rebound hammer (see notation in the text)

In Switzerland *Ernst Schmidt* developed a spring impact hammer of which handling was found to be superior to the ball penetration tester devices (Schmidt, 1950). The hardness testing method of Shore (1911) was adopted in the device developed by Schmidt, and the measure of surface hardness is the *rebound index* rather than ball penetration. With this development the hardness measurement became much easier, as the rebound index can be read directly on the scale of the device and no measurements on the concrete surface are needed (Schmidt, 1951). The original idea and design of the device was further developed in 1952 (using one impact spring instead of two) resulted in simpler use (Greene, 1954; Anderson et al, 1955). In 1954 *Proceq SA* was founded and has been producing the original Schmidt rebound hammers since then, without any significant change in the operation of the device (Proceq, 2005). Several hundred thousands of Schmidt rebound hammers are in use worldwide (Baumann, 2006). The latest development of the device was finalized in November

2007, since the Silver Schmidt hammers are available (Proceq, 2008a). The digitally recording Silver Schmidt hammers can also measure coefficient of restitution, C_R (or *Leeb hardness*; see Leeb, 1986) of concrete not only the original Schmidt rebound index. *Fig. 1.* indicates the original Schmidt hammer and the Silver Schmidt hammer in use.

The gentle reader can find detailed information about further NDT methods for concrete in the technical literature (ACI, 1998; Balázs, Tóth, 1997, Borján, 1981; Bungey, Millard, Grantham, 2006; Carino, 1994; Diem, 1985; Malhotra, 1976; Malhotra, Carino, 2004; Skramtajew, Leshchinsky, 1964).

2. OPERATION OF THE SCHMIDT REBOUND HAMMER

In the Schmidt rebound hammer (as can be studied in *Fig. 2.*) a spring (1) accelerated mass (2) is sliding along a guide bar (3) and impacts one end (a) of a steel plunger (4) of which far end (b) is compressed against the concrete surface (c). The impact energy is constant and independent of the operator, since the tensioning of the spring during operation is automatically released at a maximum position causing the hammer mass to impinge with the stored elastic energy of the tensioned spring. The hammer mass rebounds from the plunger and moves an index rider before returning to zero position. Original Schmidt rebound hammers record the rebound index (R): the ratio of paths driven by the hammer mass before impact and during rebound; see Eq. (1). Silver Schmidt hammers can record also the square of the coefficient of restitution (referred as Q-value): the ratio of kinetic energies of the hammer mass just before and right after the impact (E_0 and E_r, respectively); see Eq. (2).

$$R = \frac{x_r}{x_0} \cdot 100 \tag{1}$$

$$Q = \frac{E_r}{E_0} \cdot 100 = \frac{v_r^2}{v_0^2} \cdot 100 = C_R^2 \cdot 100 \tag{2}$$

In Eqs. (1) and (2) x_0 and v_0 indicate path driven and velocity reached by hammer mass *before impact*, while x_r and v_r indicates path driven and velocity reached by hammer mass *after impact*.

3. INTERPRETATION OF HARDNESS MEASUREMENTS

Aim of Schmidt rebound hammer tests of concrete structures is usually to find a relationship between surface hardness and compressive strength with an acceptable error. For the rebound method no general theory was developed that can describe the relationship between measured hardness values and compressive strength. The existence of only empirical relationships was already considered in the earliest publications (Anderson et al, 1955; Kolek, 1958) and also recently (Bungey et al, 2006). To find a reliable method for strength estimation one should study all the influencing factors that can have any effect on the hardness measurement, and also that can have any effect on the variability of the strength of the concrete structure examined. The estimation should be based on an extensive study with the number of test results high enough to provide an acceptable reliability level. The estimation should take care of the rules of mathematical statistics. Indications are summarized in the topics above as follows.

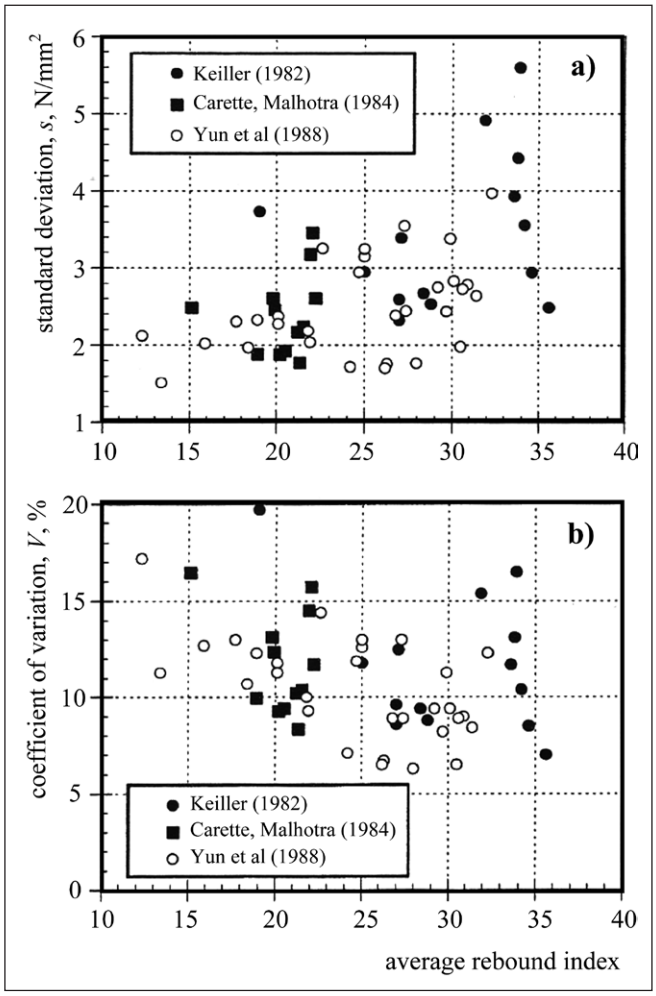

Fig. 3: Repeatability of the Schmidt hammer test (ACI, 2003b)
a) within-test standard deviation as a function of average rebound index
b) within-test coefficient of variation as a function of average rebound index

3.1 Influences by the Schmidt rebound hammer

In the Schmidt rebound hammer mechanical parts (i.e. springs, sliding hammer mass, etc.) provide the impact load and mechanical (Original Schmidt hammer) or digital (DIGI-Schmidt hammer, Silver Schmidt hammer) parts are responsible for readings. The value of the Schmidt rebound index depends on energy losses due to friction during acceleration and rebound of the hammer mass and that of the index rider, energy losses due to dissipation by reflections and attenuation of mechanical waves inside the steel plunger; and of course, energy losses due to dissipation by concrete crushing under the tip of the plunger. The value of the coefficient of restitution (thus Q-value) depends on energy losses due to dissipation by reflections and attenuation of mechanical waves inside the steel plunger and energy losses due to dissipation by concrete crushing under the tip of the plunger. *This latter loss of energy makes the Schmidt rebound hammer suitable for strength estimation of concrete*. The energy dissipated in the concrete during local crushing initiated by the impact depends both on concrete compressive strength and Young's modulus; therefore, depends on the stress-strain (σ-ε) response of the concrete tested.

The value of the Schmidt rebound index depends also on the direction of the hit by the hammer related to the direction of gravity force. The reading should be corrected accordingly (Proceq, 2006). The value of the coefficient of restitution (thus Q-value) can be considered to be independent from the direction of the hit by the hammer related to the direction of

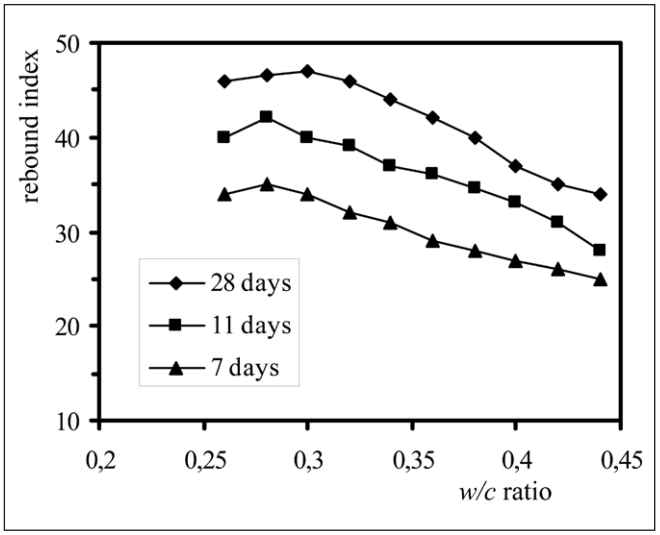

Fig. 4: Schmidt rebound hammer test results on hardened cement pastes of different w/c ratios (Kolek, 1970b)

gravity force (Proceq, 2008b). Akashi and Amasaki (1984) studied the mechanical waves in the plunger of the Original Schmidt hammer during impact. The authors have found a relationship between concrete strength and the shape of the mechanical waves as well as the maximum stress values of the mechanical waves. The authors could also demonstrate that wave propagation behaviour is considerably different in the case of different ages of concrete, and also if different test materials (aluminium, copper, steel, concrete) are studied. Nevertheless, no general explanation of the behaviour was published.

The uncertainty of the average value of the reading (either *R* or *Q*) depends on three influences: 1. the variability of the strength of concrete in the structure; 2. the repeatability of the Schmidt rebound hammer test; 3. the number of individual readings. The term *repeatability* considers the inherent scatter associated with the NDT method and is often called within-test variation. For the characterization of repeatability either the standard deviation (*s*) or the coefficient of variation (*V*) of repeated tests by the same operator on the same material can be suitable. The repeatability for the Schmidt rebound hammer test was found to be appropriately described by the within-test *coefficient of variation*, rather than the within-test standard deviation (ACI, 2003b). *Fig. 3* shows both parameters as a function of the average rebound index. A trend of increasing standard deviation with increasing average rebound index can be realized, consequently an almost constant coefficient of variation. The repeatability of the Schmidt rebound hammer test can be characterized by a V = 10 to 12 percent within-test coefficient of variation. No data are available concerning the repeatability of the Silver Schmidt rebound hammer tests for the time being.

3.2 Influences by the concrete structure

The energy dissipated in the concrete during local crushing initiated by the impact depends on the properties of the concrete in the very vicinity of the tip of the plunger. Therefore, the measurement is sensitive to the scatter of local strength of concrete due to its inner heterogeneity. For example, an air void or a bigger hard aggregate particle close to the surface is resulted in a much lower or a much higher local rebound value than that can characterize to the concrete structure globally (Herzig, 1951).

The amount of energy dissipated in the concrete can be higher for a concrete of lower strength/lower stiffness compared to the lower energy dissipation in a concrete of higher strength/higher stiffness. As it is possible to prepare concretes of the same strength but having different Young's moduli, it is also possible to measure the same rebound index for different concrete strengths or to measure different rebound indices for the same concrete strengths. Young's modulus of the aggregate has considerable influence on the rebound index.

The most significant influence on strength of concrete was found to be the water-to-cement ratio (*w/c*) of the cement paste. Schmidt hammer test results available for hardened cement pastes of different *w/c* ratios are represented in *Fig. 4* (Kolek, 1970b). Results indicate that the change of the rebound index due to the change of the *w/c* ratio is similar in nature to the relationships found between concrete compressive strength and *w/c* ratio, however, less pronounced. Even the compaction problems for low *w/c* ratios can be realized. It can be found that *measuring the surface hardness of concrete by a rebound method could provide suitable result for strength estimation*. However, it should be also noted that the *w/c* ratio of the cement paste is only one influencing parameter for the strength of concrete and several further influencing parameters should be taken into consideration in the strength estimation procedure (Granzer, 1970).

Additional important influencing parameters are:

– *the concrete mixture*: type of cement, amount of cement, type of aggregate, amount of aggregate,
– *the concrete structure*: compaction of structural concrete, method of curing, quality of concrete surface, age of concrete, carbonation depth in the concrete, moisture content of concrete, mass of the structural element, temperature and stress state.

Differences in the rebound index due to the application of different types and/or amounts of *cement* can reach 50 percent (IAEA, 2002). On the other hand, the influence of variation in fineness of cement is not considered to be significant, resulting in a scatter of about 10 percent (Bungey et al, 2006).

Type and grading of the *aggregate* have significant influence on the rebound index. The most considerable influence is attributed to the Young's modulus of the aggregate. For example, the rebound index is always found to be higher for quartz aggregate than for limestone aggregate, both corresponding to the same concrete compressive strength (Grieb, 1958; IAEA, 2002; Neville, 1981).

Fig. 5: Schematic representation of depth of carbonation in time as a function of porosity (Bindseil, 2005)

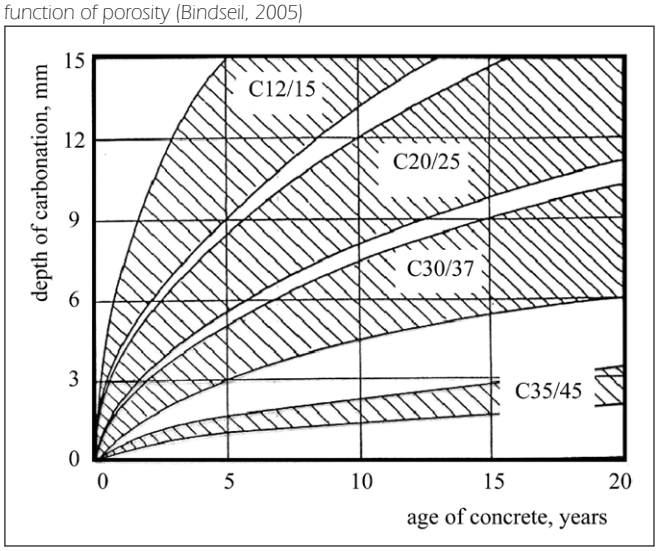

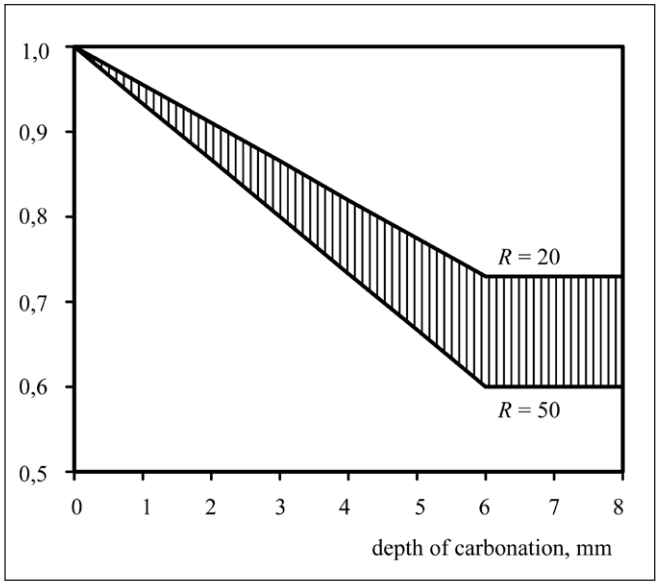

Fig. 6: Correction factor considering the depth of carbonation according to Chinese Standard JGJ/T23-2001 for rebound index R = 20-50 (after Proceq, 2003)

Moisture content of the concrete influences the rebound index (Jones, 1962; Samarin, 2004; Victor, 1963; Zoldners, 1957). Increasing the moisture content of concrete from air dry condition up to water saturated condition can be resulted in a decrease of 20 percent in the rebound index (RILEM, 1977). The situation is similar for water saturated surface dry condition, too.

Influence of the age of concrete can be realized most significantly in the effect of carbonation of concrete (i.e. the forming of limestone from the hydrated lime due to carbon-dioxide ingress from ambient air). The surface hardness of concrete and thus the rebound index increases due to carbonation. Not taking this influence into account is resulted in an *unsafe* strength estimation. The error can be more than 50 percent (Gaede, Schmidt, 1964; Pohl, 1966; RILEM, 1977; Wesche, 1967). However, the use of a reduction parameter that is a function *only* of the age of concrete should be avoided. Age of concrete can be rather taken into consideration as the *developed depth of carbonation* thus with a parameter that takes into account *porosity* of concrete (the schematic relationship between porosity and depth of carbonation is represented in *Fig. 5.*, after Bindseil, 2005). Such a parameter is introduced in Chinese Standard JGJ/T23-2001 that is adopted into the guidelines of Proceq SA (Proceq, 2003). Schematic representation is given in *Fig. 6*.

Authors of present paper do not intend to analyze mathematical statistical parameters of concrete strength in general. Only a short reference is given to the coefficient of variation due to the scatter of in-place compressive strength in concrete structures that was found to be V = 7 to 14 percent, depending on the type of structure and quality control (ACI, 2002; ACI, 2003a). The other source of variation in strength is the within-test coefficient of variation, as the measure of repeatability of strength tests. It was found experimentally that the within-test coefficient of variation is about V = 3% for moulded specimens and V = 5% for drilled cores (ASTM, 2004; ASTM, 2005). It was also demonstrated that the distribution of the within-test coefficient of variation is asymmetrical; the coefficient of variation of concrete strength is not constant with varying strength (Leshchinsky et al, 1990).

It should be mentioned that in the European practice usually the *standard deviation* is the measure for the variability of concrete strength, rather than the coefficient of variation (Rüsch, 1964; CEB-CIB-FIP-RILEM, 1974). It was found, however, that *the coefficient of variation is* less affected by the magnitude of the strength level, and is therefore *more useful than the standard deviation* in comparing the degree of control for a wide range of compressive strengths (ACI, 2002).

A selection of references is given for further details to the gentle reader's interest (Bartlett, MacGregor, 1994a; 1994b; 1994c; 1995; 1996; Neville, 1986; 2001).

3.3 Considerations about number of tests

Important question is that how many test repetitions are needed to be able to estimate concrete strength with acceptable error. Smaller number of repetitions affects the uncertainty of the average reading as it was indicated earlier. Generally, the number of repetitions depends on three influences: 1. the repeatability of the testing method (also called within-test variation); 2. the acceptable error between the sample average and the true average; 3. the desired confidence level that the acceptable error is not to be exceeded. The number of repetitions can be established from statistical principles or can be based upon usual practice.

The former RILEM Task Group suggested a minimum repetition number of 25 rebound indices for an acceptable representative value (RILEM, 1977). Borján (1968) proposed a minimum repetition number of 100 rebound indices for accuracy. The sufficiency of the collected data can be studied by an analysis of mathematical statistical parameters (average value, standard deviation, skewness and kurtosis). Asymptotic behaviour can be realized whenever the number of data is sufficient (Borján, 1968). *Fig. 7.* gives results for a concrete wall indicating the asymptotic behaviour for standard deviation (s) and kurtosis (k): after reaching a certain number of test repetitions the reliability of the sample size can not be increased further and the statistical parameters are found to be remaining constant.

Arni (1972) has demonstrated that the number of tests required to detect a strength difference of 200 psi (≈ 1.4 N/mm^2) with a 90% confidence level is 8 for standard cylinders and is 120 for rebound test readings. The technical literature demonstrates that if the total number of readings (n) taken at a location is not less than 10, then the accuracy of the mean rebound number is likely to be within $\pm 15/\sqrt{n}$ % with a 95% confidence level (Bungey et al, 2006).

ACI suggests using a number of repetitions such that the average values of the NDT results provide comparable precision to the average compressive strength (Carino, 1993). If the coefficients of variation of the compressive strength test

Fig. 7: Asymptotic behaviour of mathematical statistical parameters (standard deviation and kurtosis) by increasing sample size (number of test repetitions); Schmidt rebound hammer test results on a reinforced concrete wall (authors' results)

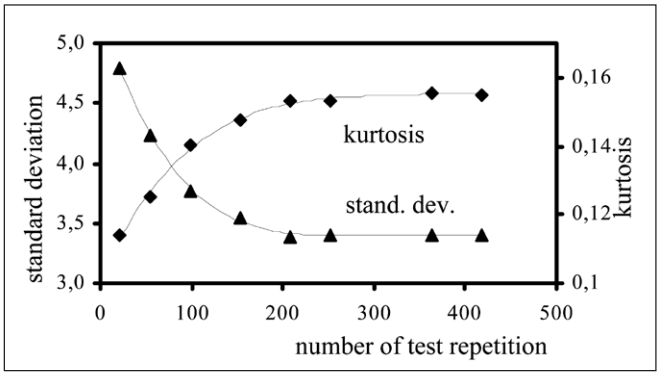

and of the NDT method are available, the ratio of the number of test repetitions can be given as:

$$\frac{n_i}{n_s} = \left(\frac{V_i}{V_s}\right)^2 \tag{3}$$

In Eq. (3) n_i and V_i refer to the number of test repetitions and coefficient of variation corresponding to the NDT (i.e. *in-place* test), while n_s and V_s refer to the number of test repetitions and coefficient of variation corresponding to the *strength* test. As a numerical example, if the number of replicate compressive strength tests is $n_s = 5$ (higher uncertainty in the estimation) or $n_s = 18$ (lower uncertainty in the estimation) at a given strength level and the coefficient of variation is $V_s = 3\%$ (moulded specimens, see *Chapter 3.2*), one can find the required number of test repetitions in case of the Schmidt rebound hammer test (with an estimated coefficient of variation $V_i = 12\%$, see *Chapter 3.1*) to be $n_i = 5 \cdot (12/3)^2 = 80$ or $n_i = 18 \cdot (12/3)^2 = 288$ at the given strength level. Results can be compared with the experimental data shown in *Fig. 7*. The user can decide which uncertainty is tolerated during Schmidt rebound hammer testing since the increase of the number of test repetitions does not have considerable economic impact but is resulted in more reliable strength estimation.

Leshchinsky et al. (1990) introduced a formula for the suggested number of NDT repetitions at a measuring location that is based on the use of empirical regression relationship from experiments as follows:

$$n = t^2 V_f^2 / p^2 \tag{4}$$

$$V_f = \frac{1}{r}\frac{\partial[\zeta(H)]}{\partial H} V_H \tag{5}$$

In Eqs. (4) and (5) V_f is the within-test coefficient of variation of the estimated concrete strength; p is the acceptable error for the evaluation of average value of concrete strength (with the present probability P); t depends on P and the number of individual NDT repetitions; $f=\zeta(H)$ is the equation of the test measure vs. concrete strength correlation relationship; f is the concrete strength; H is the indirect measure (e.g. rebound index); r is the correlation coefficient of the correlation relationship; V_H is the within-test coefficient of variation of the indirect measure.

The exact confidence interval can be also given to any number of test repetitions using a suitable reliability analysis (ACI, 2003b; Leshchinsky et al, 1990).

3.4 Considerations about mathematical statistics

The rebound index vs. strength relationship can be determined if the experimental data are available. The usual practice is to consider the average values of the replicate compressive strength and NDT results *as one data pair* at each strength level. The data pairs are presented using the NDT value as the independent variable (along the X axis) and the compressive strength as the dependent variable (along the Y axis). Regression analysis is performed as a conventional least-squares analysis on the data pairs to obtain the best-fit estimate for the strength relationship. The technical literature calls the attention that the boundary conditions of the conventional least-squares analysis are violated in the case of rebound index vs. strength relationships (Carino, 1993), therefore it is not recommended because the uncertainty in the strength relationship would be underestimated. It is useful to summarize the findings here.

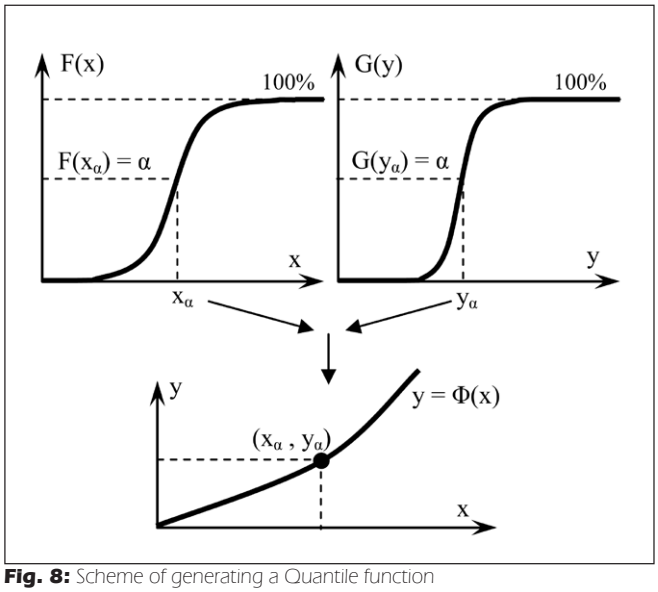

Fig. 8: Scheme of generating a Quantile function

The two most important limitations of the conventional least-squares analysis are: 1. no error (variability) is considered to be existing in the X variable (here: the rebound index); 2. the error (i.e. standard deviation) is constant in the Y variable (here: the compressive strength) over all values of Y. Regarding the findings of *Chapter 3.1* and *3.2*, it is obvious that the first assumption is violated by the uncertainty of the NDT method – characterized by its within-test coefficient of variation (which, in fact, has a larger variability than that of the strength tests); and the second assumption is violated because standard deviation increases with increasing compressive strength both for strength testing and NDT.

Mathematical statistics considers a data plot scatter to be *heteroscedastic*, when the error (i.e. standard deviation) is not constant in the Y variable; the variation in Y differs depending on the value of X (Tóth, 2007). Regression analysis of heteroscedastic data needs performing a Y variable transformation to achieve homoscedasticity (constant standard deviation in the Y variable). Conventional least-squares analysis regression can be used only if the data are homoscedastic. A suitable Y variable transformation is the *Box-Cox Normality Plot* (NIST, 2009) which is defined by a λ transformation parameter as:

$$T(Y) = (Y^{\lambda} - 1)/\lambda \tag{6}$$

For $\lambda = 0$, the natural logarithm of the data is taken; this is the most common estimation in the case of rebound index *(R)* vs. strength *(f)* relationships. If a linear relationship is used, it is formed as follows:

$$\ln(f) = a + B \cdot \ln(R) \rightarrow f = e^{a} \cdot R^{B} = A \cdot R^{B} \tag{7}$$

In Eq. (7) the exponent B determines the degree of nonlinearity of the power function. If $B = 1$, the strength relationship is a straight line passing through the origin with a slope of A. If $B \neq 1$, the relationship has curvature.

Regarding the problem of error in the X variable the regression procedure proposed by *Mandel* is suggested instead of the conventional least-squares analysis regression (Carino, 1993; ACI, 2003b). Details are not given herewith. The most

important difference to the conventional least-squares analysis is that Mandel's method minimizes the sum of squares of the deviations from the regression line in both *X* and *Y* directions, on the contrary to the conventional least-squares analysis which minimizes only the deviations from the regression line in *Y* direction.

In the 1970's Hungarian researchers (Talabér, Borján, Józsa, 1979) introduced an analysis method for the Schmidt rebound index vs. strength relationships as an adaptation of the *Quantile function* developed by *J. Reimann*, Hungarian mathematician. Quantile function can provide an estimate of the relationship of two random variables which are in a stochastic relationship (i.e. they are not independent, but one can not exactly define the other) (Reimann, 1975; Koris, 1993). Quantile functions are used in hydrology for flood analyses (Reimann, V. Nagy, 1984). Coordinates of a Quantile function can be generated easily: if the cumulative distribution functions (CDF) of *X* and *Y* random variables (being in a stochastic relationship) are known and is $F(x)$ and $G(y)$, respectively, then the values of the variables which have the same probability of occurrences $F(x_\alpha) = G(y_\alpha) = \alpha$ can be plotted as data pairs (x_α , y_α) forming the Quantile function (Reimann, 1975). Use of Quantile functions can be advantageous in the regression analysis of Schmidt rebound index vs. strength relationships because this abstraction minimizes the deviations from the regression line in both *X* and *Y* directions, eliminating the problems of the conventional least-squares analysis (Borján, 1981). Scheme of generating a Quantile function is shown in *Fig. 8*. It should be noted that the abstraction of the Quantile function is resulted in *fictitious data pairs* and omits the use of data pairs of corresponding Schmidt rebound index vs. strength measured in reality. On the other hand, it should be also noted that if Quantile functions are separated for different influencing parameters then they can represent the differences in a much noticeable way as compared to conventional least-squares analysis. Therefore, the use of Quantile functions in the analysis of influencing parameters can be reasonable. Unfortunately, the results by the Hungarian researchers mentioned above were limited to a relatively small series of tests (1152 cube specimens) and the idea was not further developed. Future work is needed in this field.

4. ESTABLISHING THE STRENGTH RELATIONSHIPS

The concrete construction practice needs in-place NDT equipment provided together with simple, easy-to-use, generalized relationships (in the form of equations, graphs or tables) which express the measured value (e.g. rebound index) as a value of compressive strength of standard concrete specimens. Such relationships, however, usually could not accurately characterize the concrete in the structure being tested.

A rigorous analysis should cover all the influences introduced in *Chapter 3* (within-test variation of the NDT method as well as of the standard strength testing; in-place variability of concrete strength in the structure; significance of the techniques of mathematical statistics both is sample size development and in regression analyses; acceptable error present in the strength estimation) and should also take into consideration the economic impact of the decision taken by the results provided.

Generalized relationships are allowed to be used only if their *validity has been established* by tests carried out on concrete similar to that being investigated and with the same type of testing device that is intended to be used in the investigation.

One should accept as a global indicator that a rigorous analysis (based on tests carried out under ideal laboratory conditions) can provide an accuracy of ±15-20% in the strength estimation; however, in a practical situation it is unlikely that a strength prediction can be made to an accuracy better than ±30-40% (Malhotra, 1976; FHWA, 1997). In practice, it is advised to use the Schmidt rebound hammer as a device of assessing relative concrete quality and uniformity (for which purpose other NDT devices are not comparable in operation and economy), rather than a device for strength estimation.

In the followings a survey is given regarding the empirical relationships found by several researchers for concrete strength estimation in the last 50 years. Due to space limitations of present paper only 40 of the formulae is summarized in *Table 1*, however, more than 60 can be found in the technical literature. Formulae are usually given in their original form but the notation is unified. Data is given in a graphical representation in *Fig. 9* with a correction to provide results for 150 mm standard cubes. For the sake of better visualization results are separated by their relation to the "*B-Proceq*" estimation curve (that is recommended by Proceq SA for the original Schmidt rebound hammers of N-type; Proceq, 2003) as follows:

- Proposal curves running continuously *over* the curve "B-Proceq" (*Fig. 9a*),
- Proposal curves running continuously *under* the curve "B-Proceq" (*Fig. 9b*),
- Proposal curves intersecting the curve "B-Proceq" *coming from below* (*Fig. 9c*),
- Proposal curves intersecting the curve "B-Proceq" *coming from above* (*Fig. 9d*).

Composition of the proposed empirical relationships can be summarized as follows (in which f_{cm} is the estimated mean strength; R is the rebound index; $a...n$ are empirical values):

- linear relationships: $f_{cm} = a + b \cdot R$,
- power function relationships: $f_{cm} = a + b \cdot R^c$,
- polynomial relationships: $f_{cm} = a + b \cdot R + c \cdot R^2 + \ldots + n \cdot R^m$,
- exponential relationships: $f_{cm} = a + b \cdot e^{c \cdot R}$,
- logarithm relationships: $\log_a(f_{cm}) = b + \log_a(R)$,
- nonlinear relationships: $f_{cm} = \zeta(R)$.

Results summarized are valid for 28 to 365 days of age, conventional, normal-weight concretes under air dry moisture condition. It can be realized that the concrete strength can be estimated at certain rebound indices by a ±40-60 N/mm^2 variation. Results clearly demonstrate that the validity of a proposal should be restricted to the testing conditions and the extension of the validity to different types of concretes or testing circumstances is impossible. It is also worth to mention that several linear estimations can be found among the proposals. This result contradicts the considerations introduced in *Chapter 3.4* and calls the attention to the linear estimation that can provide the best-fit regression if the *strength range* is chosen to be narrow in the experimental tests. Rigorous experiments were always resulted in nonlinear relationships since the very beginning of tests by the Schmidt rebound hammer (Schmidt, 1951; Gaede, 1952; Greene, 1954; Chefdeville, 1955; Zoldners, 1957; Kolek, 1958; Brunarski, 1963; Gaede, Schmidt, 1964; Granzer, 1970; Talabér, Józsa, Borján, 1979 etc.).

For the Schmidt rebound hammer tests no general theory has been developed that could describe the relationship between measured hardness values and compressive strength. Gaede and Schmidt (1964) have studied the performance in details and derived a model that can provide estimation with acceptable accuracy and can be fit to experimental data in a suitable way.

Table 1: Strength relationships in the technical literature Notations for mean concrete strength:
$f_{cm,100,cube}$ 100 mm cube, $f_{cm,150,cube}$ 150 mm cube, $f_{cm,200,cube}$ 200 mm cube, $f_{cm,cyl}$ ∅150/300 mm cylinder, $f_{cm,70\times70,core}$ ∅70/70 mm drilled core, $f_{cm,core}$ drilled core (no geometry given),
Remark: certain references give only tabulated or graphical representation; for these cases regression curves are calculated and indicated in **Table 1.**

1)	$f_{cm,200,cube} = -0{,}0003 \cdot R^3 + 0{,}0399 \cdot R^2 - 0{,}1525 \cdot R + 3{,}9976$	(N/mm^2)	Schmidt (1950)
2)	$f_{cm,200,cube} = 0{,}0477 \cdot R^{1{,}7796}$	(N/mm^2)	Chefdeville (1953)
3)	$f_{cm,cyl} = 0{,}1134 \cdot R^{1{,}4927}$	(N/mm^2)	Greene (1954)
4)	$f_{cm,cyl} = 0{,}4594 \cdot R^3 - 37{,}879 \cdot R^2 + 1175{,}7 \cdot R - 10021$	(psi)	Zoldners (1957)
5)	$f_{cm,150,cube} = 0{,}056 \cdot R^2 - 0{,}022 \cdot R + 1{,}57$	(lb/in^2 10^3)	Kolek (1958)
6)	$f_{cm,200,cube} = 0{,}019 \cdot R^{2{,}59}$	(N/mm^2)	Brunarski (1963)
7)	$f_{cm,200,cube} = 10 \cdot R - 50$	(kg/cm^2)	Victor (1963)
8)	$f_{cm,200,cube} = 0{,}06 \cdot R^{2{,}42}$	(N/mm^2)	Facaoaru (1964)
9)	$f_{cm,200,cube} = -0{,}001 \cdot R^3 + 0{,}1222 \cdot R^2 - 2{,}9185 \cdot R + 27{,}894$	(N/mm^2)	Gaede, Schmidt (1964)
10)	$f_{cm,200,cube} = 0{,}515 \cdot R^2 - 19{,}951 \cdot R + 258{,}06$	(kp/cm^2)	ÉMI (1965)
11)	$f_{cm,200,cube} = \frac{9099{,}18}{\left(2^{(5-10c)} + 3{,}178 - 0{,}65\alpha\right) \cdot i} \cdot \frac{R^2 + 0{,}067 \cdot R}{0{,}773 - \left(R^2 + 0{,}067 \cdot R\right)}$	(kp/cm^2)	Roknich (1968)
12)	$f_{cm,200,cube} = 0{,}53 \cdot R^2 - 21 \cdot R + 276$	(kp/cm^2)	Vadász (1970)
13)	$f_{cm,200,cube} = 0{,}0051 \cdot R^{2{,}3956}$	(N/mm^2)	MSZ 4715 (1972)
14)	$f_{cm,150,cube} = 2{,}0098 \cdot R - 21{,}749$	(N/mm^2)	Cianfrone, Facaoaru (1979)
15)	$\lg f_{cm,200,cube} = -1{,}055 + 1{,}805 \times \lg R + 0{,}345 \times [\lg R]^2$	(N/mm^2)	Talabér et al (1979)
16)	$f_{cm,cyl} = 54{,}1 \cdot \ln R - 148{,}4$	(N/mm^2)	Malhotra, Carette (1980)
17)	$\lg f_{cm,200,cube} = -2{,}159 + 1{,}805 \times \lg R + 0{,}345 \times [\lg R]^2$	(N/mm^2)	Borján (1981)
18)	$f_{cm,150,cube} = 0{,}00883 \cdot R^{2{,}27}$	(N/mm^2)	Di Leo et al (1984)
19)	$f_{cm,150,cube} = -0{,}00186 \cdot R^2 + 2{,}0449 \cdot R - 46{,}426$	(N/mm^2)	Knaze, Beno (1984)
20)	$f_{cm,100,cube} = 7{,}25 \cdot e^{0{,}08 \cdot R}$	(N/mm^2)	Ravindrajah (1988)
21)	$\ln f_{cm,200,cube} = -4{,}69 + 1{,}79 \times \ln R + 0{,}152 \times [\ln R]^2$	(N/mm^2)	MI 15011 (1988)
22)	$f_{cm,150,cube} = 2{,}50 \cdot R - 18{,}4$	(N/mm^2)	Mikulic et al (1992)
23)	$f_{cm,150,cube} = 1{,}0407 \cdot R^{1{,}155}$	(N/mm^2)	Almeida (1993)
24)	$f_{cm,70\times70,core} = 1{,}73 \cdot R - 34{,}3$	(N/mm^2)	Gonçalves (1995)
25)	$f_{cm,150,cube} = 0{,}403 \cdot R^{1{,}2083}$	(N/mm^2)	Kheder (1999)
26)	$f_{cm,150,cube} = 1{,}47 \cdot R - 16{,}85$	(N/mm^2)	Soshiroda (1999)
27)	$f_{cm,cyl} = 0{,}0501 \cdot R^{1{,}8428}$	(N/mm^2)	Lima, Silva (2000)
28)	$f_{cm,150,cube} = 2{,}2415 \cdot R - 30{,}762$	(N/mm^2)	Nyim (2000)
29)	$f_{cm,150,cube} = 0{,}000135 \cdot R^{3{,}4424}$	(N/mm^2)	Pascale et al (2000)
30)	$f_{cm,150,cube} = 1{,}353 \cdot R - 17{,}393$	(N/mm^2)	Qasrawi (2000)
31)	$f_{cm,150,cube} = 0{,}0244 \cdot R^{1{,}9898}$	(N/mm^2)	CPWD (2002)
32)	$f_{cm,150,cube} = 0{,}0002392 \cdot R^{3{,}299}$	(N/mm^2)	Pascale et al (2003)
33)	$f_{cm,150,cube} = 0{,}0117 \cdot R^2 + 0{,}8973 \cdot R - 13{,}213$ *(„B-Proceq")*	(N/mm^2)	Proceq SA (2003)
34)	$f_{cm,150,cube} = 0{,}0005 \cdot R^3$	(N/mm^2)	Nehme (2004)
35)	$f_{cm,150,cube} = 2{,}68 \cdot e^{0{,}06R}$	(N/mm^2)	Nehme (2004)
36)	$f_{cm,150,cube} = 0{,}00752 \cdot R^{2{,}359}$	(N/mm^2)	Fabbrocino et al (2005)
37)	$f_{cm,150,cube} = 0{,}788 \cdot R^{1{,}03}$	(N/mm^2)	Nash't et al (2005)
38)	$f_{cm,150,cube} = 2{,}1683 \cdot R - 27{,}747$	(N/mm^2)	Hobbs, Kebir (2006)
39)	$f_{cm,cyl} = 1{,}623 \cdot R - 20{,}547$	(N/mm^2)	Soshiroda et al (2006)
40)	$f_{cm,core} = 1{,}25 \cdot R - 23{,}0 \quad (20 \le R \le 24)$	(N/mm^2)	MSZ EN 13791 (2007)
	$f_{cm,core} = 1{,}73 \cdot R - 34{,}5 \quad (24 \le R \le 50)$	(N/mm^2)	

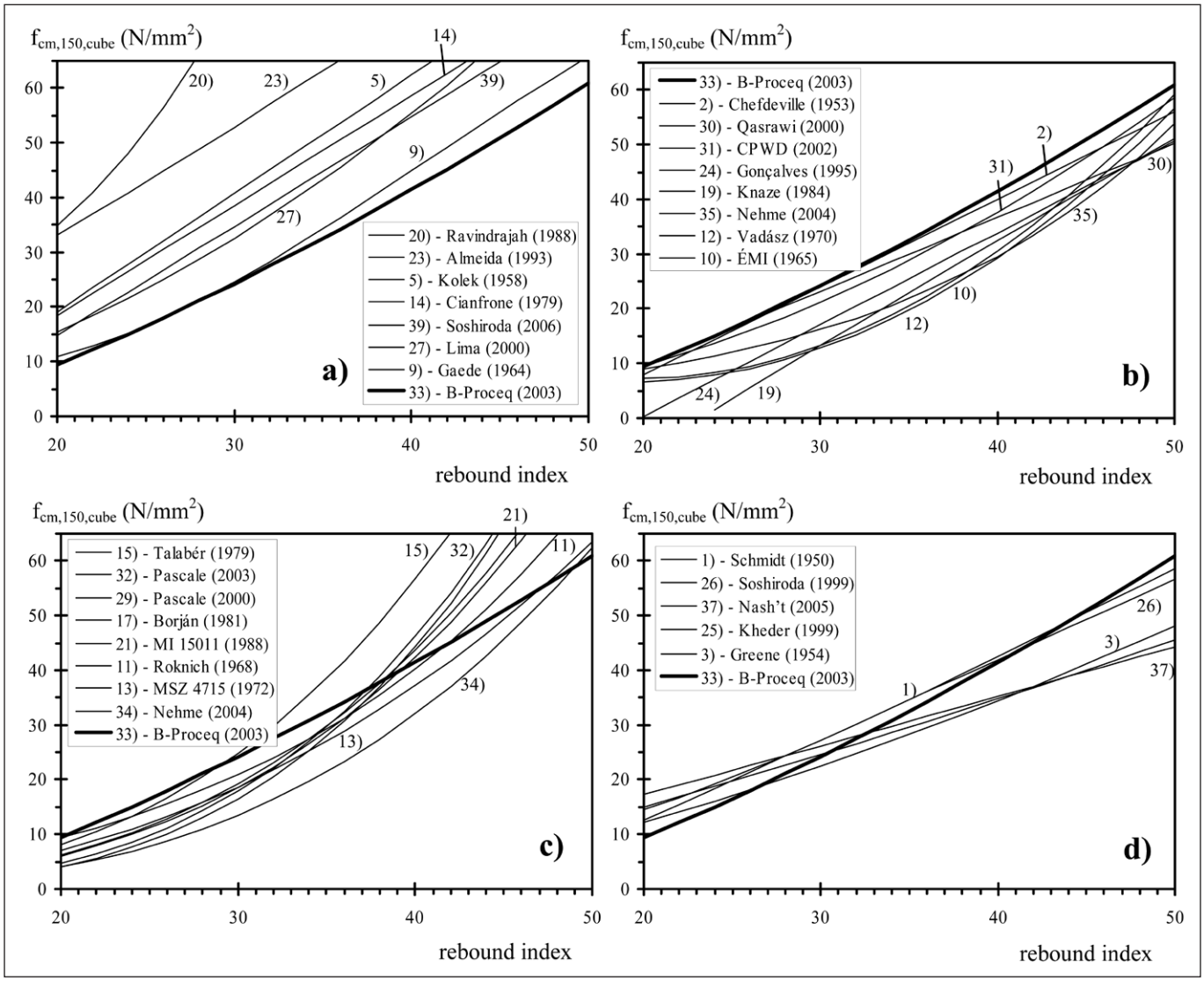

Fig.9: *Strength relationships according to Table 1 (transformed to 150 mm standard cubes)*

Unfortunately, the model does not provide the general theory because the Brinell hardness of concrete is covered in the parameters applied to the model. For the Brinell hardness of cementitious materials very limited data have been published and neither acceptable relationships with strength nor accurate theory for the hardness of porous solids is available in the technical literature. Future work is needed in this field.

For a more detailed theoretical analysis the stress wave attenuation behaviour and structural damping capacity of cementitious materials should be also studied. The relationship between rebound index and concrete strength depends on the damping capacity of concrete in the vicinity of the tip of the plunger of the Schmidt rebound hammer. Damping capacity can be described by several parameters (damping ratio; damping coefficient; logarithm decrement; Q factor; decay constant etc.), but measurements are very sensitive to the heterogeneity of the concrete. Swamy and Rigby (1971) have found the logarithm decrement of cement mortar and concrete to be dependent on the *w/c* ratio, aggregate content and moisture condition. However, limited data are available in this field in the technical literature. Based on experiments with polymer bodies Calvit (1967) has demonstrated that a simple relationship can be derived between the rebound height (h_r) of an impacting ball (falling from height h_0) and the damping capacity of a homogeneous, isotropic, viscoelastic semi-infinite solid body. Assuming that the impact is a half cycle of a sinusoidal vibration then the ratio of the energy dissipated (E_d) to the energy stored and recovered (E_r) in the half a cycle is equal to $\pi \cdot \tan\theta$, where θ is the phase shift (Ferry, 1961). The term $\pi \cdot \tan\theta$ is equal to the logarithm decrement (δ), therefore (Kolek, 1970a):

$$\frac{E_d}{E_r} = \frac{h_0 - h_r}{h_r} = \pi \cdot \tan\theta \text{, from which: } \frac{h_r}{h_0} = \frac{1}{1+\delta} \qquad (8)$$

Of course, it is not possible to derive such a simplified relationship for concrete due to the inelastic deformations in the concrete and stress wave attenuation in the plunger and in the concrete. Analytical studies need future activities.

5. TODAY TRENDS

Rapid development of concrete technology can be realized recently. New types of concretes became available for concrete construction in terms of High Strength Concrete (HSC), Fibre Reinforced Concrete (FRC), Reactive Powder Concrete (UHPC), Self Compacting Concrete (SCC) and Lightweight Concrete (LC). The strength development of concretes in the 20th century is schematically represented in *Fig. 10* (after Bentur, 2002). Technical literature considering Schmidt rebound hammer test on special concretes is very limited (e.g. Pascale et al., 2003; Nehme, 2004; Gyömbér, 2004; KTI, 2005). Considerable development is expected in this field in the future.

Environmental impact on concrete structures also tends to be changed recently. For example, the rate of carbonation

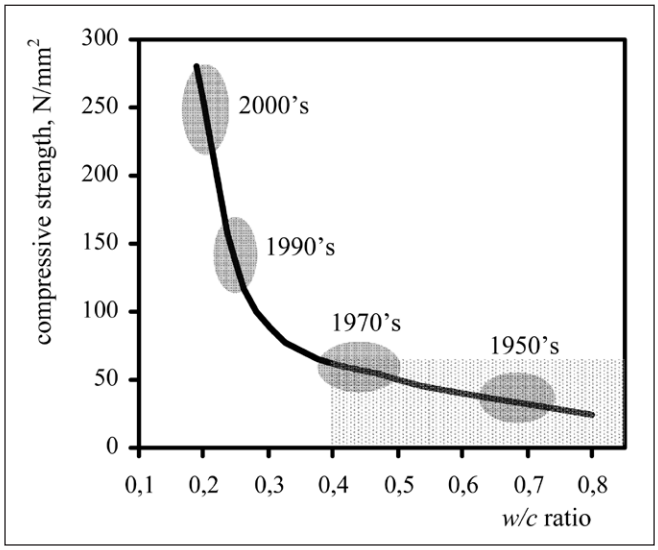

Fig. 10: *Development of concrete strengths in the last 50 years (after Bentur, 2002). Shaded region indicates validity of use for the Original Schmidt rebound hammer*

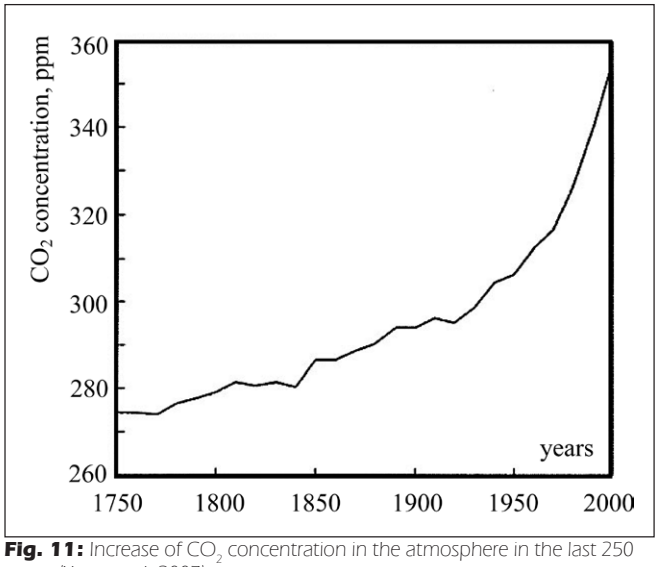

Fig. 11: *Increase of CO_2 concentration in the atmosphere in the last 250 years (Yoon et al, 2007).*

is expected to be increased due to the increasing CO_2 concentration of air in urban areas as a result of the accelerating increase of CO_2 emission worldwide. CO_2 concentration in the atmosphere is increasing by 0.5% per year on a global scale (Yoon et al, 2007). Development of CO_2 concentration in the atmospheric layer has been considerably increased in the last 50 years, as shown in *Fig. 11*. In the future, extensive studies are needed in this field to be able to develop relationships for the rate of carbonation considering special concretes available recently.

6. CONCLUSIONS

The Schmidt rebound hammer was developed in 1950 by a Swiss engineer, *Ernst Schmidt* and became the most widespread surface hardness testing device of concrete in the last 50 years. Several thousand hundreds of Schmidt rebound hammers are in use worldwide recently. The apparently simple operation, easy and quick use and its economy made the device successful. On the other hand, if users are not skilled well usually overestimate the reliability of the Schmidt rebound hammer.

If the estimation of the compressive strength of structural concrete is the purpose of the user, empirical relationships are available that are established between rebound index and compressive strength. Empirical formulae based on laboratory tests can be used only within their limits of application. Extension of the validity of the curves is usually not possible. In such cases the error of the strength estimation by the Schmidt rebound hammer can be higher than expected. The detailed literature review given in present paper reflects to the sensitive nature of the testing method.

The widespread use of the Schmidt rebound hammer is expected to be maintained in the future. Rapid development of concrete technology makes special concretes available for the concrete construction industry. Several research programmes are expected to study the application of the Schmidt rebound hammer for novel types of concretes.

7. ACKNOWLEDGEMENTS

Authors gratefully acknowledge the support of the *Bolyai János* research scholarship by the Hungarian Academy of Sciences (MTA). Special thanks to Mr. Kurt Baumann (Proceq), Mr. Sándor Boros (ÉMI), Dr. Olivier Burdet (EPFL), Dr. Attila Erdélyi (BME), Dr. Zsuzsanna Józsa (BME), Mr. László Kutassy (MSZT) and Dr. István Zsigovics (BME) for their help provided in the literature review and to Dr. Lars Eckfeldt (TUD) for his ever initiative ideas.

8. REFERENCES

ACI (1998) „Nondestructive Test Methods for Evaluation of Concrete in Structures", ACI 228.2R-98, *American Concrete Institute*, Farmington Hills, Michigan

ACI (2002) „Evaluation of Strength Test Results of Concrete", ACI 214R-02, *American Concrete Institute*, Farmington Hills, Michigan

ACI (2003a) „Guide for Obtaining Cores and Interpreting Compressive Strength Results", ACI 214.4R-03, *American Concrete Institute*, Farmington Hills, Michigan

ACI (2003b) „In-Place Methods to Estimate Concrete Strength", ACI 228.1R-03, *American Concrete Institute*, Farmington Hills, Michigan

Akashi, T., Amasaki, S. (1984) „Study of the Stress Waves in the Plunger of a Rebound Hammer at the Time of Impact", *ACI Publication SP-82 In Situ/ Nondestructive Testing of Concrete*, Malhotra, V. M. (Editor), *American Concrete Institute*, Detroit, Michigan, 1984, pp. 17-34.

Almeida, I. R. (1993) „Qualitative evaluation of high performance concretes by means of rebound and ultrasonic testing (Emprego do esclerômetro e do ultra-som para efeito da avaliação qualitativa dos concretos de alto desempenho)", *Professoral Thesis*, Universidade Federal Fluminese, Niterói, Brasil, 124 p. (in Portuguese)

Anderson, A. R., Bloem, D. L., Howard, E. L., Klieger, P., Schlintz, H. (1955) „Discussion of a paper by Greene, G. W.: Test Hammer Provides New Method of Evaluating Hardened Concrete", *Journal of the American Concrete Institute*, December 1955, Vol. 27, No. 4, Part 2 (Disc. 51-11), pp. 256-1…256-20.

Arni, H. T. (1972) „Impact and Penetration Tests of Portland Cement Concrete", *Highway Research Record 378*, Highway Research Board, Washington D.C., pp. 55-67.

ASTM (2004) „Standard Test Method for Obtaining and Testing Drilled Cores and Sawed Beams of Concrete", ASTM C42/C42M-04, *ASTM International*, C09.61 Subcommittee, 6 p.

ASTM (2005) „Standard Test Method for Compressive Strength of Cylindrical Concrete Specimens", ASTM C39/C39M-05e1, *ASTM International*, C09.61 Subcommittee, 7 p.

Balázs Gy., Tóth E. (1997) „Diagnostics of concrete- and reinforced concrete structures, Vol. 1. (Beton- és vasbetonszerkezetek diagnosztikája I.), *Műegyetemi Kiadó*, 396 p. (in Hungarian)

Bartlett, F. M., MacGregor, J. G. (1994a) „ Effect of Core Moisture Condition on Concrete Core Strengths", *ACI Materials Journal*, V. 91, No. 3, May-June 1994, pp. 227-236.

Bartlett, F. M., MacGregor, J. G. (1994b) „Effect of Core Length-to-Diameter Ratio on Concrete Core Strengths", *ACI Materials Journal*, V. 91, No. 4, July-August 1994, pp. 339-348.

Bartlett, F. M., MacGregor, J. G. (1994c) „ Effect of Core Length-to-Diameter Ratio on Concrete Core Strengths", *ACI Materials Journal*, V. 91, No. 5, September-October 1994, pp. 460-470.

Bartlett, F. M., MacGregor, J. G. (1995) „Equivalent Specified Concrete Strength from Core Test Data", *Concrete International,* V. 17, No. 3, March 1995, pp. 52-58.

Bartlett, F. M., MacGregor, J. G. (1996) „Statistical Analysis of the Compressive strength of Concrete in Structures", *ACI Materials Journal*, V. 93, No. 2, March-April 1996, pp. 158-168.

Baumann, K. (2006) *personal communication* (Schwerzenbach, Switzerland)
Bentur, A. (2002) „Cementitious Materials – Nine Millenia and a New Century: Past, Present and Future", *ASCE Journal of Materials in Civil Engineering*, Vol 14, Issue 1, February 2002, pp. 2-22.
Bindseil, P. (2005) „On-site inspection of concrete structures: state-of-the-art and practical applications", *University of Applied Sciences Kaiserslautern, Department of Civil Engineering,* www.fh-kl.de/~bindseil
Borján J. (1968) „Mathematical statistical analysis of nondestructive testing of concrete (Roncsolásmentes betonvizsgálatok értékelése matematikai statisztikai módszerrel)", *Mélyépítéstudományi Szemle*, XVIII. évf., 7. sz., pp. 294-297. (in Hungarian)
Borján J. (1981) „Nondestructive testing of concrete (Roncsolásmentes betonvizsgálatok)", *Műszaki Könyvkiadó*, 204 p.(in Hungarian)
Brinell, J.-A. (1901) „Steel ball test report (Mémoire sur les épreuves à bille en acier)", *Communications presentés devant le congrés international des méthodes d'essai des matériaux de construction*, Vol. 2., 1901, pp. 83-94. (in French)
Brunarski, L. (1963) „Combined use of non-destructive testing methods in quality control of concrete (Gleichzeitige Anwendung verschiedener zerstörungsfreier Prüfmetoden zur Gütekontrolle des Betons)", *Wissenschaftliche Zeitschrift der Hochschule für Bauwesen Leipzig*, Sonderdruck, 1963 (in German)
Bungey, J. H., Millard, J. H., Grantham, M. G. (2006) „Testing of Concrete in Structures", *Taylor and Francis*, New York, 352 p.
Calvit, H. H. (1967) „Experiments on rebound of steel balls from blocks of polymers", *Journal of the Mechanics and Physics of Solids*, V.15, No. 3, May 1967, Pergamon Press Ltd., Oxford, pp. 141-150.
Carette, G. G., Malhotra, V. M. (1984) „In Situ Tests: Variability and Strength Prediction at Early Ages", *ACI Publication SP-82 In Situ/Nondestructive Testing of Concrete*, Malhotra, V. M. (Editor), *American Concrete Institute*, Detroit, Michigan, 1984, pp. 111-141.
Carino, N. J. (1993) „Statistical Methods to Evaluate In-Place Test Results", *New Concrete Technology: Robert E. Philleo Symposium*, ACI SP-141, T. C. Liu and G. C. Hoff, eds., American Concrete Institute, Farmington Hills, Michigan, pp. 39-64.
Carino (1994) „Nondestructive Testing of Concrete: History and Challenges", ACI SP-44, Concrete Technology – Past, Present and Future, Ed. Mehta, P. K., *American Concrete Institute*, 1994, pp. 623-678.
CEB-CIB-FIP-RILEM (1974) „Recommended principles for the control of quality and the judgement of acceptability of concrete", *Materials and Structures*, V. 8, No. 47, RILEM, 1974, pp. 387-403.
Chefdeville, J. (1953) „Application of the method toward estimating the quality of concrete", *RILEM Bulletin*, No. 15, Special Issue – Vibration Testing of Concrete, Part 2, RILEM, Paris, 1953
Chefdeville, J. (1955) „Nondestructive testing of concrete. Part 2. Compressive strength of concrete and its measurement by the Schmidt rebound hammer (Les essais non destructifs du béton. II. La résistance à la compression du béton. Sa mesure par le scléromètre Schmidt)", *Annales de l'Institut Technique du Batiment et des Travaux Publics*, Huitième année, No. 95., Novembre 1955, pp. 1137-1182. (in French)
Cianfrone, F., Facaoaru, I. (1979) „Study on the introduction into Italy on the combined non-destructive method, for the determination of in situ concrete strength", *Matériaux et Constructions*, Vol. 12, No. 71., pp. 413-424.
CPWD (2002) „Handbook on repair and rehabilitation of RCC buildings", Central Public Works Department, Government of India, *India Press*, Mayapuri, New Delhi, 498 p.
Crepps R. B., Mills R. E. (1923) „Ball Test Applied to Cement Mortar and Concrete", Bulletin No. 12., Engineering Experiment Station, Purdue University, LaFayette, Indiana, May 1923, 32 p.
Di Leo, A., Pascale, G., Viola, E. (1984) „Core Sampling Size in Nondestructive Testing of Concrete Structures", *ACI Publication SP-82 In Situ/ Nondestructive Testing of Concrete*, Malhotra, V. M. (Editor), *American Concrete Institute*, Detroit, Michigan, 1984, pp. 459-478.
Diem, P. (1985) „Nondestructive testing methods in the construction industry (Roncsolásmentes vizsgálati módszerek az építőiparban)", *Műszaki Könyvkiadó*, 233 p. (in Hungarian)
Dutron, R. (1927) „Ball tests for the determination of compressive strength of neat cement mortars (Essais à la bille pour la determination de la résistance à la compression des pates de ciment pur)", *Brochure - Le laboratoire Groupement Professionnel des Fabricants de Ciment Portland artificial de Belgique*, Bruxelles, Belgium, 1927 (in French)
Einbeck, C. (1944) „Simple method to determine concrete quality in structures (Einfaches Verfahren zur Feststellung der Betongüte im Bauwerk", *Bauwelt*, Vol. 35, 1944, p. 131 (in German)
ÉMI (1965) „Concrete strength evaluation by N-type Schmidt rebound hammer (A beton szilárdságának vizsgálata N-típusú Schmidt-féle rugós kalapáccsal)", *Építőipari Minőségvizsgáló Intézet private standard*, HSz 201-65, Prepared by János Vadász, 1 Dec 1965 (in Hungarian)
Fabbrocino, G., Di Fusco, A. A., Manfredi, G. (2005) „In situ evaluation of concrete strength for existing constructions: critical issues and perspectives of NDT methods",*Proceedings of the **fib** Symposium Keep Concrete Attractive 2005 Budapest*, Balázs, G. L. and Borosnyói, A. (Editors), Műegyetemi Kiadó, Budapest, 2005. pp. 811-816.
Facaoaru, I. (1964) „Experiences of the application of Romanian standards for the strength testing of concrete by the Schmidt rebound hammer (L'expérience de l'application des normes roumaines provisoires pour la déterminition de la résistance du béton à l'aide du scléromètre Schmidt)", RILEM Publication – Non-destructive testing of concrete, Meeting in Bucharest, 1964 (in French)
Ferry, J. D. (1961) „Viscoelastic properties of polymers", *John Wiley and Sons Inc*., New York, 1961, 482 p.
FHWA (1997) „Guide to Nondestructive Testing of Concrete", *FHWA Publication SA-97-105*, U.S. Department of Transportation, Federal Highway Administration, September 1997, 60 p.
Forslind, E. (1944) „Determination of Concrete Strength by Means of Shock and Drill Tests (Hållfasthetsbestämnig hos betong medelst slag- och borrprov)", *Meddelanden (Bulletins) Nr. 2.*, Swedish Cement and Concrete Research Institute, Stockholm, 1944, 20 p. (in Swedish)
Gaede, K. (1934) „A new method of strength testing of concrete in structures (Ein neues Verfahren zur Festigkeitsprüfung des Betons im Bauwerk)", *Bauingenieur*, 1934/15, Vol. 35-36., pp. 356-357. (in German)
Gaede, K. (1952) „Impact ball tests for concrete (Die Kugelschlagprüfung von Beton)", Deutscher Ausschuss für Stahlbeton, 1952, Heft 107, *Ernst & Sohn*, Berlin, p. 73. (in German)
Gaede, K., Schmidt, E. (1964) „Rebound testing of hardened concrete (Rückprallprüfung von Beton mit dichtem Gefüge)", *Deutschen Ausschusses für Stahlbeton*, Heft 158, p. 37. (in German)
Gonçalves, A. (1995) „In situ concrete strength estimation. Simultaneous use of cores, rebound hammer and pulse velocity", *Proc. International Symposium NDT in Civil Engineering*, Germany, pp. 977-984.
Granzer, H. (1970) „About the dynamic hardness testing of hardened concrete (Über die dynamische Härteprüfung von Beton mit dichtem Gefüge)", *Dissertationen der Technischen Hochschule Wien*, No. 14, Verlag Notring, Wien, 1970, p. 103. (in German)
Greene, G. W. (1954) „Test Hammer Provides New Method of Evaluating Hardened Concrete", *Journal of the American Concrete Institute*, November 1954, Vol. 26, No. 3 (Title No. 51-11), pp. 249-256.
Grieb, W. E. (1958) „Use of the Swiss Hammer for Estimating the Compressive Strength of Hardened Concrete", *Public Roads*, V. 30, No. 2, June 1958, pp. 45-50.
Gyömbér Cs. (2004) „Nondestructive testing of lightweight concrete (Könnyűbeton roncsolásmentes vizsgálata)", *MSc Thesis*, Budapest University of Technology and Economics, Faculty of Civil Engineering (in Hungarian)
Herzig, E. (1951) „Tests with the new concrete rebound hammer at the Dept. of Concrete and Reinforced Concrete, Material Testing Institute of Zurich (Versuche mit dem neuen Beton-Prüfhammer an der Abteilung für Beton und Eisenbeton der Eidg. Materialprüfungs- und Versuchsanstalt, Zürich)", *Schweizer Archiv für angewandte Wissenschaft und Technik*, V. 17, Mai 1951, pp. 144-146. (in German)
Hobbs, B., Kebir, M. T. (2006) „Non-destructive testing techniques for the forensic engineering investigation of reinforced concrete buildings", *Forensic Science International*, V. 167, 2006, Elsevier Ireland Ltd., pp. 167-172.
IAEA (2002) „Guidebook on non-destructive testing of concrete structures", Training Course Series No. 17, *International Atomic Energy Agency*, Vienna, 231 p.
Jones, R. (1962) „Non-Destructive Testing of Concrete", Cambridge Engineering Series (Ed. Baker, J.), *Cambridge University Press*, 1962, 104 p.
Keiller, A. P. (1982) „Preliminary Investigation of Test Methods for the Assessment of Strength of In Situ Concrete", *Technical Report* No. 42.551, Cement and Concrete Association, Wexham Springs, 1982, 37 p.
Kheder, G. F. (1999) „A two stage procedure for assessment of in situ concrete strength using combined non-destructive testing", *Materials and Structures*, Vol. 32., July 1999, pp. 410-417.
Knaze, P., Beno, P. (1984) „The use of combined non-destructive testing methods to determine the compressive strength of concrete", *Matériaux et Constructions*, Vol. 17, No. 99., pp. 207-210.
Kolek, J. (1958) „An Appreciation of the Schmidt Rebound Hammer", *Magazine of Concrete Research*, Vol. 10, No. 28, March 1958, pp. 27-36.
Kolek, J. (1970a) „Non-destructive testing of concrete by hardness methods", *Proceedings of the Symposium on Non-destructive testing of concrete and timber*, 11-12 June 1969, Institution of Civil Engineers, London, 1970, pp. 19-22.
Kolek, J. (1970b) „Discussion of the paper 3A: Non-destructive testing of concrete by hardness methods, by Kolek, J.", *Proceedings of the Symposium on Non-destructive testing of concrete and timber*, 11-12 June 1969, Institution of Civil Engineers, London, 1970, pp. 27-29.
Koris K. editor (1993) „Hydrology calculus (Hidrológiai számítások)", *Akadémiai Kiadó*, Budapest, 567 p. (in Hungarian)
KTI (2005) „Nondestructive testing of high strength concretes by the Schmidt rebound hammer (Nagyszilárdságú betonok roncsolásmentes vizsgálata Schmidt kalapáccsal)", *Research Report*, Prepared by Gáspár L., Tóth Z., Skokán G., KTI Kht., 2005 (in Hungarian)
Leeb, D. (1986) „Definition of the hardness value "L" in the Equotip dynamic measurement method", VDI Berichte 583, 1986, pp. 109-133.
Leshchinsky, A. M., Leshchinsky, M. Yu., Goncharova, A. S. (1990) „Within-Test Variability of Some Non-Destructive Methods for Concrete Strength Determination", *Magazine of Concrete Research*, V. 42, No. 153, pp. 245-248.

Lima, F. B., Silva, M. F. B. (2000) „Correlation between the compressive strength and surface hardness of concrete (Correlação entre a resistência à compressão do concreto e a sua dureza superficial)", *Proc. IV. Congresso de Engenharia Civil*, Ed. Interciência, Juiz de Fora, pp. 429-440. (in Portuguese)
Long, B. G., Kurtz, H. J., Sandenaw, T. A. (1945) „An Instrument and a Technic for Field Determination of Elasticity, and Flexural Strength of Concrete (Pavements)", *Journal of the American Concrete Institute*, Vol. 16., No. 3., *Proceedings* Vol. 41., January 1945, pp. 217-231.
Malhotra, V. M. (1976) „Testing Hardened Concrete: Nondestructive Methods", *ACI Monograph*, No. 9., American Concrete Institute, Detroit, 188 p.
Malhotra, V. M., Carette, G. (1980) „Comparison of Pullout Strength of Concrete with Compressive Strength of Cylinders and Cores, Pulse Velocity, and Rebound Number", *ACI Journal*, May-June 1980, pp. 161-170.
Malhotra, V. M., Carino, N. J. (2004) „Handbook on nondestructive testing of concrete", Second edition, *CRC Press LLC*, 384 p.
MI 15011 (1988) „Sectional analysis of existing load bearing elements of structures (Épületek megépült teherhordó szerkezeteinek erőtani vizsgálata)", Technical Guideline, *Hungarian Institute of Standardization* (*Magyar Szabványügyi Hivatal)*, 27 p. (in Hungarian)
Mikulic, D., Pause, Z., Ukraincik, V. (1992) „Determination of concrete quality in a structure by combination of destructive and non-destructive methods", *Materials and Structures*, Vol. 25, pp. 65-69.
MSZ 4715/5 (1972) „Testing of hardened concrete. Nondestructive testing (Megszilárdult beton vizsgálata. Roncsolásmentes vizsgálatok)", *Hungarian Standard (Magyar Népköztársasági Országos Szabvány)*, 13 p. (in Hungarian)
MSZ EN 13791 (2007) „Assessment of in-situ compressive strength in structures and precast concrete components", *European Standard*
Nash't, I. H., A'bour, S. H., Sadoon, A. A. (2005) „Finding an Unified Relationship between Crushing Strength of Concrete and Non-destructive Tests", *Proc. 3rd MENDT – Middle East Nondestructive Testing Conference and Exhibition*, Bahrain, Manama, www.ndt.net
Nehme, S. G. (2004) „Porosity of concrete (A beton porozitása)", *PhD Thesis*, Budapest University of Technology and Economics, Faculty of Civil Engineering (in Hungarian)
Neville, A. M. (1981) „Properties of Concrete", *Pitman,* London, 532 p.
Neville, A. M. (1986) „Properties of Concrete - An Overview, Part 3", *Concrete International*, Volume 8, Issue 4, April 1, 1986, pp. 53-57.
Neville, A. M. (2001) „Core Tests: Easy to Perform, Not Easy to Interpret", *Concrete International,* American Concrete Institute, November 2001, pp. 59-68.
NIST (2009) „NIST/SEMATECH e-Handbook of Statistical Methods", source: www.itl.nist.gov/div898/handbook/, *National Institute of Standards and Technology*, January 2009
Nyim, C. K. (2000) „Reliability in integrating NDT results of concrete structures", *MSc Thesis*, Universiti Teknologi Malaysia, 2000
Pascale, G., Di Leo, A., Bonora, V. (2003) „Nondestructive Assessment of the Actual Compressive Strength of High-Strength Concrete", *ASCE Journal of Materials in Civil Engineering*, Vol. 15., No. 5., pp. 452-459.
Pascale, G., Di Leo, A., Carli, R., Bonora, V. (2000) „Evaluation of Actual Compressive Strength of High Strength Concrete by NDT", *Proc. 15th WCNDT*, Roma, Italy, www.ndt.net
Pohl, E. (1966) „Nondestructive testing of concrete (Zerstörungsfreie Prüfmethoden für Beton)", *VEB Verlag für Bauwesen Berlin*, 1966, p. 160. (in German)
Proceq SA (2003) „Concrete Test Hammer N/NR,L/LR and DIGI SCHMIDT ND/LD – Rebound Measurement and Carbonation", *Info sheet,* ver 10 2003, Schwerzenbach, Switzerland
Proceq SA (2005) „Non-Destructive testing of concrete – Schmidt concrete test hammer", *Training course handout,* October 2005, Schwerzenbach, Switzerland
Proceq SA (2006) „Operating Instructions – Concrete Test Hammer N/NR – L/LR", *Manual*, ver 09 2006, Schwerzenbach, Switzerland
Proceq SA (2008a) „Silver Schmidt product launch", *Info sheet,* May 2008, Schwerzenbach, Switzerland
Proceq SA (2008b) „Silver Schmidt Operating Instructions", *Manual,* ver 04 2008, Schwerzenbach, Switzerland
Qasrawi, H. Y. (2000) „Concrete strength by combined nondestructive methods – Simply and reliably predicted", *Cement and Concrete Research*, Vol. 30., pp. 739-746.
Ravindrajah, R. S., Loo, Y. H., Tam, C. T. (1988) „Strength evaluation of recycled-aggregate concrete by in-situ tests", *Materials and Structures*, Vol. 21, pp. 289-295.
Reimann J. (1975) „Mathematical statistical analysis of characteristic flood data (Árvizek jellemző adatainak matematikai statisztikai elemzése)", *Hidrológiai Közlöny*, 1975/4, pp. 157-163. (in Hungarian)
Reimann J., V. Nagy I. (1984) „Statistics in Hydrology (Hidrológiai statisztika)", *Tankönyvkiadó*, Budapest, 1984, 519 p. (in Hungarian)
RILEM (1977) „Recommendations for testing concrete by hardness methods", Tentative Recommendation, 7-NDT Committee – Non Destructive Testing, *Matériaux et Constructions*, Vol. 10, No. 59., pp. 313-316.
Roknich Gy. (1968) „Nondestructive testing of concrete (A beton roncsolásmentes vizsgálata)", *Mélyépítéstudományi Szemle*, XVIII. évf., 7. sz., pp. 298-301. (in Hungarian)
Rüsch, H. (1964) „Statistical quality control of concrete (Zur statistischen Qualitätskontrolle des Betons)", Materialprüfung, V. 6, No. 11, November 1964, pp. 387-394. (in German)
Samarin A., (2004) „Combined Methods", Chapter 9 in Malhotra, V. M., Carino, N. J. (Editors) „Handbook on nondestructive testing of concrete", Second edition, *CRC Press LLC*, pp. 9-1 to 9-12.
Schmidt, E. (1950) „Rebound hammer for concrete testing (Der Beton-Prüfhammer)", *Schweizerische Bauzeitung*, 15. Juli 1950, 68. Jahrgang, Nr. 28, pp. 378-379. (in German)
Schmidt, E. (1951) „Quality control of concrete by rebound hammer testing (Versuche mit dem neuen Beton-Prüfhammer zur Qualitätsbestimmung des Betons)", *Schweizer Archiv für angewandte Wissenschaft und Technik*, V. 17, Mai 1951, pp. 139-143. (in German)
Sestini, Q. (1934) „Strength test of cementitious materials by Brinell testing (La prova Brinell applicata al materiali cementizi come prova di resistenza)", *Le Strade*, 1934/7, Vol. 16. (in Italian)
Shore, A. T. (1911) „Property of Hardness in Metals and Materials", *Proceedings*, ASTM, Vol. 11., 1911, pp. 733-739.
Skramtajew, B. G. (1938) „Determining Concrete Strength in Control for Concrete in Structures", *Journal of the American Concrete Institute*, Jan-Feb 1938, Vol. 9 (Proceedings Vol. 34), No. 3, pp. 285-303.
Skramtajew, B. G., Leshchinsky, M. Y. (1964) „Strength testing of concrete (Испытание прочности бетона)", *Sztroizdat*, Moscow, 1964, 176 p. (in Russian)
Soshiroda, T., Voraputhaporn, K. (1999) „Recommended method for earlier inspection of concrete quality by non-destructive testing", *Proc. Symp. Concrete Durability and Repair Technology*, Dundee, UK, pp. 27-36.
Soshiroda, T., Voraputhaporn, K., Nozaki, Y. (2006) „Early-stage inspection of concrete quality in structures by combined nondestructive method", *Materials and Structures (2006)*, DOI 10.1617/s11527-005-9007-6.
Steinwede, K. (1937) „Application of ball hardness tests for the determination of strength of concrete (Über die Anwendung des Kugelhärteversuches zur Bestimmung der Festigkeit des Betons), *Doctoral Thesis*, University of Hannover, Faculty of Civil Engineering, 20 Feb 1937, *Gebrüder Jänecke*, Hannover, 69 p. (in German)
Swamy, N., Rigby, G. (1971) „Dynamic properties of hardened paste, mortar and concrete", *Matériaux et Constructions*, Vol. 4, No. 19., pp. 13-40.
Talabér J., Borján J., Józsa Zs. (1979) „Influences of concrete technology parameters to the strength estimation relationships based on non-destructive testing (Betontechnológiai paraméterek hatása a roncsolásmentes szilárdságbecslő összefüggésekre)", *Tudományos Közlemények 29.*, Budapest University of Technology, Dept. of Building Materials, 97 p. (in Hungarian)
Tóth, J., editor (2007) „Oxford-Typotex Encyclopaedia of mathematics (Oxford-Typotex Matematikai Kislexikon)", *Typotex publishing*, 2007, source: www.tankonyvtar.hu (in Hungarian)
Vadász J. (1970) „Nondestructive testing of concrete strength in structures (A beton nyomószilárdságának roncsolásmentes meghatározása szerkezetekben)", *Doctoral Thesis*, Budapest University of Technology, Faculty of Civil Engineering (in Hungarian)
Vandone, I. (1933) „Indentation testing for the determination of compressive strength of cements (La prova d'impronta per determinare la resistenza a compressione dei cementi)", *Le Strade*, 1933/9, Vol. 15. (in Italian)
Victor, D. J. (1963) „Evaluation of hardened field concrete with rebound hammer", Indian Concrete Journal, November 1963, pp. 407-411.
Wesche, K. (1967) „Strength testing of concrete in structures (Die Prüfung der Betonfestigkeit im Bauwerk)", *Betonstein-Zeitung*, Heft 6/1967, pp. 267-277. (in German)
Williams, J. F. (1936) „A Method for the Estimation of Compressive Strength of Concrete in the Field", *The Structural Engineer* (London), Vol. 14., No. 7., July 1936, pp. 321-326.
Yoon, I.-S., Copuroglu, O., Park, K.-B. (2007) „Effect of global climatic change on carbonation progress of concrete", *Atmospheric Environment*, Elsevier, doi: 10.1016/j.atmosenv.2007.05.028.
Yun, C. H., Choi, K. R., Kim, S. Y., Song, Y. C. (1988) „Comparative Evaluation of Nondestructive Test Methods for In-Place Strength Determination", *ACI Publication SP-112 Nondestructive Testing*, Lew, H. S. (Editor), *American Concrete Institute*, Farmington Hills, Michigan, 1984, pp. 111-136.
Zoldners, N. G. (1957) „Calibration and Use of Impact Test Hammer", *Journal of the American Concrete Institute*, V. 29, No. 2, August 1957, Proceedings V. 54, pp. 161-165.

Katalin Szilágyi (1981) civil engineer (MSc), PhD candidate at the Department of Construction Materials and Engineering Geology, Budapest University of Technology and Economics. Main fields of interest: diagnostics of concrete structures, non-destructive testing of concrete, concrete technology, self-compacting concretes. Member of the Hungarian Group of fib.

Dr. Adorján Borosnyói (1974) civil engineer (MSc), PhD, senior lecturer at the Department of Construction Materials and Engineering Geology, Budapest University of Technology and Economics. He received the MTA Bolyai János research fellowship for 2006-2009. Main fields of interest: application of non-metallic (FRP) reinforcements for concrete structures, bond in concrete, non-destructive testing of concrete. Member of the Hungarian Group of fib and of fib TG 4.1 „Serviceability Models".